Analysis of Molecular Components Essential for the Formation of Signaling-competent TNF-TNFR Complexes

Von der Fakultät Geo- und Biowissenschaften der Universität Stuttgart
zur Erlangung der Würde eines Doktors der
Naturwissenschaften (Dr. rer. nat.) genehmigte Abhandlung

vorgelegt von

Marcus Branschädel

aus Heilbronn

Hauptberichter: Prof. Dr. Peter Scheurich
Mitberichter: Prof. Dr. Klaus Pfizenmaier
Tag der mündlichen Prüfung: 17.07.2007

Institut für Zellbiologie und Immunologie
Universität Stuttgart
2007

Die experimentellen Arbeiten für die vorliegende Dissertation wurden unter der Leitung von Prof. Dr. P. Scheurich am Institut für Zellbiologie und Immunologie der Universität Stuttgart durchgeführt.

»Gleich. Nur noch anderthalb Seiten.«

aus “Der Leseteufel” von Siegfried Lenz

Table of contents

ABBREVIATIONS

aa	Amino acids
Å	Angstrom (0.1 nm)
ADAM	A disintegrin and metalloprotease
Amp	Ampicillin
April	A proliferation-inducing ligand
APS	Ammonium persulfate
BAFF	B cell activating factor belonging to the TNF family
β-ME	Beta-Mercaptoethanol
BS^3	Bis-(sulfosuccinimidyl)-suberate
BSA	Bovine serum albumin
°C	Degree Celsius
Ci	Curie
CD	Cluster of differentiation
CDR	Complementary determining region
cpm	Counts per minute
CRD	Cysteine rich domain
CT	Chloramine T
CysTNF	Cysteine-TNF (a membrane-like TNF variant)
ddH_20	Twice distilled water (“bidest”)
DMSO	Dimethylsulfoxide
DR	Death receptor
EC50	Effector concentration 50%
EDA	Ectodysplasin-A
EDTA	Ethylene di-amine tetra-acetic acid
EGF	Epidermal growth factor
ELISA	Enzyme-linked immunosorbent assay
EPO	Erythropoietin
Fab	Fragment antigen binding
FACS	Fluorescence-activated cell sorter
FADD	Fas-associating protein with a death domain
Fc	Fragment crystallizable (constant region)
FCS	Fetal calf serum
Fig.	Figure
FITC	Fluorescein isothiocyanate
GFP	Green fluorescing protein

h	Hour
H398	Hugo, clone 398
HEK cells	Human embryonal kidney cells
HVEM	Herpes virus entry mediator
HPLC	high performance liquid chromatography
HSA	Human serum albumin
Ig G	Immunoglobulin G
IL	Interleukin
IMAC	Immobilized metal affinity chromatography
k	Boltzmann constant, 1.38065 x 10-23 JK^{-1}
K	Kelvin (0 K = -273.15 °C)
KD	Saturation affinity constant
kDa	Kilo Dalton
LB	Luria Bertani
LPS	Lipopolysaccharide
LTα	Lymphotoxin alpha
M	Molar
mAb	Monoclonal antibody
MD	Molecular dynamics
MEF	Mouse embryonic fibroblast
min	Minute
mM	Milli-molar (10^{-3} M)
ml	Milliliter (10^{-3} l)
MS	Mass spectrometry
mTNF	Membrane-bound TNF
Mw	Molecular weight
NF-κB	Nuclear factor-kappa B
nm	Nano-meter (10^{-9} m)
nM	Nano-molar (10^{-9} M)
o.n.	Over night
OD	Optical density
pAb	Polyclonal antibody
PAGE	Polyacrylamide electrophoresis
PMSF	Phenylmethylsulfonyl fluoride
PBA	PBS with BSA and azide
PBS	Phosphate buffered saline
PBS-T	PBS with Tween-20

PBS-TBA	PBS with Tween-20, BSA and azide
PCR	Polymerase chain reaction
Pfu	*Pyrococcus furiosus*
PLAD	Pre-ligand binding assembly domain
pM	Pico-molar (10^{-12} M)
PMSF	Phenylmethylsulfonylfluoride
RIA	Radio-immuno-assay
RING	Really interesting new gene
RPM	Rotations per minute
RT	Room temperature
SDS	Sodium dodecyl sulfate
SPOTS	Signaling protein oligomerization transduction structures
sTNF	Soluble TNF
S/N	Supernatant
TACE	TNFα converting enzyme
TACI	Transmembrane activator and CAML interactor
TAE	Tris-acetate-EDTA
TEMED	N,N,N´,N´-tetramethylethyl-diamine
TNF	Tumor Necrosis Factor
TNFSF	TNF super family
TNFR1 (p55/60, CD120a)	TNF receptor 1
TNFR2 (p75/80, CD120b)	TNF receptor 2
TRADD	TNFR1 associated death domain
TRAF	TNF receptor associated factor
TRAIL(R)	TNF-related apoptosis-inducing ligand (receptor)
TRIS	Tris-(hydroxymethyl)-amino-methane
U	Units
UV	Ultra violet
μm	Micrometer
μM	Micro-molar (10^{-6} M)
VMD	Visual molecular dynamics
Vol	Volume
wt	Wild type
YNB	Yeast nitrogen base
zVADfmk	N-benzyloxycarbonyl-Val-Ala-Asp-fluoromethyl ketone

SUMMARY

Signaling of Tumor Necrosis Factor Receptors (TNFR) coincides with the formation of microscopically visible aggregates. At least two interactions are required for such cluster formation: One ligand-dependent, and one ligand-independent. The second type of interaction was investigated by using chimeric receptors consisting of TNFR1 or TNFR2 that were fused to the intracellular parts of Fas. These molecules were used as a model system to analyze the role(s) of the extracellular cysteine rich domains (CRDs) as well as the stem- and transmembrane regions during signal formation. Whereas CRD2 and -3 directly contact the ligand within a signaling-competent complex, the CRD1 has several roles: It is a scaffold for CRD2, necessary for receptor-receptor interactions without ligand and essential for the formation of signaling competent complexes after ligand binding. In addition, the exchange of the CRD1 between receptors revealed that this domain also contributes to the discrimination of soluble versus membrane-bound ligand.

Furthermore, the stem- and transmembrane regions influence the chemical reactivity towards the homo-bifunctional crosslinker BS^3. The amount of cross-linkable receptors may be indicative for the strength of a homophilic receptor-receptor interaction that, together with the half-times of the ligand-receptor interaction, determine the generation of an intracellular signal.

The experimental data are summarized into a hypothetical model of a ligand-induced hexagonal lattice of ligand-receptor complexes. Such a pattern would allow the efficient activation of intracellularly recruited and enzymatically active proteins (e.g. kinases and caspases) as these are believed to require a dimerization for activation, although ligands of the TNF family display a three-fold symmetry.

ZUSAMMENFASSUNG

Die Entstehung eines Signals, ausgehend von einem der zwei Rezeptoren des Tumor Nekrose Faktors (TNF), korreliert mit der Bildung von lichtmikroskopisch beobachtbaren Ligand-Rezeptor-Aggregaten auf der Zelloberfläche. Mindestens zwei molekulare Interaktionen sind notwendig, um solche Proteinkomplexe aufzubauen: Eine ligand-abhängige und eine ligand-unabhängige. Um den zweiten Typus der Interaktion näher zu charakterisieren wurden chimäre Rezeptoren hergestellt, die aus den extrazellulären und trans-membranären Anteilen von TNFR1 oder TNFR2 bestehen und mit der intrazellulären Domäne des Fas Moleküls fusioniert sind. Dieses Modellsystem wurde verwendet um die Rollen der extrazellulären, Cystein-Reichen Domänen (CRDs), sowie der sog. Stiel- und transmembranären Domänen bei der Signalentstehung zu untersuchen. Während die CRD2 und -3 den Liganden in einem signalfähigen Komplex direkt kontaktieren, hat die CRD1 mehrere Funktionen: Sie ist ein Stützgerüst für die CRD2, notwendig für eine ligand-unabhängige Rezeptor-Rezeptor Interaktion und essentiell für die Bildung signalfähiger Komplexe nach Ligand-Bildung. Weiterhin konnte durch den Austausch der CRD1 zwischen den TNF-Rezeptoren gezeigt werden, dass diese Domäne darüber mitbestimmt, ob ein Rezeptor gegenüber dem löslichen Liganden responsiv ist, oder eine höher vernetzende Form des Liganden benötigt wird.

Weiterhin beeinflussen die Stiel- und transmembranären Domänen die chemische Reaktivität gegenüber dem homo-bifunktionellen, quervernetzenden Agens BS^3. Die Stärke dieser Quervernetzbarkeit könnte als Hinweis für das Ausmaß einer homophilen Rezeptor-Rezeptor Interaktion interpretiert werden, die zusammen mit den Halbwertszeiten der Rezeptor-Ligand Interaktion darüber bestimmt, ob ein starkes Signal innerhalb der Zelle zustande kommt.

Die experimentellen Daten wurden in ein hypothetisches Modell zusammengefasst, das die Bildung eines hexagonalen Gitters aus Ligand-Rezeptor Komplexen vorschlägt. Ein solches Muster würde die effiziente Aktivierung von intrazellulär rekrutierten und enzymatisch aktiven Proteinen (z.B. Kinasen und Caspasen) ermöglichen, da man annimmt, dass diese eine Dimerisierung zur Aktivierung benötigen, die Liganden der TNF Familie jedoch eine dreifache Symmetrie aufweisen.

1. INTRODUCTION

1.1 Tumor Necrosis Factor

Cells are the smallest biological units that can exist autonomously. Even the smallest bacterial cell can sense differences in appropriate nutritients in the surrounding medium and for instance change its “swimming” direction accordingly. This simple task, however, results into a quite complex signaling network within the cell. Metazoans, consisting of ~10^{12} cells, have acquired cellular communication mechanisms to maintain the balance between individual cells and the organism. One class of proteins utilized for cellular communication contains molecules of the cytokine family. They deliver information between cells, especially cells of the immune system. Besides the interleukins, colony-stimulating factors, growth hormones, interferons and chemokines, the tumor necrosis factor (TNF) family has gained a lot of interest in recent years. Although not defined at the time, the anti-tumoral bioactivity of TNF was already used by Dr. William B. Coley, a New York surgeon at the 19th century. He noticed that in patients with certain cancer types sometimes a spontaneous regression of the tumor could be observed during a bacterial infection. This observation was exploited to treat cancer patients with bacteria or bacterial products (Coley, 1896). Although in some cases indeed a tumor response could be observed, the side effects of this treatment regime often could not be controlled, even leading to the death of some patients. Leaping forward into the 20th century, the genetic information of a protein that causes dramatic weight loss albeit sufficient calory uptake (cachexin) was reported. In parallel, a protein was isolated that exhibited the impressive capability to cure mice from a certain type of chemically induced sarcoma. Since the sarcomas in these animal models were observed to be eliminated by starvation and subsequent necrosis, this factor was named tumor necrosis factor and is known today to be identical to cachexin (Aggarwal, 2003)

1.2 The TNF receptor/ligand superfamily

TNF is the prototypic member of a family of proteins called the TNF superfamily (TNFSF). The discovery rate of new family members has decelerated in recent years, thus making it likely that the list of family members is almost complete. Today, 21 TNFSF members have been identified that are mirrored by roughly 30 binding partners of the TNF receptor superfamily, TNFRSF (Branschädel et al., 2007). Some ligands bind to several receptors and some receptors bind more than one ligand. For instance, TNF can bind two receptors, TNFR1 and TNFR2 (Hohmann et al., 1989) and TNFR1 can interact with TNF and lymphotoxin α (LTα). Some orphan receptors exist for which the ligand remains to be identified such as death receptor 6 (DR6). Gene deletion studies (“knock out”) and other experiments have established essential roles for many members of the TNF-ligand/-receptor

family during the development of the embryo, control of the immune system, control of the immune response and some rather special functions such as development of skin appendices like hair, sweat glands and teeth (Locksley et al., 2001). The network-like pattern of ligand/receptor interactions within the TNF ligand and receptor families is further complexed by recent data showing that some receptors of the TNFR family are rather promiscuous with respect to their interaction partners. For instance, HVEM (herpes virus entry mediator), besides capable of interacting with the TNFSF ligands LTα and LIGHT, also binds to members of the B7 family of co-stimulatory molecules and viral glycoproteins. In addition, TNFR1 can interact with a poxvirus protein (Sedger et al., 2006) and CD40 can interact with its ligand CD154 as well as with the heat shock protein hsp70. Especially TNF has gained popularity in recent years as it plays a major role in the development and progression of chronic inflammatory diseases such as rheumatoid arthritis and others (Feldmann and Maini, 2003).

1.3 Signaling pathways of TNF Receptors

The intracellular signaling pathways that are activated by members of the TNFRSF are highly complex and are far from being understood. There exists an overwhelming body of literature on TNF itself. Accordingly, with the recent establishment of the new field of systems biology, besides cell biologists, immunologists and physicians mathematicians, physicists and system engineers have recently been attracted by this field. Clearly the cooperation of scientific disciplines will be crucial for understanding the complex nature of TNFR signaling pathways in the future.

TNF signaling has been discussed in several excellent reviews and will here be presented only in parts. In contrast to some other plasma-membrane located receptors, members of the TNFRSF have no intrinsic enzymatic activity and thus rely on the recruitment of intracellular proteins. These include adapter proteins, kinases, enzymes involved in ubiquitination and de-ubiquitination and proteases. Two principal classes of TNFR family members can be distinguished based on the mainly induced cellular responses. One receptor class induces gene expression leading to proliferation, survival and secretion of other cytokines, whereas the other leads to the coordinated break down of the cell. The latter process is also called apoptosis and is a form of programmed cell death (PCD) which has to be distinguished from other forms of cell death like necrosis mentioned in the tumor model above. Whereas necrosis leads to the release of intracellular material followed by local inflammation, apoptosis is a silent and genetically determined form of death. Apoptosis is essential during development and to maintain homeostasis of the adult organism. Many intermediate forms of PCD have been described (Leist and Jaattela, 2001). Apoptosis, however, is biochemically defined by the activation of intracellular proteases called the caspases. Caspases are

zymogens, i.e. inactive enzymes that are activated by limited proteolysis. For instance this activation mechanism is also found in the blood-clotting cascade and digestive enzymes. So far, 14 human caspases have been identified that reside in different cellular compartments. They all contain a cysteine at their active sites and cleave their substrates after an aspartate, hence the name, caspase. Once sufficiently activated, caspases pave the way to death by cleaving substrates that bring about morphological cellular changes. Typically, these involve the formation of small membrane-attached vesicles ("blebbing"), loss of plasma-membrane polarity, loss of mitochondrial potential and integrity, release of mitochondrial proteins, chromatin condensation, nuclear fragmentation and the cleavage of DNA between chromatin-organizing proteins (nucleosomes) by the caspase-activated DNAse (CAD). Eventually, the dying cell dissects itself into handy packets that are engulfed by phagocytic cells such as macrophages. Many positive and negative feedback-loops exist, so there is not just one way to kill a cell. It is clear, that the caspase activation process must be highly regulated. As members of the TNF family are capable of killing cells, they are also of great therapeutical interest to treat diseases such as cancer. By the means of recombinant DNA technology, it is possible to create "magic bullets" or "Swiss army knives" (Watermann et al., 2007) that are specifically activated at the tumor-site with reduced targeting of the healthy tissue.

1.4 Activation of intracellular proteins by the TNFR family

So far, the scientific community is in agreement that caspases are activated by bringing the so-called initiator caspases (caspase-2, -8, -9, and -10) into close proximity (Boatright and Salvesen, 2003; Boatright et al., 2003; Salvesen and Dixit, 1999; Muzio et al., 1998). This can happen when plasma-membrane resident receptors of the TNFR family that contain the cytoplasmatic "death domain" (DD) are activated by their respective homotrimeric ligands. Examples for DD containing receptors are TNFR1, Fas, DR6 and TRAIL-R1, -2. The DD is a homotypic interaction domain that subsequently recruits cytoplasmic adaptor proteins such as the TNF receptor adaptor protein with a DD (TRADD) and/or Fas-associated factor with a DD (FADD). These, in turn, bind via homotypic interactions the death-effector domain (DED) of caspase-8 or -10 to generate the death-inducing signaling complex, DISC (Scaffidi et al., 1999). The auto-processed and active caspase-8 then cleaves/activates effector caspases such as caspase-3. Although the molecular components involved in caspase activation have been identified, the process how two caspase molecules are activated by a ligand-induced homotrimerization of receptor chains is rather unclear.

Besides the cell-surface induced apoptotic process an intracellular activation mechanism exists that was termed the intrinsic pathway. Here, no ligand is required and mitochondria serve as Pandora's box that contains pro-apoptotic molecules (Zamzami and Kroemer,

2001). Currently it is believed that the permeability for pro-apoptotic molecules of the outer mitochondrial membrane is hierarchically controlled by members of the B-cell lymphoma (BCL) class of proteins (Galonek and Hardwick, 2006).

On the other hand, the non-apoptotic signaling pathways rely on the recruitment of adaptors belonging to the TNF-receptor-associated factors, TRAFs (Wajant et al., 2001). Characteristic for the six known human TRAF proteins is the existence of a C-terminal TRAF-domain, however, other motifs such as RING (really interesting new gene) and zinc-fingers are also found. The crystal structures of several C-terminal TRAF-domains have been solved and revealed that TRAFs are homotrimeric and mushroom-shaped molecules (Park et al., 1999; Ye et al., 1999). TRAFs bind with their C-termini to sequences of the cytoplasmatic parts from TNFRSF family members with relatively low affinities ranging from 40 μM to 2 mM (Ye and Wu, 2000). Subsequently, upstream kinases of the MAPK (mitogen activating protein kinases) family are recruited and activated involving a complex molecular mechanism of phosphorylation and ubiquitination events (Sebban et al., 2006; Kovalenko and Wallach, 2006). Downstream kinases such as the MAPK c-Jun N-terminal kinase (JNK) and others culminate in the activation of several transcription factors including AP2 and nuclear factor-kappa B (NF-κB). NF-κB belongs to a family of five transcription factors that homo- or hetero-dimerize via their characteristic, N-terminal Rel homology domain also required for DNA binding. At least two pathways have been described that lead to the activation of NF-κB. For TNFR1 it has been shown that the so-called “canonical” mode is utilized, typically leading to a fast translocation of NF-κB into the nucleus and characterized by the involved kinases such as inhibitor of NF-κB kinase β (IKKβ) and the NF-κB subunits p50/p65. Other members of the TNFRSF including LTβR, CD40 and B cell activating factor belonging to the TNF family (BAFF)-R3 utilize the “non-canonical” pathway (Pomerantz and Baltimore, 2002) that is believed to lead to a prolonged survival signal (Sen, 2006; Karin and Lin, 2002) and involves the molecules NF-κB inducing kinase (NIK) in combination with IKKα as well as the heterodimer p52/RelB.

Interestingly, caspases are not exclusively used for killing of cells (Lamkanfi et al., 2007; Lamkanfi et al., 2006). For instance, the founding member, caspase 1, was historically found to be required for processing the cytokine interleukin 1β (IL-1β) into the biologically active form by a meanwhile characterized multi-protein complex termed the inflammasome (Martinon et al., 2002). In addition, it has been shown that patients with certain mutations in caspase 8 show defects in the activation of T-lymphocytes (Su et al., 2005; Bidere et al., 2006; Budd et al., 2006). Additional post-translational modifications besides limited proteolysis, such as phosphorylation and ubiquitination, are responsible for the functional regulation of proteins. These examples impressively demonstrate that higher eukaryotes have pursued the evolutionary strategy to use one protein for several functions, brought

about by increasing the number of modifying enzymes. The combinatorial variety of interactions is thus more effective than inventing one protein for every task. This principle is for instance impressively demonstrated by the adaptive branch of the immune response that creates a huge panel of antibodies by combining a limited set of encoding genes. So far, most if not all of the proteins involved in TNFR signaling, including the receptors themselves, have been shown to be post-translationally modified in one way or the other. Whereas TNFR1 unifies both basic signaling pathways described (inflammatory/gene induction and pro-apoptotic), TNFR2 is rather anti-apoptotic. Whereas TNFR1 is ubiquitously expressed on most cells, TNFR2 is highly regulated and mainly confined to the immune system. In addition, TNFR1 signaling functions have been correlated with the subcellular localization of the receptor when ligated with TNF, thus forming a new layer of regulation. Whereas the TNFR1-complex 1 is located at the plasma-membrane and induces gene expression via NF-κB, the complex 2 is found intracellularly and induces apoptosis. Issues concerning the precise molecular composition of these two complexes are still debated (Schneider-Brachert et al., 2004; Micheau and Tschopp, 2003).

1.5 The TNF ligand(s)

Whereas receptors of the TNF superfamily can signal when ligated, some ligands can do so likewise if presented in the membrane-bound form by another cell. This pathway has been called “retrograde” or “reverse” signaling and has for instance been demonstrated for CD40 (Blotta et al., 1996) and TNF (Friedmann et al., 2006), however with rather unclear relevance for the latter. In addition, ligands can be rendered soluble by several proteases, such as TNF that can be cleaved by a metalloproteinase of the ADAM (a disintegrin and metalloprotease) family, called TNFα converting enzyme or simply TACE (Zheng et al., 2004) to generate soluble TNF (sTNF). For TNF, the biological function of this principle likely is to systemically activate signaling of TNFR1 bearing cells. Other ligands are required to be rendered soluble in order to reach their target cell, such as ectodysplasin-A (EDA) that is involved in hair and teeth formation (Chen et al., 2001). On the other hand, the membrane-anchored ligand locally transfers information between cells, a process termed juxtatropic signaling. For instance membrane-bound TNF (mTNF) can efficiently activate both TNFRs; further examples are known in which a membrane variant is required to efficiently activate the respective receptor (CD40L-CD40, FasL-Fas and TRAIL-TRAILR2). But how can a receptor distinguish between the two forms of the same ligand? It has been demonstrated that the TNF system is controlled by the action of mass law. In more detail, the dissociation rates (k_{off}) between the receptor-ligand pairs decide if the receptors are kept in a signaling competent state or not. Whereas TNFR1 has a slow off rate for sTNF and thus a long half-time at 37°C (k_{off} = 0.021 min^{-1}, $t_{½}$ = 30 min), it seems that TNFR2 can easily capture the ligand, but as

easily looses it, as reflected by the fast off-rate and short half-time (k_{off} = 0.631 min^{-1}, $t_{½}$ = 1.1 min) (Grell et al., 1998). Thus, the ability to "hold on to" the ligand correlates with the ability to signal but may not be the only determinant, as will be shown later.

1.6 Functions and structure of TNF

The typical *in vivo* sources of TNF are white blood cells of the myeloid branch such as macrophages (MΦ) and neutrophils, but T- and B-cells are also known to produce TNF. Upon encountering bacteria, MΦ secrete TNF that induces many effects such as the activation of the endothelium from blood vessels to produce selectins such as CD62E that allows white blood cells to adhere. In addition, TNF is vaso-relexative to ease the crossing of immune-cells and fluids and induces the secretion of chemotactic factors such as IL-8. TNF also activates MΦ to efficiently digest phagocytized or intracellular pathogens, such as Mycobacterium spec., that is responsible for diseases such as tuberculosis and leprosy. However, there also is a "dark side" attached to TNF, namely if acutely released in huge concentrations such as observed during sepsis, or if chronically elevated. The latter is observed during chronic auto-inflammatory disorders of the joints (rheumatoid arthritis), gastrointestinal tract (Crohn disease, Morbus), arthritis associated with skin psoriasis (psoriatic arthritis), sacroiliac joints, enthuses and spine (ankylosing spondylitis). However, additional cytokines have been identified to be important for progression of these diseases, such as IL-12 and IL-23 during Morbus (Neurath, 2007). As a first line therapy for most of these chronic diseases, immunosuppressive drugs such as corticosteroids or metothrexate are typically administered. However, these disease modifying drugs can become ineffective after some time. Currently, three so-called "biologicals" are approved for this scenario and all target TNF itself, namely infliximab (Remicade; the variable region of a mouse monoclonal anti-TNF antibody coupled to the constant region of human IgG1), adalimumab (Humira; full-length human IgG1) and Eternacept® (soluble TNFR2 fused with the Fc fragment of human IgG1). Biochemical and structural data indicate that the ligands of the TNF superfamily are homotrimeric molecules (Jones et al., 1990; Reed et al., 1997), held together by hydrophobic interactions over a broad concentration range (Corti et al., 1992). Chemical compounds that favor the dissociation of TNF have been developed that may serve as future therapeutics (He et al., 2005). Each subunit of the homotrimeric ligand is composed of several β-sheets. Their organization, if drawn on a paper, is reminiscent of a cut-open cake and is therefore called the "jelly roll fold". Besides members of the TNFSF, the jelly roll fold is also found in capsid proteins of small RNA viruses (Jones and Liljas, 1984). Although the important roles of TNF and its alike *in vivo* are well established, the super-structural organization of ligands, receptors and adaptors on and within the cell leading to a strong signal are only beginning to be understood (Carrington et al., 2006).

1.7 Structure of TNF receptors

Whereas the primary structures of TNF receptors show low homology, tertiary structures determined by X-ray crystallography from the extracellular parts of members from the TNFRSF are quite similar. Solved structures include TNFR1 bound to LTα (Banner et al., 1993), TNFR1 without ligand (Naismith et al., 1995; Naismith et al., 1996a; Naismith et al., 1996b), TRAILR2 bound to TRAIL (Hymowitz et al., 1999; Cha et al., 2000), HVEM bound to a viral glycoprotein (Carfi et al., 2001), TACI bound to its ligand April (Hymowitz et al., 2005) and OX40 bound to OX40L (Compaan and Hymowitz, 2006). Characteristically, receptors contain regularly dispersed cysteines that form disulfide-bridge stabilized cysteine-rich domains (CRDs). This feature is likely to be required for structural stability because the receptors form elongated molecules with little space for hydrophobic cores. The nomenclature of CRDs has been refined recently (Naismith and Sprang, 1998) and dissects these motifs into modules followed by a number indicating the amount of intra-chain disulfide bridges (Table 1 and Fig. 1). For instance, the first three CRDs of TNFR1 and the first two CRDs of TNFR2 are built by one A1 and one B2 module.

Module	Structure	Number of residues	Number of disulfide bridges	Disulfide connectivity	Consensus sequence
A1	Three short strands linked by two loops; S-shaped	12 – 17	1	$Cys^1 \rightarrow Cys^2$	**Cys^1**-x-x-Gly-x-Tyr/Phe-x-x-x-x-x-(x-x-x-x-x)-**Cys^2**
B2	Three anti-parallel strands reminiscent of a paper clip	21 – 24	2	$Cys^1 \rightarrow Cys^3$ $Cys^2 \rightarrow Cys^4$	**Cys^1**-x-x-**Cys^2**-x-x-x-(x-x-x)-x-x-x-x-x-**Cys^3**-Thr-x-x-(x-x-x)-Asn-Thr-Val-**Cys^4**

Table 1: Features of the A1 and B2 modules (Naismith and Sprang, 1998). Within the consensus sequence the 'x' indicates intervening amino acids. Residues within brackets indicate variable lengths at these positions. For instance, within the A1 module the distance between Tyr/Phe and the second cysteine (Cys^2) is at least five variable residues long, but up to ten residues can be found at this site. The conserved aromatic residues are thought to stabilize disulfide bridges between cysteines.

Additional modules within the TNFRSF have been identified that are described elsewhere (Naismith and Sprang, 1998). Whereas TNFR1 (Fig. 1A), TNFR2 and HVEM contain four CRDs, Fas, TRAILR, EDAR and XEDAR (Hymowitz et al., 2003) contain three CRDs and BAFF-R3 only a partial CRD (Gordon et al., 2003). However, the BAFF system may represent a special case within the TNF superfamily and is discussed at the end of this work.

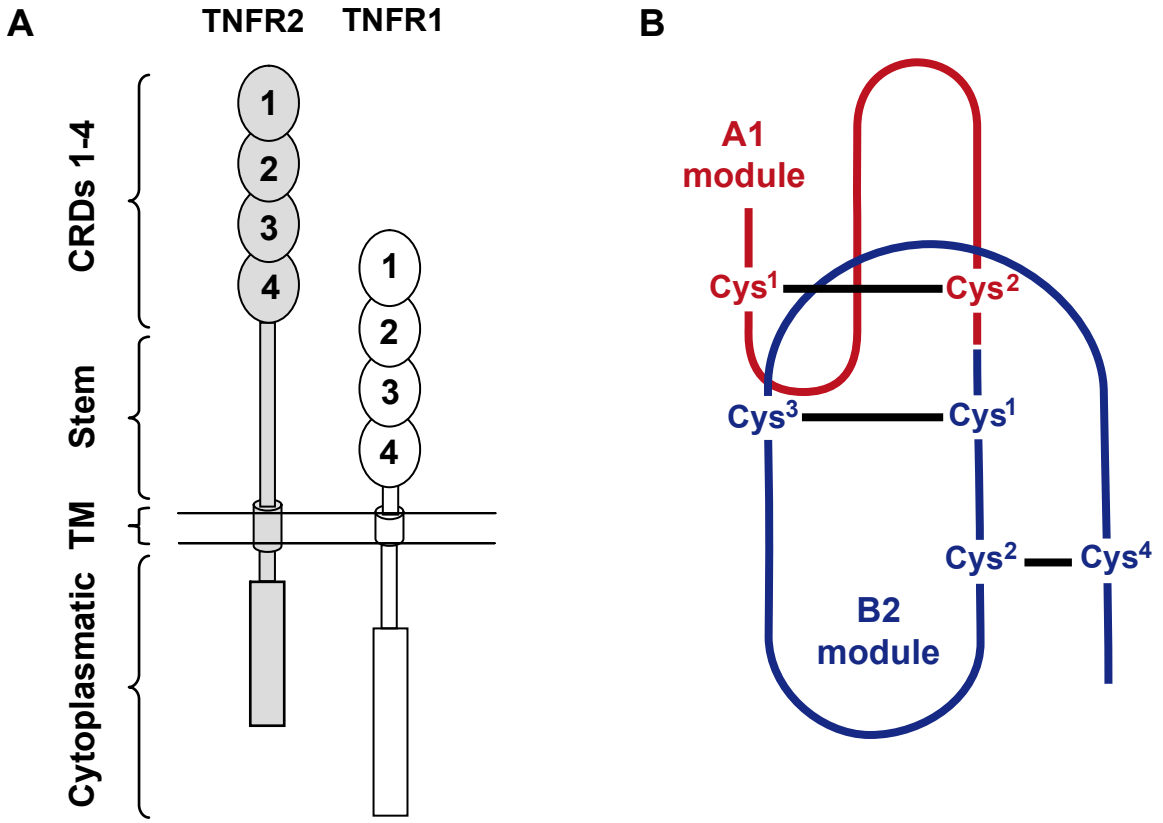

Figure 1: Structure of TNFR1, TNFR2 and their modules. A, Schematic drawing of TNFR2 (gray color) and TNFR1 (no filling). Both molecules consist of four CRDs shown as ovals labeled 1 – 4. The CRDs are followed by the stem regions as indicated at the left. The transmembrane domains (TM) are depicted as cylinders and precede the cytoplasmatic domains. Note the differences in length for the stem and TM regions between the two receptors. **B**, Schematic drawing of the A1 and B2 modules (adapted from Naismith and Sprang, 1998). The A1 and B2 modules are shown in red and blue, respectively. Disulfide bridges between cysteines are indicated by black lines. Cysteines within modules are labeled by superscript numbers.

For TNFR1 four crystal structures of the extracellular domains ($TNFR1_{ex}$) are accessible through the Protein Data Bank. Two structures are without ligand and show a dimerized $TNFR1_{ex}$ either with a parallel organization (head-to-head) found at pH 7.5 (Naismith et al., 1995) or with a completely overlapping anti-parallel organization (head-to-tail) observed at pH 3.7 (Naismith et al., 1996b). Besides the parallel dimer an additional interaction type has been identified within the same unit cell of the pH 7.5 crystal (Naismith et al., 1995). This anti-parallel dimer of receptors forms homophilic contacts mainly between CRD2 and thus also occludes the ligand binding site as will be explained below. This interesting type of interaction will be further discussed in section 4. In addition, one $TNFR1_{ex}$ crystal structure complexed with the ligand LTα has been solved (Banner et al., 1993). Therein, the homotrimeric ligand binds to three receptor chains. All receptor-ligand contacts are formed by CRD2 and to a minor extent by CRD3 of $TNFR1_{ex}$ (Banner et al., 1993). Therefore, all anti-parallel crystal structures cannot bind to ligand. Homology modeling showed that the

interactions of TNFR1 and -2 with TNF (Fu et al., 1995) are likely to be similar to these observed within the LTα complex. The fourth available crystal structure of $TNFR1_{ex}$ was determined in complex with a small chemical inhibitor of TNF binding (Carter et al., 2001). However, this structure will not be further considered as there again two $TNFR1_{ex}$ molecules formed a parallel dimer identical to that reported by Naismith and colleagues (Naismith et al., 1995). The four CRDs of TNFR1 and TNFR2 are separated from their transmembrane domains by a stretch of amino acid residues termed the stem region (Fig. 1A).

Since the seminal report of the LTα-TNFR1 structure by the Basel-based group of Werner Lesslauer it had been widely accepted that signaling emanates from ligand-induced trimerization of TNFRs. However, microscopical and biochemical data show that upon ligation, large aggregates of TNF and TNFRs are formed at 37°C (Krippner-Heidenreich et al., 2002). Similar observations have been made for the Fas system (Algeciras-Schimnich et al., 2002). Therein, the observed aggregates were subsequently termed signaling protein oligomerization transduction structures, or simply SPOTS (Siegel et al., 2004). The understanding of how such clusters within the TNF(R)SF are made and what they look like on the structural level could be of great therapeutic use.

1.8 Aim of the work

The aim of this work was to characterize extracellular molecular components of TNFR1 that are required for efficient ligand binding, the formation of ligand-receptor clusters and efficient signaling. In more detail, the work focuses on the roles of the N-terminal CRD1 of TNFR1 and of TNFR2 as well as on the stem and transmembrane regions of these two receptors.

2. Materials and Methods

2.1 Materials

2.1.1 Chemicals and reagents	
Acetonitrile	Carl Roth GmbH & Co., Karlsruhe
Acrylamide (Rotiphorese^{R} Gel 30)	Carl Roth GmbH & Co., Karlsruhe
Agarose	Carl Roth GmbH & Co., Karlsruhe
Ampicillin (Amp)	Sigma, Steinheim
Aprotinin	Sigma, Steinheim
Ammonium persulfate (APS)	Carl Roth GmbH & Co., Karlsruhe
Beta-mercaptoethanol (βME)	Sigma, Steinheim
Biotin	Invitrogen
Bradford reagent	Bio-Rad, München
Blasticidin S	Invitrogen
Bovine Serum Albumin (BSA)	Sigma-Aldrich Chemie GmbH
Bradford protein reagent	Carl Roth GmbH & Co., Karlsruhe
Blotting-paper, 3MM	Whatman International, England
Bromphenol blue	Serva, Heidelberg
Cell culture flasks and dishes	Greiner, Frickenhausen
Cell culture glass bottom dishes (microscopy)	Mattek Corporation, USA
Cobalt(II)-chloride	Merck, Darmstadt
Cytochrome *c*	Sigma-Aldrich Chemie GmbH
Crystal violet	Merck, Darmstadt
Di-butyl phtalat (scatchard oil 1)	Sigma-Aldrich Chemie GmbH
Di-octyl phtalat (scatchard oil 2)	Sigma-Aldrich Chemie GmbH
Dimethylsulfoxide (DMSO)	Carl Roth GmbH & Co., Karlsruhe
DMEM (4.5 g/l glucose, + L-glutamine)	Invitrogen (Gibco®)
DNA size standards	Gibco Life Technol. GmbH, Karlsruhe
Ethylene di-amine tetra-acetic acid (EDTA)	Sigma-Aldrich Chemie GmbH
Electroporation cuvettes, 4 mm (*Pichia*)	Equibio, Peqlab Biotechnologie GmbH
Eosine	Merck, Darmstadt
Fetal Calf Serum (FCS) Standard quality, EU approved	PAA Laboratories GmbH, Austria
Hygromycin A	Invitrogen
Imidazol	Amersham (GE Healthcare)
Iodine-125 ($Na^{125}I$)	Amersham (GE Healthcare)

MES (2-N-morpholino-ethansulfonic acid)	Carl Roth GmbH & Co., Karlsruhe
Methanol	Carl Roth GmbH & Co., Karlsruhe
Milk powder, non-fat	Applichem
Nitrocellulose	Pall Life Sciences, USA
OptiMEM®	Invitrogen (Gibco®)
PD10 column	GE Healthcare
Phenylmethylsulphonyl fluoride (PMSF)	Sigma-Aldrich Chemie GmbH
Poly-L-lysine (10x)	Sigma-Aldrich Chemie GmbH
Protease inhibitor cocktail tablets	Roche
Prestained protein marker	New England Biolabs, Frankfurt
Protein marker, unstained (PageRuler^{TM})	Fermentas
Protein marker, unstained, (High Mark^{TM})	Invitrogen
Puromycin A	Calbiochem, San Francisco, USA
Radio-Immuno-Assay (RIA) tubes	Sarstedt AG, Nümbrecht
RPMI 1640 (+ L-glutamine)	Invitrogen (Gibco®)
Scatchard centrifugation tubes (Micro tube 0.3 ml)	Sarstedt AG, Nümbrecht
Sinapinic acid (3,5-dimethoxy-4-hydroxycinnamic acid)	Sigma-Aldrich Chemie GmbH
Sodium azide (NaN_3)	Sigma-Aldrich Chemie GmbH, Deisenhofen
Sodiumdisulfite ($Na_2S_2O_5$)	Merck, Darmstadt, #6528
Sodiumiodide (NaI)	Merck, Darmstadt, #6523
Sorbitol	Carl Roth GmbH & Co., Karlsruhe
Talon® Superflow metal affinity resin	Clontech
TEMED (N,N,N´,N´-tetramethylethyl-diamine)	Sigma-Aldrich Chemie GmbH
Tetracycline hydroxide	Calbiochem, San Francisco, USA
Tris	Carl Roth GmbH & Co., Karlsruhe
Triton X-100	Merck, Darmstadt
Tween-20	Merck, Darmstadt
Trypsin/EDTA (10 x solution)	Invitrogen
Yeast extract	Carl Roth GmbH & Co., Karlsruhe
Yeast nitrogen base (YNB) without amino acids and ammonium sulphate	Difco^{TM} (Becton and Dickinson)
Whatman paper (3 mm)	Whatman Intl., Great Britain
Zeocin	Invitrogen
zVADfmk	Bachem, Germany

2.1.2 Cell culture media and reagents	
HEK293 Flp-In T-REx selection medium	DMEM + 10% FCS + 15 μg/ml blasticidin + 100 μg/ml hygromycin
MEF culture medium	RPMI 1640 + 5% FCS
MEF selection medium	RPMI 1640, 5% FCS, 2.5 μg/ml puromycin
HEK293 transfection medium	OptiMEM® (Invitrogen)
Trypsin/EDTA (in PBS) 0.5 mg/ml Trypsin, 0.2 mg/ml EDTA	Invitrogen
FCS + DMSO (cryo-conservation)	90% (v/v) FCS, 10% (v/v) DMSO
LB-medium (*E. coli*)	0.5% (w/v) yeast extract, 1% (w/v) trypton, 1% (w/v) NaCl, pH 7.0
LB-medium/low salt (*E. coli*)	0.5% (w/v) yeast extract, 1% (w/v) trypton, 0.5% (w/v) NaCl, pH 7.5
LB^{Amp} medium (*E. coli*)	LB-medium + 100 µg/ml ampicillin
LB^{Zeo} medium (*E. coli*)	LB-medium/low salt + 25 µg/ml zeocin
LB^{Amp}-agar plates (*E. coli*)	LB-medium + 1.5% (w/v) agarose, 100 µg/ml ampicillin
LB^{Zeo}-agar plates (*E. coli*)	LB-medium/low salt + 1.5% (w/v) agarose + 25 µg/ml zeocin
SOC++ (*E. coli*)	2% trypton, 0.5% yeast extract, 10 mM NaCl, 2.5 mM KCl, 20 mM glucose, 10 mM $MgCl_2$, pH 7.0
YPG^{Zeo} medium (*Pichia*)	1% (w/v) yeast extract, 2% (w/v) peptone, 2% (w/v) glucose, 100 μg/ml zeocin, pH 7.0
YPG^{Zeo} agar plates (*Pichia*)	YPG^{Zeo} medium + 2% agar (w/v)
$YPGS^{Zeo}$ agar plates (*Pichia*)	YPG^{Zeo} medium + 2% agar (w/v) + 18.2% (w/v) sorbitol
BMGY medium (*Pichia*) buffered complex medium containing glycerol	1% yeast extract, 2% peptone, 100 mM potassium phosphate (pH 6.0), 1.34% yeast nitrogen base, 4 x 10^{-5}% biotin, 1% glycerol
BMMY medium (*Pichia*) buffered complex medium containing methanol	1% yeast extract, 2% peptone, 100 mM potassium phosphate (pH 6.0), 1.34% yeast nitrogen base, 4 x 10^{-5}% biotin, 0.5% methanol

2.1.3 Buffers and solutions	
Crystal violet solution (cytotoxicity assay)	0.5% (w/v) crystal violet, 20% (v/v) MeOH
DNA sample buffer (6 x fold)	0.25% (w/v) bromphenol blue, 0.25% (w/v) xylencyanol, 30% (v/v) glycerol
Blocking buffer (Western blotting)	PBS, 0.01% (v/v) Tween-20, 10% (w/v) nonfat milk powder
Buffer A (solubisation buffer)	20 mM Tris/HCl pH 7.4, 150 mM NaCl, 1% TritonX-100
Buffer EL (elution buffer)	50 mM Na/H-PO_4, 300 mM NaCl, 100 mM imidazol, pH 6.4
Buffer EQ (equilibration buffer)	50 mM Na/H-PO_4, pH 7.50
Buffer W (washing buffer)	50 mM Na/H-PO_4 + 300 mM NaCl, pH 7.05
PBS	2.67 mM KCl, 1,47 mM KH_2HPO_4, 137.9 mM NaCl, 8.06 mM Na_2HPO_4, pH 7.2
PBS-T (Western Blotting)	0.05% (v/v) Tween-20 in PBS, pH 7.2
PBS-T/B/A (primary antibody buffer during western blotting)	PBS-T + 0.025% (v/v) BSA + 0.02% (v/v) NaN_3
PBA (FACS buffer)	PBS + 0.025% (v/v) BSA, 0.02% (v/v) NaN_3, pH 7.2
PBS/B (radioactive labeling / gel filtration)	PBS + 5 % (m/v) BSA
PFA (Scatchard buffer)	PBS + 2% FCS + 0.02% (v/v) NaN_3
Ponceau S	0.1% (w/v) ponceau red in 5% (w/v) sodium acetate
MS-solution1 (mass spectroscopy)	Acetonitril in ddH_20 (9:1 v/v) + 20 mg/ml sinapinic acid
MS-solution2 (mass spectroscopy)	Acetonitril : 0.1% trifluoracetic acid (1:3 v/v) + 20 mg/ml sinapinic acid
MES buffer (IMAC regeneration)	20 mM 2-(N-morpholine)-ethanesulfonic acid (MES), pH 5.0
Radioactive labeling reaction buffer	Na/H-PO_3, pH 7.4
SDS-sample buffer (4x)	40 mM Tris/HCl, pH 8.0, 0.4 mM EDTA, 140 mM SDS, 4.4 M glycine, 0.4% (w/v) bromphenol blue (20% (v/v) β-ME added fresh)
SDS-PAGE electrophoresis running buffer (1x)	50 mM Tris/HCl, 380 mM glycine, 4 mM SDS, pH 8.3

Separating gel SDS buffer (4 x fold)	375 mM Tris/HCl, pH 8.8, 3.75 mM SDS
Stacking gel SDS buffer (4 x fold)	125 mM Tris/HCl, pH 6.8, 3.75 mM SDS
Scatchard oil mixture	53% di-butylphtalate + 47% di-octylphtalate (v/v)
Transfer buffer (Western blotting)	192 mM glycine, 25 mM Tris, 20% (v/v) methanol, pH 8.3
TAE-buffer (DNA-agarose gels)	40 mM Tris, pH 8.3, 0.11% (v/v) Acetate, 50 mM EDTA

2.1.4 Kits	
NucleoBond® AX PC100 (DNA extraction from *E. coli* cultures)	Macherey-Nagel, Düren
NucleoSpin® Extract II (DNA extraction from agarose)	Macherey-Nagel, Düren
Lipofectamine™	Invitrogen
IL-8 ELISA kit (BD OptEIA™)	BD Biosciences
Protein Silver Staining Kit	Amersham Biosciences
TransIT® 293	Mirus Bio Corporation
Super Signal® West Dura ECL Substrate	Pierce, Rockford/Illinois, USA

2.1.5 Proteins

Recombinant human soluble TNF ($2x10^7$ U/mg) was provided by Knoll AG (Ludwigshafen, Germany). The cloning, recombinant expression and purification of CysTNF has been described (Bryde et al., 2005). In brief, the protein was expressed in *E. coli*, purified by ion-metal affinity chromatography to homogeneity and endotoxins were removed (Endotrap). Soluble TNFR1 (TNFR1ex; aa Leu_1 – Cys_{162} of the mature protein with an additional Arg and Leu residues at the C-terminus) and full-length TNFR2 were purified from a baculoviral expression system (Moosmayer et al., 1996). The TNFR2-Fc protein (Enbrel®) was from Wyeth.

2.1.6 Enzymes

DNA-modifying enzymes (T4 DNA-ligase, T4 polynucleotide kinase, calf intestinal alkaline phosphatase (CIAP), DNA polymerase I large fragment (Klenow) and restriction endonucleases) were from New England Biolabs. For cloning-PCR, the *Pfu* DNA polymerase was used (Promega) and for colony-PCR of *Pichia* clones Taq polymerase (Gibco) was used. Factor Xa protease was obtained from Boehringer Mannheim.

2.1.7 Antibodies	
anti-huTNFR1 (mouse; clone mAb225; FACS)	R&D
anti-huTNFR1 (mouse; clone H398; FACS)	IZI, University of Stuttgart
anti-huTNFR2 (mouse; clone 80M2; FACS and cytotoxicity assay)	IZI, University of Stuttgart
anti-huTNFR2 (rabbit; polyclonal; HP9003s-3720A09; FACS)	Hbt HyCult, The Netherlands
anti-huTNFR2 (rabbit; M80 serum; FACS)	IZI, University of Stuttgart
anti-huTNFR2 (mouse; clone MR2-1; FACS)	Hbt HyCult, The Netherlands
anti-huCD95/Fas (mouse; clone CH-11; FACS)	Beckman Coulter
anti-mouse IgG + IgM FITC (goat; FACS)	Dianova
anti-rabbit FITC (mouse; FACS)	Dianova
anti-huTNFR1 (mouse; clone H5; Western blot)	Santa Cruz Biotechnology
anti-hu cytoplasmatic Fas (mouse; clone B10; Western blot)	Santa Cruz Biotechnology
anti-huTNFR2 (goat; Western Blot)	R&D
anti-myc (mouse; clone 9E10; Western blot)	IZI, University of Stuttgart
anti-huTNF (mouse; clone T3; Western blot)	IZI, University of Stuttgart
anti-mouse-IgG HRP (goat; Western blot)	Dianova
anti-goat-IgG HPR (bovine, sc-2350; Western blot)	Santa Cruz Biotechnology

2.2. Methods

2.2.1 Molecular biochemistry – Polymerase chain reaction (PCR), DNA phosphorylation, DNA de-phosphorylation, fill-in reaction and restriction endonuclease treatment were performed as recommended by the supplier of corresponding enzymes. For the amplification of DNA fragments by PCR usually a gradient of annealing temperatures was applied (MasterCycler Gradient, Eppendorf).

2.2.2 Transformation of *E. coli* – Chemically competent bacterial cells (*E.coli* XL1 Blue (Stratagene), or DH5α (Invitrogen) were stored as 50 µl aliquots at -80°C. Cells were unthawed on ice and incubated for 20 min. on ice with the DNA (300 ng) of interest. Heat

shock was performed by placing cells into a water bath of 37°C for 30 sec. and followed by incubation for 1 min. on ice. SOC++ medium (950 μl) was added and cells were allowed to grow 1h at 37°C followed by plating on LB agar plates containing the appropriate antibiotics (100 μg/ml ampicillin or 25 μg/ml zeocin).

2.2.3 Propagation of Vectors in *E. coli* – Cells were transformed with vectors as described and one clone was used to inoculate 1.2 ml cultures of LB^{Amp} or LB^{Zeo}. The pre-culture was then used as an inoculum for an over night culture (125 ml LB^{Amp} or LB^{Zeo} medium) at 37°C. Cells were harvested by centrifugation and circular DNA was extracted with a commercial kit (Midiprep kit 100, Nucleobond). Vectors were checked for purity and concentration by measuring the absorption in 1 cm cuvettes (UVette, Eppendorf) at 260 nm and 280 nm with a spectrometer (Eppendorf). Restriction endonuclease treatment and agarose gel electrophoresis were used to assure the correctness of isolated vectors.

2.2.4 Tissue culture – Mouse embryonic fibroblasts (MEF (-/-)(-/-), MEF TNFR1-Fas, MEF TNFR2-Fas, MEF $\Delta A1_{CRD1}$-TNFR1-Fas, MEF $CRD1_{TNFR2}$-TNFR1-Fas, MEF ΔCRD1-TNFR1-Fas, MEF ΔCRD1-TNFR2-Fas, MEF TNFR1-$(S/TM)_{TNFR2}$-Fas and MEF TNFR2-$(S/TM)_{TNFR1}$-Fas) were cultured in RPMI + 5% FCS. HEK293 Flp-In T-REx cells (TNFR1-Fas, $\Delta A1_{CRD1}$-TNFR1-Fas and ΔCRD1-TNFR1-Fas) were cultured in DMEM (4.5 g/l glucose, with glutamine) + 10% FCS + 15 μg/ml blasticidin + 100 μg/ml hygromycin. Kym-1 cells were cultured in RPMI + 10% FCS. All cell lines were incubated at 37°C with a 5% CO_2 atmosphere. Cells were not allowed to grow further than 90% confluency, as it was observed to reduce the cell-surface expression of chimeric TNFR-Fas receptors on MEF cells. Kym-1 cells were cultured in RPMI + 10% FCS.

2.2.5 Transfection of MEFs – Mouse embryonic fibroblasts were transfected with the Lipofectamine™ Plus (Invitrogen) method. The day prior to transfection 2 x 10^5 cells per well were seeded in 6-well plates. The following day, DNA (2.5 µg) was diluted with 100 µl of RPMI and 20 µl of PLUS reagent were added. Parallel, 5 µl of the Lipofectamine reagent were added to 100 µl RPMI and both solutions were incubated for 15 minutes at RT, before they were mixed and incubated for another 15 minutes at RT. The medium of cells was replaced with 1 ml of RPMI (w/o FCS) prior to addition of the transfection mixture. Cells were placed in the incubator and the transfection mixture was replaced with RPMI + 5% FCS after 3 hours of incubation.

2.2.6 Transfection of HEK cells – HEK293 cells (3 x 10^5 cells/well) were seeded over night into 6-well plates in DMEM + 10% FCS. The following day, medium was replaced with OptiMEM® medium (600 µl) and cells were transfected with a TNFR1-GFP expression construct (500 µg DNA/well; internal number #250) using the *Trans*It®-293 system (Mirus Bio). Therefore, 100 µl OptiMEM® were mixed with 6 µl *Trans*It, vortexed and incubated 5 min. at RT. DNA was added and after a further incubation time of 15 min. at RT the solution was transferred onto the cells. After three hours at 37°C, the medium was replaced with fresh medium containing 20 µM of zVADfmk to prevent cell death due to ligand-independent TNFR1 signaling. The following day, cells were used for chemical crosslinking as described in the corresponding section.

For the generation of stable cell lines, HEK293 Flp-In T-REx cells ($2x10^6$) were grown in 10 cm petridishes over night and co-transfected in a 1:10 ratio with pcDNA5/FRT/TO (1 µg DNA encoding for the different TNFR1-Fas constructs #358, #359 or #361) and the pOG44 vector (9 µg DNA encoding the Flp recombinase). Therefore, for one dish 500 µl OptiMEM® were mixed with 25 µl *Trans*It and 10 µg DNA as described above and transferred onto cells.

2.2.7 Generation of stably expressing Mouse Fibroblast cell lines – Simian virus 40 large T-immortalized mouse fibroblasts have been generated from TNFR1 and TNFR2 double knockout mice and were generously supplied by Daniela Männel (University of Regensburg, Germany). The generation of cell lines expressing TNFR1-Fas or TNFR2-Fas has been described (Krippner-Heidenreich et al., 2002) and further MEF cell lines used here were produced accordingly.

Therefore, the coding sequences for ΔA1-TNFR1-Fas, ΔCRD1-TNFR1-Fas or ΔCRD1-TNFR2-Fas were created by PCR and the used oligonucleotides are listed below in Table 2 “Primers”. The pEFpgkpuroA-based expression vectors encoding full length TNFR1-Fas (number #113) or TNFR2-Fas (number #114) were used as templates to generate the N-terminal deletion mutants $\Delta A1_{CRD1}$-TNFR1-Fas, ΔCRD1-TNFR1-Fas or ΔCRD1-TNFR2-Fas. First, oligonucleotides (signal $sequence_{sense/antisense}$) comprising the secretory signal sequence from mus musculus immunoglobulin heavy chain (VDJ-region; NCBI CoreNucleotide database-ID 195747) were annealed, phosphorylated and ligated with the vector pCDNA3.1 previously treated with BamHI/EcoRI yielding pCDNA3.1-Ig-signal (number #254). The Ig heavy chain signal sequence was used to replace the endogenous secretion signals of TNFR1 or TNFR2. Second, sequences encoding $\Delta A1_{CRD1}$-TNFR1-Fas (lacking aa Leu_1-Cys_{29} of huTNFR1, adding N-terminal the residues Asp and Val), ΔCRD1-TNFR1-Fas (lacking aa Leu_1-Arg_{53} of huTNFR1) or ΔCRD1-TNFR2-Fas (lacking aa Leu_1-Cys_{53} of huTNFR2) were amplified by PCR (primer pairs $\Delta A1_{for}$/$huFas_{rev}$, $\Delta PLADR1_{for}$/$huFas_{rev}$ and $\Delta PLADR2_{for}$/$huFas_{rev}$ respectively) and cloned in-frame to the pCDNA3.1 based

immunoglobulin heavy chain secretory signal sequence using EcoRI/XbaI sites. The resulting vectors, pCDNA3.1 Ig signal- $\Delta A1_{CRD1}$-TNFR1-Fas (number #311), -ΔCRD1-TNFR1-Fas (number #255) and -ΔCRD1-TNFR2-Fas (number #256) were sequenced and sub-cloned via BamHI/XbaI sites into the expression vector pEFpgkpuroA. The yielded constructs were pEFpgkpuroA $\Delta A1_{CRD1}$-TNFR1-Fas (number #312), ΔCRD1-TNFR1-Fas (number #259) or ΔCRD1-TNFR2-Fas (number #260). Parental MEFs were transfected, selected with puromycin A (2.5 μg/ml), sorted with a FACS and yielded MEF $\Delta A1_{CRD1}$-TNFR1-Fas, MEF ΔCRD1-TNFR1-Fas or MEF ΔCRD1-TNFR2-Fas.

The CRD1 exchange mutant ($CRD1_{TNFR2}$-TNFR1-Fas) has been generated by Sylvia Willi (University of Stuttgart) and the detailed construction is described elsewhere (Branschaedel et. al, manuscript in preparation). In brief, the coding sequence of CRD1 of TNFR2 was amplified by PCR and was used to replace the CRD1 of TNFR1 with that of TNFR2. Site directed mutagenesis was used to introduce a glutamate (E) at the fusion site of $CRD1_{TNFR2}$ (TVCD) and $CRD2_{TNFR1}$ (TVCDECESGS). The generation of stem- and transmembrane exchange mutants TNFR1-$(S/TM)_{TNFR2}$-Fas and TNFR2-$(S/TM)_{TNFR1}$-Fas is described elsewhere (Messerschmidt, 2006).

Name	**Nucleotide sequence (5' → 3')**
signal $sequence_{sense}$	GAT CCG CCA CCA TGA AAT GCA GCT GGG TTA TGT TCT TCC TGA TGG CAG TGG TTA CAG GGG TG
signal $sequence_{antisense}$	AAT TCA CCC CTG TAA CCA CTG CCA TCA GGA AGA ACA TAA CCC ACC TGC ATT TCA TGG TGG CG
$\Delta A1_{for}$	CAG TGA ATT CAG ATG TCT GTA CCA AGT GCC A
$\Delta PLADR1_{for}$	AGT GAA TTC CAG GGA GTG TGA GA
$\Delta PLADR2_{for}$	AGT GAA TTC TGA CTC CTG TGA GGA
$huFas_{reverse}$	CTA GTC TAG ACT AGA CCA AGC TTT
$PLAD1_{for}$	TAT GAA TTC CTG GTC CCT CAC CTA
$PLAD1_{rev}$	ATA TAG CGG CCG CTC TAC CTT CAA TAG CAC CCT CTC TGC AGT CCG T
$PLAD2_{for}$	ACG GAA TTC TTG CCA GCC CAG GTG
$PLAD2_{rev}$	ATA TAG CGG CCG CTC TAC CTT CAA TAG CAC CAG AGT CAC ACA CGG TG
5´ *Pichia* primer	GAC TGG TTC CAA TTG ACA AGC
3´ *Pichia* primer	GCA AAT GGC ATT CTG ACA TCC

Table 2, Primers: List of used oligonucleotides with corresponding nucleotide sequences. Forward, for; reverse, rev.

2.2.8 Generation of stable and inducible HEK293 cell lines – Stable and doxycycline-inducible HEK293 cell lines expressing TNFR1-Fas and the N-terminal deletion mutants thereof were generated using the Flp-In T-REx system (Invitrogen). Therefore, the coding

sequences for $\Delta A1_{CRD1}$-, ΔCRD1- or full length TNFR1-Fas were ligated into the inducible expression vector pcDNA5/FRT/TO in three steps. First, the pEFpgkpuroA-based expression vectors (DNA numbers #312, #259 and #113, respectively) were linearized by treatment with XbaI, followed by a fill-in reaction to create a "blunt" end. The coding sequences were then liberated by treatment with BamHI, separated from empty pEFpgkpuroA vector by agarose gel electrophoresis and fragments were extracted (NucleoSpin®). Second, the pCDNA5/FRT/TO vector (DNA number #357) was treated with the enzymes BamHI and EcoRV, purified by agarose gel electrophoresis, extracted (NucleoSpin®), de-phosphorylated and purified again (NucleoSpin®). Third, the inserts were finally ligated into pCDNA5/FRT/TO to generate constructs for TNFR1-Fas (#358), $\Delta A1_{CRDD1}$-TNFR1-Fas (#361), and ΔCRD1-TNFR1-Fas (#359). All expression vectors were verified by sequencing (MWG) using the CMV-forward priming site. The constructs were transfected into HEK293 Flp-In T-REx cells and after two days, a selective medium containing 15 μg/ml blasticidin S and 100 μg/ml hygromycin B was applied and replaced every 5-6 days. Typically, five to ten isogenic clones were obtained per plate.

2.2.9 Cell death assay – Mouse fibroblasts were analyzed with the crystal violet assay. Cells (1×10^4 cells/well) were seeded in 96-well flat-bottom plates and treated as indicated with reagents (sTNF, CysTNF, antibodies) 6 h later. The next day cells were stained by crystal violet (20% methanol, 0.5% crystal violet) for 15 min. The plates were gently washed under the water tap, air-dried, dissolved (100 μl methanol / well) and optical density was determined at 550 nm with an ELISA plate reader (SPECTRAmax 340PC, Molecular Devices Corp., Sunnyvale, CA).

2.2.10 Light microscopy – HEK293 Flp-In T-REx cells (3×10^5 cells/well) were grown over night in a six-well plate and were induced the following day by addition of doxycycline (4 ng/ml) for 18h in the presence or absence of 20 μM zVADfmk. Cells were cultured and pictures were taken at 10x magnification with a light microscope (Leitz DM-IRB, Leica Germany) coupled to digital camera (AxioCam, Carl Zeiss, Germany).

2.2.11 Confocal microscopy – HEK293 Flp-In T-REx cells (3×10^5 cells/well) were seeded over night in microscopy plates (Mattek) that were pre-coated with poly-L-lysine (Invitrogen) as described by the manufacturer. Cells were induced over night with 4 ng/ml doxycycline in the presence of 20 μM zVADfmk. Staining was performed by incubation with 0.5 ml medium containing 2 μg/ml of Alexa-546 coupled TNF for 4 minutes on ice. Then 2.5 ml medium were added and dishes were placed into a temperature-controlled chamber (37°C, 5% CO_2) and analyzed by live imaging using confocal laserscanning microscopy (Leica TCS SL).

2.2.12 Immuno-staining and flow cytometry – Cells ($5x10^5$) were harvested by trypsinisation, washed once with PBS and stained one hour on ice with antibodies (2.5 μg/ml in PBA buffer) specific for TNFR1 (mAb225 or H398) or TNFR2 (hbt-pAb, M80-serum or 80M2). Cells were washed once with ice-cold PBA, incubated for 45 min. on ice with 3.75 μg/ml secondary FITC-labeled antibodies specific for goat or mouse (Dianova, Germany), washed again and analyzed by flow cytometry (EPICS, Backman Coulter). For the FACS-sorting of mouse embryonic fibroblasts (FACSDiva, Becton Dickinson), cells were pre-incubated for one hour with the caspase inhibitor zVADfmk (20 μM) before harvesting and immuno-staining. Typically, 20,000 cells were sorted into 2.5 ml RPMI + 5% FCS + 20 μM zVADfmk.

2.2.13 IL-8 ELISA – HEK293 Flp-In T-REx cells ($1x10^4$ cells/well) were seeded into 96-well tissue culture plates and the following day expression of chimeric receptors was induced for 18 h by incubation with 4 ng/ml doxycycline. The next day, cells were stimulated with TNF as indicated. In each step, cells were treated with 20 μM zVAD-fmk. Supernatants were collected 24 h later and tested for IL-8 with the BD OptEIA™ human IL-8 ELISA kit (Becton and Dickinson). ELISA plates were measured with an ELISA reader (SPECTRAmax 340PC, Molecular Devices Corp., Sunnyvale, CA) at OD_{405nm}.

2.2.14 Chemical crosslinking – Mouse fibroblasts expressing TNFR1-Fas (3×10^5 cells/well) were grown over night in 6-well tissue culture plates. The next day cells were washed on ice with PBS and then incubated for 30 minutes with varying concentrations of the NH_2-reactive crosslinker bis-(sulfosuccinimidyl)-suberate, BS^3 (Perbio). The crosslinker was prepared freshly for each experiment. The reaction was stopped by the addition of 10 mM Tris/HCl pH 7.0. Cells were scraped off and pellets were lysed in buffer A, supplemented with protease inhibitors (Roche). Soluble protein content was determined with the Bradford reagent (Biorad). To equalize cell surface expressed receptors loaded protein amounts used were adjusted to FACS analyses performed in parallel for corresponding cells. Proteins were boiled in SDS sample buffer with 10% (v/v) ß-mercaptoethanol and subjected to SDS-PAGE and Western Blot analysis.

For the crosslinking of purified proteins, TNF (2 μg/lane), soluble $TNFR1_{ex}$ (600 ng/lane), full-length TNFR2 (560 ng/lane) and the CRD1 from TNFR2 ($CRD1_{TNFR2}$; 1.5 μg/lane) were incubated in 20 μl PBS with increasing concentrations (0 – 500 μM) of BS^3 for 30 min. on ice. Samples were quenched and subjected to reducing SDS-PAGE and Western Blotting as described above.

2.2.15 Western Blotting – Samples (maximal 100 μg protein/lane of cell lysate) were resolved by Tris/glycin SDS-PAGE using a vertical, water-cooled electrophoresis system (Owl, Portsmouth, NH). Proteins were transferred onto nitrocellulose membranes (Pall, Pensacola, FL) for 90 min. at 1.5 mA / cm^2. Membranes were incubated for one hour at RT with blocking buffer (PBS, 10% (w/v) nonfat milk powder, 0.01% (v/v) Tween-20). Proteins were detected by incubation over night at 4°C with specific monoclonal antibodies for $TNFR1_{ex}$ (H5, Santa Cruz Biotechnology), Fas (B10, Santa Cruz Biotechnology), TNFR2 (gt anti-TNFR2, R&D) and TNF (clone T3, IZI Stuttgart) respectively. Secondary antibodies were horseradish peroxidase-coupled (goat anti-mouse, Dianova or bovine anti-goat, SantaCruz). Chemiluminescence was generated by using the ECL Dura kit (Perbio). The non dye-labeled protein markers (PageRuler™ and HighMark™) were visualized by staining with 0.1% (w/v) ponceau red in 5% (w/v) sodium acetate.

2.2.16 Radioactive labeling of TNF and saturation binding experiments – Receptor-ligand affinities were determined by performing saturation binding experiments as described (Grell et al., 1998). Labeling of TNF with $Na^{125}I$ (Amersham) was done with the chloramine-T (CT) method. Therefore, 1 mCi of ^{125}I were added to 10 µg of recombinant soluble human TNF in a total volume of 70 μl with $NaPO_3$ (400 mM, pH 7.4) as the reaction buffer. The redox-reaction was started by addition of 5 µg of CT (10 μl of 0.5 mg/ml) as oxidant. After one minute, the reaction was stopped by treatment with 10 µg (10 μl of 10 mg/ml) of the reducing agent sodiumdisulfite ($Na_2S_2O_5$), given for another minute. Remaining CT or $Na_2S_2O_5$ were inactivated by incubation for 5 min. with 6.3 mg of NaI (70 μl of 90 mg/ml). Radioactively labeled TNF was then isolated using gel filtration by applying the solution onto a pre-packed Sephadex G-25M column (PD-10), pre-equilibrated with PBS/B. Ten milliliter PBS/B were used for elution and the flow-through was collected in one milliliter fractions, of which radioactivity was measured in a γ-counter (LB 2100, Berthold). Usually the ligand was present in fractions number three and four, with free ^{125}I being in fractions seven and eight. Ligand containing fractions were pooled and concentration set to 1 mg/ml with PBS/B, assuming that approximately 20 % TNF were lost during gel filtration. Typically, 20,000 - 40,000 cpm/ng were achieved. Bioactive material was determined by cell death assay on Kym-1 cells using unlabeled TNF as a reference.

Murine fibroblasts ($1x10^5$ cells/ml) or HEK293 FlpIn T-REx ($2x10^5$ cells/ml) were then incubated in PFA binding buffer for two hours on ice with varying concentrations of ^{125}I-TNF (0.25 – 25 ng/ml) in the presence or absence of a 100-fold excess of unlabeled TNF to determine nonspecific binding (NSB). The total volume was 150 μl and RIA tubes (Sarstedt) mounted on a ice-cooled, metallic 96-well plate were used to incubate cells. Cell-bound ^{125}I-TNF (TB) was determined with a γ-counter after centrifugation (20 sec., 13,000 rpm, RT) of

the cells through a phthalate oil mixture (200 µl; density was ς = 1.014) using scatchard centrifugation tubes. Specific binding was calculated by subtraction of NSB from TB and obtained data points were used for fitting a one-site binding hyperbola with the program Prism v4.00 (GraphPad Software Inc.).

2.2.17 Cloning of expression-vectors for $CRD1_{TNFR1}$ and $CRD1_{TNFR2}$ – The coding sequences for the cysteine-rich domains 1 of TNFR1 and TNFR2 were amplified by PCR using the primer pairs $PLAD1_{for/rev}$ and $PLAD2_{for/rev}$ (Table 2 'Primers'). As template blue script vectors (pBS) containing TNFR1 (internal DNA number #78) or TNFR2 (internal DNA number #79) were used. The amplified sequences of CRD1 were treated with the restriction endonucleases EcoRI and NotI, resolved by 2% agarose gel-electrophoresis, excised with a scalpel and extracted from the gel (NucleoSpin®). In parallel, the expression vector pPICZαA was cut with EcoRI/NotI, treated with calf intestine phosphatase (CIAP) and extracted as above. The vector was ligated with the CRD1 sequences over night at 4°C and transformed into *E.coli* XLI blue that were allowed to grow on LB^{Zeo} agar plates. Positive clones were expanded in LB^{Zeo} medium, vectors (pPICZαA/PLAD1, internal number #248; pPICZαA/PLAD2, internal number #249) were extracted and verified by sequencing.

2.2.18 Generation of stable *Pichia pastoris* X33 clones – Stable clones of the methylotrophic yeast *Pichia pastoris* X33 were generated as described in the Invitrogen EasySelect™ manual. In brief, yeast cells were grown in YPG medium in baffled flask at 30°C until they had reached an $OD_{600nm,\ 1cm}$ of 1.3. Cells were harvested by centrifugation and made electro-competent by washing twice with ice-cold ddH_2O and once with 1M sorbitol. Cells were finally dissolved in 250 µl of 1M sorbitol, transferred into a sterile electroporation cuvette, and were incubated 10 min. on ice with 5 µg of pPICZαA expression vectors that were in advance linearized with the endonuclease SacI to increase the recombination rate. Electroporation was performed with a twin pulse program (pulse 1: 1500 Volt, 25 µF, 201 Ω, 5 ms; pulse 2: 104 Volt, 1500 µF, 201 Ω, 302 ms) with an Easyject Plus 70–1010 electroporator (Equibio, Peqlab Biotechnologie GmbH, Erlangen). One ml sorbitol was immediately added and cells were incubated 1h at 30°C without shaking, followed by plating on $YPGS^{Zeo}$ agar plates. Typically, one to ten clones were grown on five agar plates. Clones were screened by colony PCR for positive integration and by small-scale expression (10 ml) in BMMY medium followed by SDS-PAGE and Western Blotting with a myc-specific antibody (clone 9E10).

2.2.19 PCR screening of *Pichia* clones – The gene of interest (e.g. the CRD1s of TNFR1 or TNFR2) within the pPICZαA vector is flanked by sequences (5' AOX1 and 3'AOX1) that are used for homologous recombination by *Pichia*. Primer pairs complimentary to these regions (5´ AOX1 primer and 3´ AOX1 primer; Invitrogen) can be utilized for PCR. The procedure was carried out as described in the EasySelect™ manual (Invitrogen). In brief, clones were stroked on YPG^{Zeo} agar plates and incubated for three days at 30°C. One colony was picked with a plastic tip and directly used as template with the following PCR reaction mixture and program:

Sterile water	15.5 µl
10X PCR reaction buffer (Gibco)	2.5 µl
25 mM $MgCl_2$ (Gibco)	0.75 µl
25 mM dNTPs	0.5 µl
Taq polymerase (Gibco)	0.25 µl
5´ AOX1 primer (10 pmol/µl)	0.5 µl
3´ AOX1 primer (10 pmol/µl)	0.5 µl
Total Volume	25 µl

Step		Temp.	Time
1	Denaturation	94°C	5 min.
2	Denaturation	94°C	30 sec.
3	Annealing	60°C	30 sec.
4	Extension	72°C	70 sec.
5	Goto step #2 and repeat 35x		
6	Extension	72°C	5 min.
7	Hold	4°C	

As negative control for the PCR reaction water and as positive control the pPICZαA vectors containing the coding sequences of $CRD1_{TNFR1}$ or $CRD1_{TNFR2}$ were used. DNA loading buffer was added and samples were analyzed by agarose gel electrophoresis for a band at ~700 bp (~500 bp from the vector, ~200 bp from the CRD1).

2.2.20 Expression and purification of recombinant, soluble $CRD1_{TNFR2}$ – Positive clones of the yeast *Pichia pastoris* X33 were stroked onto YPG^{Zeo} agar plates and one colony was used to inoculate 25 ml of BMGY^{Zeo} medium. Cells were grown over night (30°C, 250 rpm) to give an $OD_{600nm,1cm}$ of ~8. Cells were harvested by centrifugation and transferred into 500 ml expression medium (BMMY) to give an $OD_{600nm,1cm}$ of ~0.4 and were continued to grow in 2000 ml baffled flasks (30°C; 200 rpm) for five days. Methanol (0.5% vol/vol) was added manually every 24h. During this period the pH value usually dropped below 4 and the $OD_{600nm,1cm}$ reached a plateau at ~22. The supernatant was cleared by centrifugation (2,000 rpm, 20 min.) using 250 ml plastic flasks. The resulting S/N was sterile filtered and the pH adjusted to 7.5 by titration with 1M KOH. White salt precipitates were removed by centrifugation and filtration.

For purification by immobilized metal ion affinity chromatography (IMAC), a column (XK16, Pharmacia) was packed with 5 ml of the cobalt-loaded Talon® Superflow resin, equilibrated with 10 column volumes of buffer EQ at pH 7.5 and the supernatant was pumped onto the

column (pump P1, Pharmacia) with a flow-rate of 1 ml/min at RT. The flow-through was passed through a UV-detector (Uvicord II, Pharmacia) connected to a writer. Non-specific proteins were removed by washing with 10 column volumes (50 ml) of buffer W. Elution was done with “buffer EL” and sixteen 1 ml fractions were collected manually. The column material was cleaned with MES buffer and stored in a ddH_2O + 20% (v/v) ethanol at 4°C. Eluted protein samples were tested for $CRD1_{TNFR2}$ by performing Western Blot analysis with a myc-specific antibody (clone 9E10). Positive fractions (usually fractions 6 - 14) were pooled and protein purity and concentration (usually ~100 μg/ml, total protein 0.8 mg) were checked by silver gel and serial dilutions of cytochrome *c* as a standard. Proteins were dialyzed against PBS containing 2.5% glycerol (vol/vol). The myc-his-tag was removed by incubation with Factor Xa for 2h at RT (1U per 100 μg protein) and the reaction was stopped with 1 mM of the protease inhibitor PMSF. The solution was dialyzed again for 24h against PBS, sterile filtered and stored at -80°C in aliquots. The cleaved product was again checked by silver-gel, HPLC and mass spectrometry for purity, size and concentration.

2.2.21 Mass Spectrometry – The purified, Factor Xa-cleaved $CRD1_{TNFR2}$ (400 ng protein) or sTNF were first de-salted by repeated ultrafiltration (MWCO 5,000 Da; Millipore) and dilution with ultrapure water (resistance ~18 MΩ). A gold-carrier in 96-well format was prepared by first rinsing with 2-propanol, second sonification in a bath of ultrapure water and third drying under nitrogen gas. For the embedding of the protein samples, 0.5 μl of MS-solution1 were applied onto the gold-layer, air-dried and overlaid with 1 μl of a 1:1 (vol/vol) mixture of salt-free protein in MS-solution2. The samples were air-dried and analyzed by mass spectrometry (Ultraflex II TOF/TOF, Bruker) using the time-of flight modus with both flight tubes connected to one. The spectrometer was externally calibrated with protein standards (Calibration starter kit, Standard No. 1, Bruker).

2.2.22 High performance liquid chromatography (HPLC) – The $CRD1_{TNFR2}$ (400 ng protein; 7.1 μM) was injected into a sample loop of 20 μl volume with a glass syringe (Hamilton). Proteins were separated with a BioSep-SEC-S 2000 column (300 x 7.8 mm; Phenomenex) coupled to a Waters 486 UV-detector (Millipore). As mobile phases, PBS or PBS + 1M NaCl were used. The flow rate was 1 ml/min and size standards used were thyroglobulin (669 kDa), apoferritin (443 kDa), β-amylase (200 kDa), BSA (66 kDa), carbonic anhydrase (29 kDa), cytochrome *c* (12.4 kDa) and aprotinin (6.5 kDa).

2.2.23 Structural data manipulation and analysis – The superimposition of TNFR1 crystal structures obtained with ligand (Banner et al., 1993) and without ligand (parallel dimer) at pH 7.5 (Naismith et al., 1995; Naismith et al., 1996a; Naismith et al., 1996b) was performed with the program Visual Molecular Dynamics (VMD) (Humphrey et al., 1996). The arguments used for this operation were typed in the TK console and are given below:

Load 1NCF.pdb file for $[TNFR1]_2$		The Molecule-ID in the Main VMD window shall be called “0”
Load pdb file for homotrimeric LTα bound to $[TNFR]_3$		The Molecule-ID in the Main VMD window shall be called “1”

Input	**Reply of the Tk console**	**Remark**
set dimer [atomselect 0 "chain A and resid 30 to 143 and backbone"]	atomselect0	Definition of a variable named “dimer” with a selection of coordinates from the molecule with the ID “0”
$dimer num	456	The number of atoms in the variable named “dimer” are replied
set trimer [atomselect 1 "segname R1 and resid 30 to 143 and backbone"]	atomselect1	
$trimer num	456	
set matrix [measure fit $dimer $trimer]	{-0.43745419383 0.864523530006 -0.247452676296 48.7688598633} {0.897764503956 0.435636848211 -0.0651128068566 -14.0403432846} {0.0515078417957 -0.250638246536 -0.9667096138 91.8691253662} {0.0 0.0 0.0 1.0}	Definition of the rotational/ translational matrix to move the receptor chain A (dimeric structure) onto the receptor chain R1 (LTα-TNFR complex)
atomselect 0 all	atomselect3	Selection of all atoms within the dimeric TNFR1 structure
Atomselect3 move $matrix		Movement of both TNFR1 chains within the dimeric TNFR structure
set dimer [atomselect 0 "chain B and resid 30 to 143 and backbone"]	atomselect4	New definition of the variable “dimer”; note that the second receptor molecule (chain B) was selected
set trimer [atomselect 1 "segname R1 and resid 30 to 143 and backbone"]	atomselect5	
$trimer num	456	
$dimer num	456	
set matrix [measure fit $trimer $dimer]	{-0.759644806385 -0.0625143796206 0.647327184677 41.7915840149} {-0.276713877916 -0.869701504707 -0.408715635538 51.0996284485} {0.58853161335 -0.489602535963 0.643365561962 -1.84568870068} {0.0 0.0 0.0 1.0}	Definition of the rotational/ translational matrix to move the receptor chain R1 (LTα-$[TNFR]_3$) onto the receptor chain B (dimeric structure)
atomselect 1 all	atomselect6	Selection of all atoms within the LTα-$[TNFR1]_3$ structure
atomselect6 move $matrix		
atomselect 0 all	atomselect7	
atomselect7 writepdb “TNFR_dimer_moved.pdb”		Saves the coordinates for the moved TNFR1-dimer into a new file
atomselect 1 all	atomselect8	
atomselect8 writepdb “TNF-TNFR_trimer_moved.pdb”		

2.2.24 Determination of the angle between two LTα homotrimers –The central, horizontal axes of the LTα-TNFR1 complexes were visualized with the program VMD. Therefore, two cylinders were drawn through two calculated central points (one on the top, one on the bottom) for each LTα molecule:

draw color blue
draw cylinder {14.75 0 85.969} {6.395 0 38.247} radius 0.5
draw color red
draw cylinder {86.237 11.881 58.978} {61.565 33.652 26.623} radius 0.5

The angle between the two LTα-TNFR1 complexes was determined in two steps. First, the scalar dot product of two vectors running centrally through the LTα molecules was determined using the program VMD (arguments see below) and second, this value was used to manually calculate the inverse cosine (arccos 0.782827701726 = 38.48°).

Input	Reply of the Tk console	Remark
set v1 [vecsub {14.75 0 85.969} {6.395 0 38.247}]	8.355 0.0 47.722	Definition of a variable named "v1" for the first vector
set v2 [vecsub {86.237 11.881 58.978} {61.565 33.652 26.623}]	24.672 -21.771 32.355	Definition of a variable named "v2" for the second vector
veclength $v1	48.4478617949	Calculates the length of the vector v1
veclength $v2	46.1468311945	Calculates the length of the vector v2
set v1 [vecnorm $v1]	0.172453431183 0.0 0.985017671203	Re-defines vector v1 after it has been normalized (length = 1)
set v2 [vecnorm $v2]	0.534641260545 -0.471776705712 0.701131565538	Re-defines vector v2 after it has been normalized (length = 1)
set cosa [vecdot $v1 $v2]	0.782827701726	Returns the scalar dot product of the two vectors

2.2.25 Calculation of the electrostatic potential from the LTα-TNFR1 complex – First, the structural data of LTα-TNFR1 ((Banner et al., 1993); 1TNR.pdb) was converted into data that contained hydrogen atoms, per-atom charges and radii (*.pqr file) by using the web-based program pdb2pqr (Dolinsky et al., 2004) (utilizing the Amber99 force field and pH 7.0). Second, the *.pqr files were loaded into the program PyMol (DeLano Scientific, San Carlos, CA, USA) and the built-in Poisson–Boltzmann solver APBS (Baker et al., 2001) was used to calculate the electrostatic potential at 310K and physiological salt concentrations (0.15 M of +/-1 charged ions and 0.01 M +/-2 charged ions) and displayed as solvent accessible surfaces.

2.2.26 Production of a physical "real" model of the LTα-TNFR1 complex – The coordinates of the LTα-TNFR1 crystal structure (1TNR.pdb) (Banner et al., 1993) were used to generate a 'real' three dimensional solid. Therefore, the coordinates were loaded into the program VMD (Humphrey et al., 1996) and the molecule was displayed in surface representation modus. In brief, the surface is generated by scanning the molecule with a probe that has a defined radius (1.4 Å). The built-in rendering function of VMD was used to export the surface into the VRML format that was used to print layers of a plaster-like material to generate the three-dimensional solid. The final printing process was carried-out by 4D Concepts (Gross-Gerau, Germany).

2.2.27 Molecular Dynamics Simulation – The MD simulation has been performed in cooperation with Andrew Aird (University of Stuttgart) and is described in depth elsewhere (Branschadel et. al, manuscript in preparation). In brief, all simulations were carried out using the program NAMD2 with the CHARMM27 force field. The extracellular part of TNFR1 from the LTα-TNFR1 crystal structure (pdb entry 1TNR) was hydrated, minimized and equilibrated for 6 ns (complete extracellular domain of TNFR1). Thereof, N-terminal deletion mutants $\Delta A1_{CRD1}$-TNFR1-Fas and ΔCRD1-TNFR1-Fas were constructed and equilibrated for further 4.25 ns. During the first ns of equilibration, a harmonic constraint on the protein backbone atoms of 70 pN/Å was gradually removed to allow relaxation of the solvent molecules. The C-terminus was fixed to mimic membrane anchoring. The temperature was kept at 300 K and the pressure at 1 bar. Visualization and data analysis was done with the program VMD (Humphrey et al., 1996).

3. Results

3.1. Chapter I

3.1.1 The CRD1 is required for ligand binding

It is well established that soluble versions of members from the TNFRSF antagonize signaling. Whereas it is clear that proteins such as soluble Fas or soluble TNFR1 can competitively bind to their ligands, Fas mutants were described that lacked ligand-binding capability, yet were still antagonistic molecules (Papoff et al., 1999; Papoff et al., 1996). The membrane-distal, first of three cysteine rich domains (CRDs) was required for this Fas variant to be an antagonist. In addition, previous data showed that deletion of the CRD1 from Fas (Orlinick et al., 1997) or TNFR1 (Marsters et al., 1992) lead to a complete loss of ligand binding capability. Subsequently, the group of Michael Lenardo reported that TNFR1, TNFR2, CD40, Fas and TRAIL all homo-multimerize on the plasma-membrane already in the absence of ligand (Chan et al., 2000; Siegel et al., 2000). The region required for the homo-multimerization was shown to require the CRD1 and was termed the pre-ligand binding assembly domain (PLAD). The deletion of the membrane-distal CRD of TNFR1 (= $CRD1_{TNFR1}$) abolished the binding of fluorescently labeled TNF, as determined by FACS analyses. The authors argued that efficient ligand binding requires preassociated receptors and that the lack of receptor-trimerization due to the CRD1 deletion causes a non-binding receptor.

To analyze the effects of the CRD1 deletion in more detail, TNFR1 and TNFR2 (Fig. 1A) were fused to the intracellular parts of Fas, thus unifying the signaling pathways (Krippner-Heidenreich et al., 2002). This step was necessary since TNFR1 utilizes a plethora of intracellular signaling molecules that are partly different from that of TNFR2, not mentioning different subcellular localization of receptor-protein-complexes. In contrast to TNFR1, Fas is a rather simple molecule that leads to apoptosis via the classical formation of the death-inducing signaling complex (DISC) composed of the adapter FADD that recruits the caspase 8, as described in the introduction. From these chimeric TNFR-Fas molecules, the CRD1 of TNFR1 and the CRD1 of TNFR2 were deleted, thus creating ΔCRD1-TNFR1-Fas and ΔCRD1-TNFR2-Fas and both molecules were expressed in mouse fibroblasts derived from *tnfr1/tnfr2* deficient mice. All four chimeric molecules could be expressed on the cell surface, as determined by FACS analyses using specific antibodies for TNFR1 or TNFR2 (Fig. 2A - D). Interestingly, whereas the full-length TNFR1-Fas molecule containing CRD1-4 could be easily detected with monoclonal antibodies (mAb; mAb225, agonist; H398, antagonist), the deletion of CRD1 only allowed binding of mAb225 (Fig. 2A and B). Deleting the CRD1 of TNFR2 allowed binding of polyclonal rabbit sera (hbt, Fig. 2D; M80, not shown), but abolished binding of monoclonal antibodies (80M2, Fig. 2D; MR2-1, not shown).

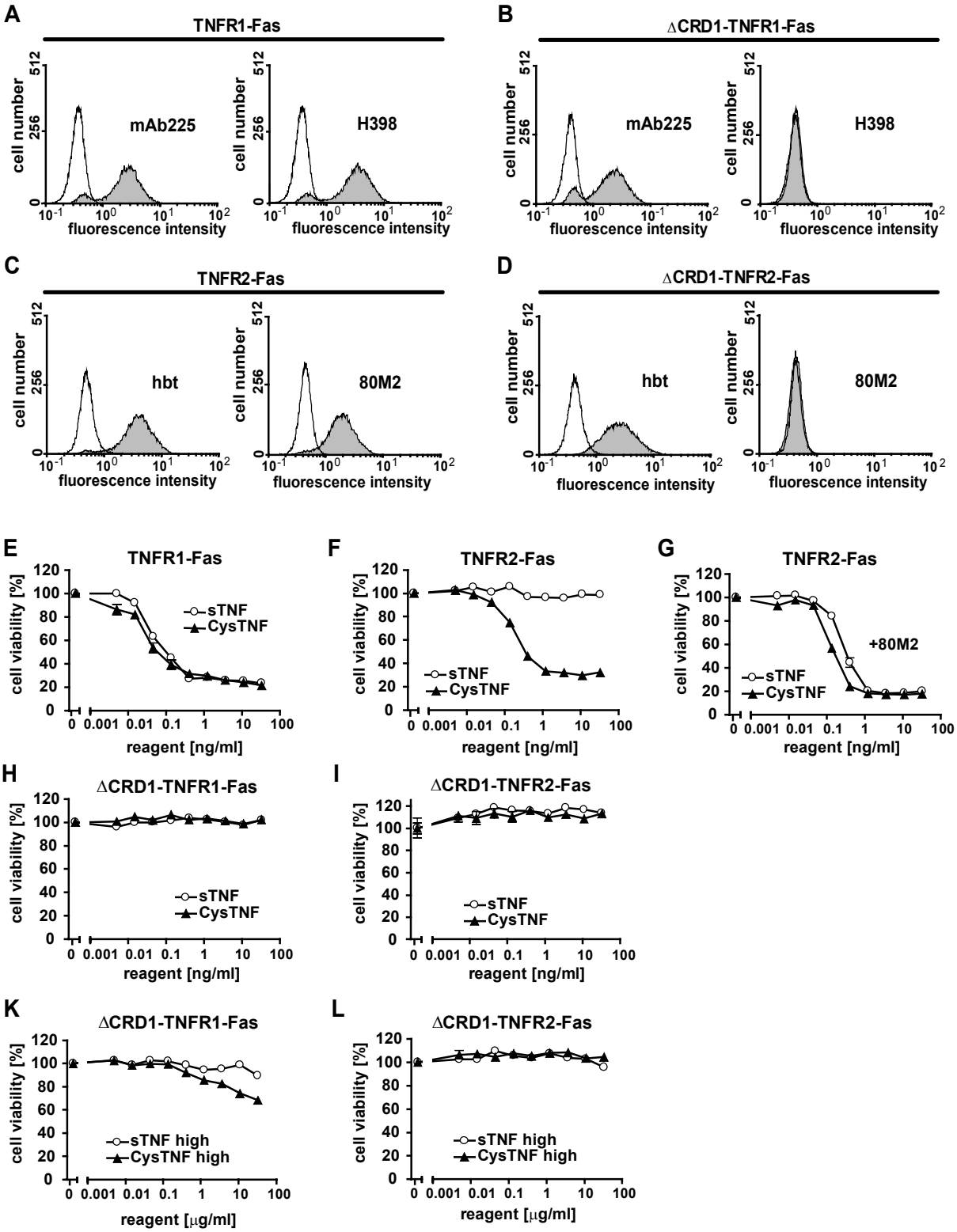

Figure 2: Deletion of CRD1 leads to unresponsive TNF-receptors. A-D, FACS analyses of chimeric receptors. Mouse embryonic fibroblasts (MEFs) expressing TNFR1-Fas (A), ΔCRD1-TNFR1-Fas (B), TNFR2-Fas (C) or ΔCRD1-TNFR2-Fas (D) were stained with TNFR1-specific antibodies (A and B; mAb225 or H398, filled histograms) or TNFR2-specific antibodies (C and D; hbt or 80M2, filled histograms) or were only stained with the secondary FITC-labeled antibodies (open histograms). **E-L,** Cytotoxicity assays. MEF TNFR1-Fas (E), TNFR2-Fas (F and G), ΔCRD1-TNFR1-Fas (H and K) and ΔCRD1-TNFR2-Fas (I and L) cells were cultured for 18 hours with soluble TNF or CysTNF. Cell viability was assessed by crystal violet staining followed by OD measurement at 550 nm. TNFR2-Fas cells were pre-treated with 1 μg/ml of the antibody 80M2 where indicated (G). The shown data are representative of at least three independent experiments.

The mAb 80M2 is normally used in combination with soluble TNF to mimic membrane-bound ligand. The functionality of CRD1-deleted molecules was assessed by performing cytotoxicity assays with the respective full-length molecules as positive controls (Fig. 2E - L). In accordance with reported data (Krippner-Heidenreich et al., 2002), TNFR1 was responsive towards sTNF and CysTNF. CysTNF is a genetically modified TNF variant that contains a cysteine residue at the C-terminus of each protomer (Bryde et al., 2005). These three cysteines per homotrimer allow the spontaneous formation of several disulfide-linked TNF molecules. Size exclusion chromatography showed an about 9- to 10-fold increase in molecular size of CysTNF, as compared to sTNF (data not shown). The use of CysTNF thus allowed the stimulation of TNFR2 (Fig. 2F), whereas sTNF requires the TNFR2-specific mAb 80M2 (Fig. 2G). The CRD1-deleted molecules, however, were not responsive to both TNF variants at comparable and physiological concentrations, (Fig. 2H and I). To see if high amounts of ligand rendered the receptors active, ligands were applied at a 1000-fold increased concentration (Fig. 2K and L). However, even the use of high μg/ml concentrations only induced slight cytotoxic effects (Fig. 2K), thus proving that the intracellular parts are capable of transducing a cytotoxic signal. Control experiments with agonistic mAb225 also showed that ΔCRD1-TNFR1 was principally signaling-competent (not shown). These data indicated that ΔCRD1 molecules were not capable to bind to ligand with high affinity.

3.1.2 The deletion of CRD1 leads to partial unfolding of CRD2

To address the question whether the deletion of CRD1 causes structural changes that could lead to a non-ligand binding receptor, molecular dynamics (MD) simulations of TNFR1 were performed (Fig. 3) in cooperation with Andrew Aird (3rd Physical Institute, University of Stuttgart). MD simulations are used to analyze and predict the structure and dynamics of proteins *in silico*, i.e. with the help of computers. In brief, molecules are set in motion by heating the aquaeous system to a specified temperature that allows the molecule(s) to overcome potential energy barriers. The interaction potentials between atoms are calculated and Newton's equation of motion is used to predict where a particle will be after a short time interval of a few femtoseconds. The calculation is then repeated for several million time steps leading to a trajectory that describes the dynamics of the molecule. Different amino acid compositions or partial deletions thus lead to different trajectories.

Therefore, the available crystal structures of the extracellular parts of TNFR1 ($TNFR1_{ex}$) were first structurally aligned and were found to be virtually identical. However, structures without ligand were found to be slightly more curved. Therefore, the structure of TNFR1 bound to LTα (pdb databank entry 1TNR) was chosen to analyze the effect of the CRD1 deletion. Second, the structure of $TNFR1_{ex}$ was allowed to equilibrate in water (Fig. 3B and E-Nr.I).

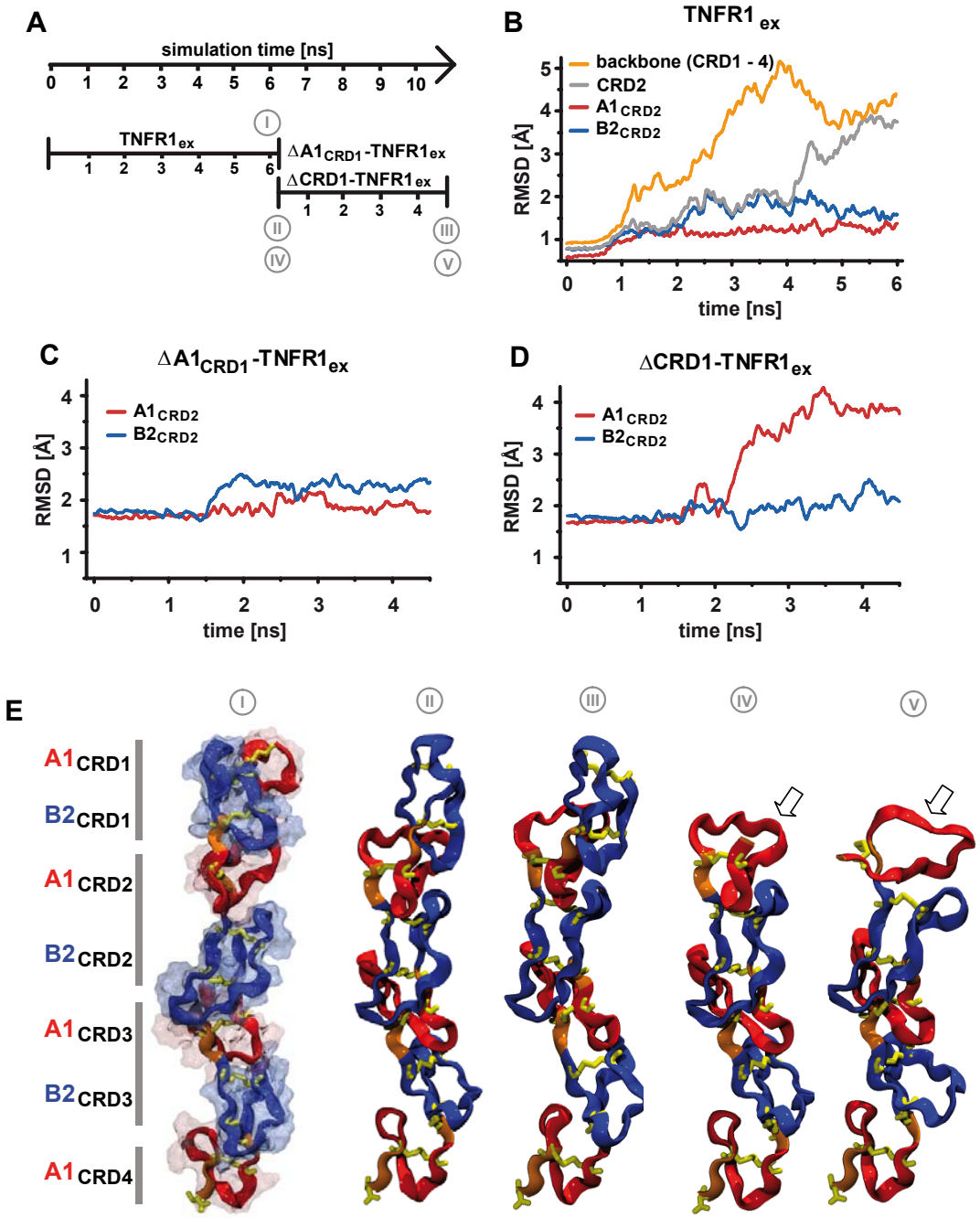

Figure 3: The deletion of CRD1 leads to unfolding of $A1_{CRD2}$. A, Delineation of the molecular dynamics simulations performed with $TNFR1_{ex.}$ First, the extracellular domain of TNFR1 was equilibrated in water for 6 ns. From the equilibrated structure, the N-terminal deletion mutants $\Delta A1_{CRD1}$-$TNFR1_{ex}$ and ΔCRD1-$TNFR1_{ex}$ were generated and allowed to equilibrate for further 4.25 ns to analyze if these deletions cause any structural changes. The structures shown in E are indicated by encircled latin numbers (I-V). **B-D**, The structural dynamics of $TNFR1_{ex}$ (B), $\Delta A1_{CRD1}$-$TNFR1_{ex}$ (C) and ΔCRD1-$TNFR1_{ex}$ (D) were analyzed by calculating the root mean square deviation (RMSD) values between the simulated structure and the reference structure (pdb entry 1TNR). **B**, Whereas the complete molecule (backbone; orange) is quite flexible, the flexibility decreases for the individual CRDs (CRD2, gray line) and even more for the modules (A1 and B2 of CRD2 are shown; red and blue, respectively). **C**, The deletion of $A1_{CRD1}$ has no structural effects for the A/B modules of CRD2. **D**, The deletion of the complete CRD1 leads to the destabilization of the A1 module of CRD2 ($A1_{CRD2}$, red). **E**, structures of the simulated $TNFR1_{ex}$ molecules in ribbon representation. The location of the A and B moduls are given at the left. (E-I), $TNFR1_{ex}$ after equilibration. $\Delta A1_{CRD1}$-$TNFR1_{ex}$ before (E-II) and after (E-III) equilibration. ΔCRD1-$TNFR1_{ex}$ before (E-IV) and after (E-V) equilibration. Black arrows are intendet to focus on $A1_{CRD2}$.

The experiment showed that the $TNFR1_{ex}$ molecule is quite flexible, as demonstrated by the root mean square difference (RMSD) value of the protein backbone of >4Å (Fig. 3B, orange line). RMSD values for a given time point indicate the difference in position and thus flexibility with respect to a reference structure. When analyzing the individual CRDs, this flexibility decreased but was still evident (Fig. 3B, gray line as an example for CRDs). Thus, the extracellular domain can be regarded as a chain of marbles, with the marbles being the CRDs. However, the real building blocks of the molecule, as shown by their low molecular movement are the A and B modules of the CRDs, as defined by Naismith and colleagues (Naismith et al., 1996b; Naismith and Sprang, 1998). For instance, the CRD1 of TNFR1 is composed of $A1_{CRD1}$ and $B2_{CRD1}$ (Fig. 3E, at the left and Fig. 1B). The MD simulation showed that the A/B modules for full-length TNFR1 quickly equilibrated and remained stable (Fig. 3B, red and blue line) with a RMSD value around 2Å. Next, the CRD1 was deleted (ΔCRD1-$TNFR1_{ex}$, Fig. 3D) and the RMSD value of the A/B modules of CRD2 were analyzed, because CRD2 forms extensive contacts with LTα in the crystal structure (Banner et al., 1993). Interestingly, whereas the $B2_{CRD2}$ remained stable, the $A1_{CRD2}$ showed large movements of 4 Å (Fig. 3D, red line). This indicated that the CRD1 is a scaffold for the subsequent A1 loop of CRD2. In an additional simulation experiment, only “half” of the CRD1 was removed yielding $\Delta A1_{CRD1}$-$TNFR1_{ex}$ and analyzed as above (Fig. 3C). This molecule still contained the B2 of CRD1 that could potentially stabilize A1 of CRD2. This hypothesis was confirmed by RMSD values for the A/B modules of CRD2 being stable at around 2Å (Fig. 3C, red and blue line). Pictures of protein structures are also given in Fig. 3E.

3.1.3 The CRD1 is a scaffold for CRD2

To verify the predictions of the MD simulations, the $\Delta A1_{CRD1}$-TNFR1-Fas was constructed and expressed in MEFs (Fig. 4) as described above. Here it was noticed that several rounds of FACS sorting were required to produce cells that could be immunostained at the cell surface with antibodies specific for TNFR1. In addition, cells were unresponsive two weeks after cell sorting. MEF $\Delta A1_{CRD1}$-TNFR1-Fas were functionally analyzed by performing cytotoxicity assays and by their ability to bind to radiolabeled TNF in equilibrium saturation binding experiments performed at 4°C (Fig. 4 and not shown). Saturation binding experiments with these cells were rather inconsistent with K_D values between 70 and 350 pM, whereas the full-length molecule TNFR1-Fas displayed a K_D of ~100 pM, as expected (not shown). However, in all functional experiments performed, MEF $\Delta A1_{CRD1}$-TNFR1-Fas were not responsive towards sTNF. Instead, the ability to signal cytotoxicity was strictly dependent on additional crosslinking by the ligand such as CysTNF (Fig. 4D). To have an alternative cellular expression system, a human embryonal kidney cell line (HEK293) was

used. To prevent the development of toxic effects of the TNFR-Fas constructs used, an inducible cell line (HEK293 Flp-In T-REx) was chosen. These cells allow the site-specific integration into the genome, due to the presence of a nucleotide sequence that is recognized

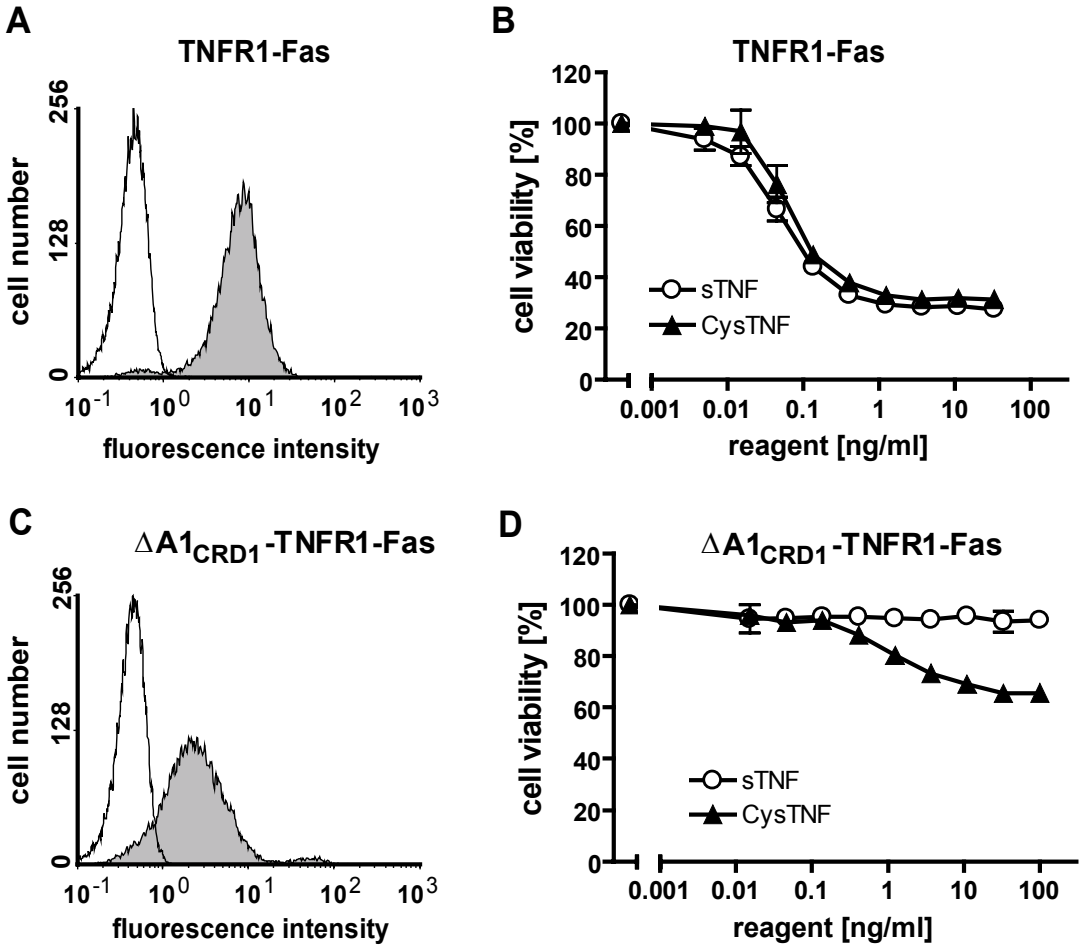

Figure 4: The $A1_{CRD1}$ module is required for efficient TNFR1-Fas signaling. Shown is the analysis of the two receptors TNFR1-Fas (**A** and **B**) and $\Delta A1_{CRD1}$-TNFR1-Fas (**C** and **D**) expressed in mouse embryonic fibroblasts. **A** and **C**, FACS analyses of receptor expression. Cells were stained with a TNFR1-specific antibody (mAb225, filled histograms) or were only stained with the secondary anti-mouse FITC antibody (open histograms) and analyzed by flow cytometry. **B** and **D**, Cytotoxicity assays. Indicated cells were seeded, prepared and treated as described before. Note that whereas TNFR1-Fas is responsive towards sTNF (B), the deletion of $A1_{CRD1}$ leads to a receptor that requires CysTNF for apoptosis signaling (D). Shown data were performed in parallel and are representative for five independent experiments.

by the Flp recombinase. In addition, the promoters of the used pCDNA5-FRT-TO vectors that carried the different TNFR1-Fas genes were under control of the tetracycline repressor, also encoded by the host cell line. Thus, three stable and inducible HEK293 Flp-In T-REx cell lines were created expressing TNFR1-Fas, $\Delta A1_{CRD1}$-TNFR1-Fas or ΔCRD1-TNFR1-Fas. First, cells were analyzed for the inducer concentration required to detect receptors by FACS analysis (not shown). Instead of tetracycline the more stable derivative doxycycline was used and cells were incubated with increasing concentrations from 0 - 8 ng/ml over night at 37°C.

molecules with increasing deletions, i.e. TNFR1-Fas < $\Delta A1_{CRD1}$ < ΔCRD1. The kinetics of cell surface expression was also assessed and receptors were detected starting 6h post-induction, with maximal expression observed after 18h of induction (data not shown). To address the question whether the two deletion mutants bind TNF with high affinity, saturation binding experiments with ^{125}I-labeled TNF were performed at 4°C (Fig. 5). In accordance with previous experiments using MEF cells, TNFR1-Fas, expressed on the inducible HEK cell line, displayed a high TNF affinity (Fig. 5A; K_D = 94 $\pm$ 78 pM). FACS analyses performed in parallel (Fig. 5B) correlated with the determined number of binding sites for iodinated TNF (113,000 $\pm$ 30,000). Cells expressing $\Delta A1_{CRD1}$-TNFR1-Fas were also strongly stained in FACS analysis when induced with doxycycline (Fig. 5D) and displayed an approximately 2-fold lower TNF affinity (Fig. 5C; K_D = 195 $\pm$ 40 pM). However, although more or equivalent binding sites as compared to the full-length TNFR1 were expected from FACS analyses (Fig. 5B versus 5D), the number of binding sites for ^{125}I-TNF was 66,000 $\pm$ 26,000 on $\Delta A1_{CRD1}$-TNFR1-Fas cells. Thus, the number of binding sites was lower on $\Delta A1_{CRD1}$-TNFR1-Fas cells as compared to TNFR1-Fas positive cells, indicative of non-functional receptor species. The third construct, ΔCRD1-TNFR1-Fas, was also highly expressed on the cell surface (Fig. 5F), but no saturatable binding was observed (Fig. 5E). Identical results were obtained with MEFs stably expressing ΔCRD1-TNFR1-Fas (Fig. 10H). Confocal microscopy with fluorescently labeled TNF was used to confirm TNF binding for TNFR1-Fas and $\Delta A1_{CRD1}$-TNFR1-Fas (Fig. 6). Inducible HEK cells expressing one of these two receptors were incubated on ice with Alexa-546-labeled TNF and analyzed at 37°C by live imaging. Whereas for TNFR1-Fas red TNF could easily be detected (Fig. 6A) the ΔA1-mutant also showed red staining, although strongly reduced (Fig. 6C). No staining was observed for the CRD1 deletion mutant (not shown).

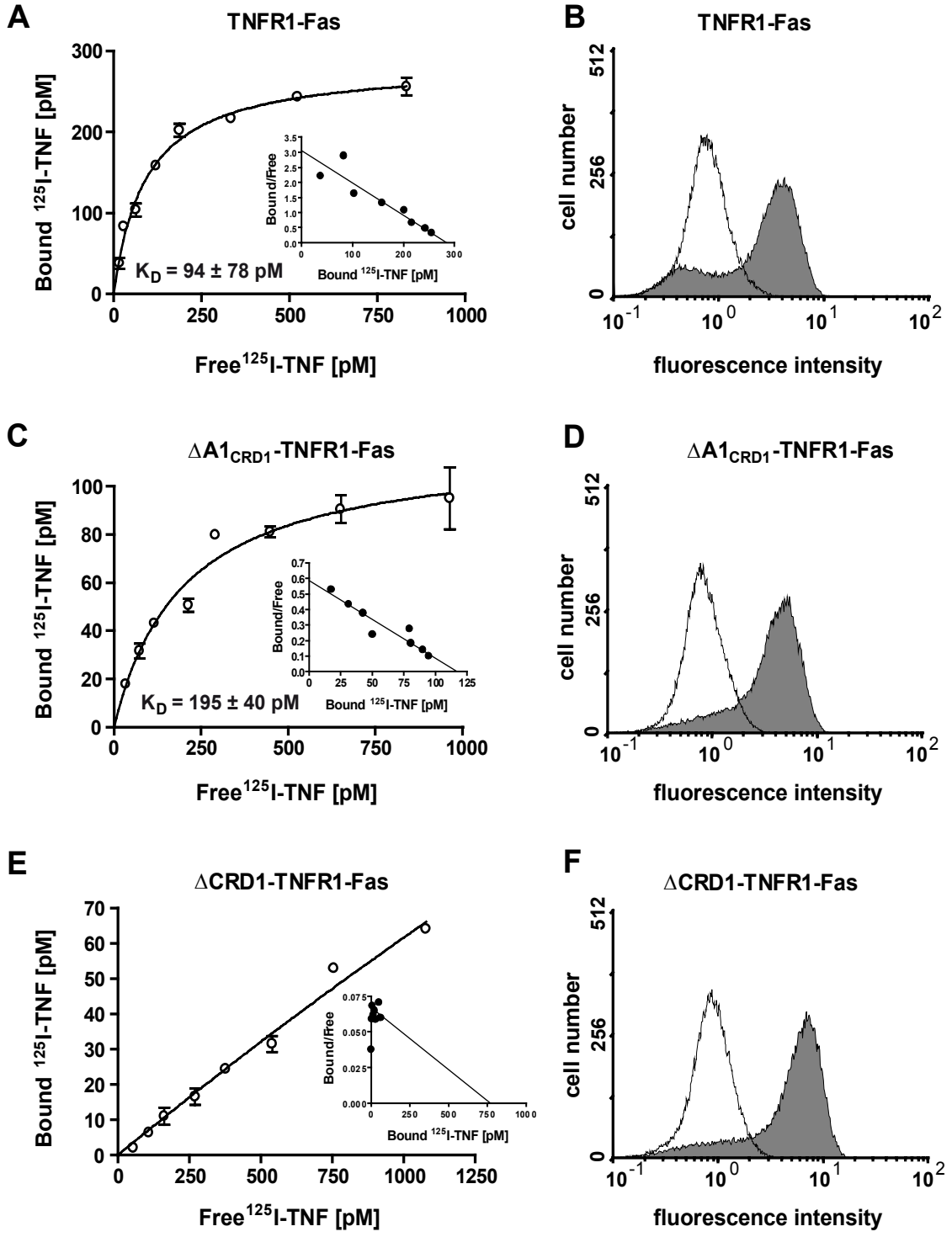

Figure 5: The B2 module of CRD1 is essential for high affinity TNF binding by TNFR1. **A, C, E,** Saturation binding data determined at 4°C using ^{125}I-TNF on HEK 293 Flp-In T-REx cell lines that were induced to express chimeric receptors; the insets represent the Scatchard plots of corresponding data. **B, D, F**, FACS analyses. Flow cytometry was used to monitor the expression of TNFR1-Fas (B), $\Delta A1_{CRD1}$-TNFR1-Fas (D) and ΔCRD1-TNFR1-Fas (F). Therefore, un-induced cells (open histograms) and induced cells (18h of doxycycline treatment; grey histogram) were stained with a TNFR1-specific antibody (mAb225) followed by incubation with a FITC-labeled goat anti-mouse antibody. Shown are typical data from four independent experiments. Note that ligand binding to ΔCRD1-TNFR1-Fas (E) is not saturable under these conditions, whereas TNFR1-Fas (A) and $\Delta A1_{CRD1}$-TNFR1-Fas (C) bind TNF with high affinity.

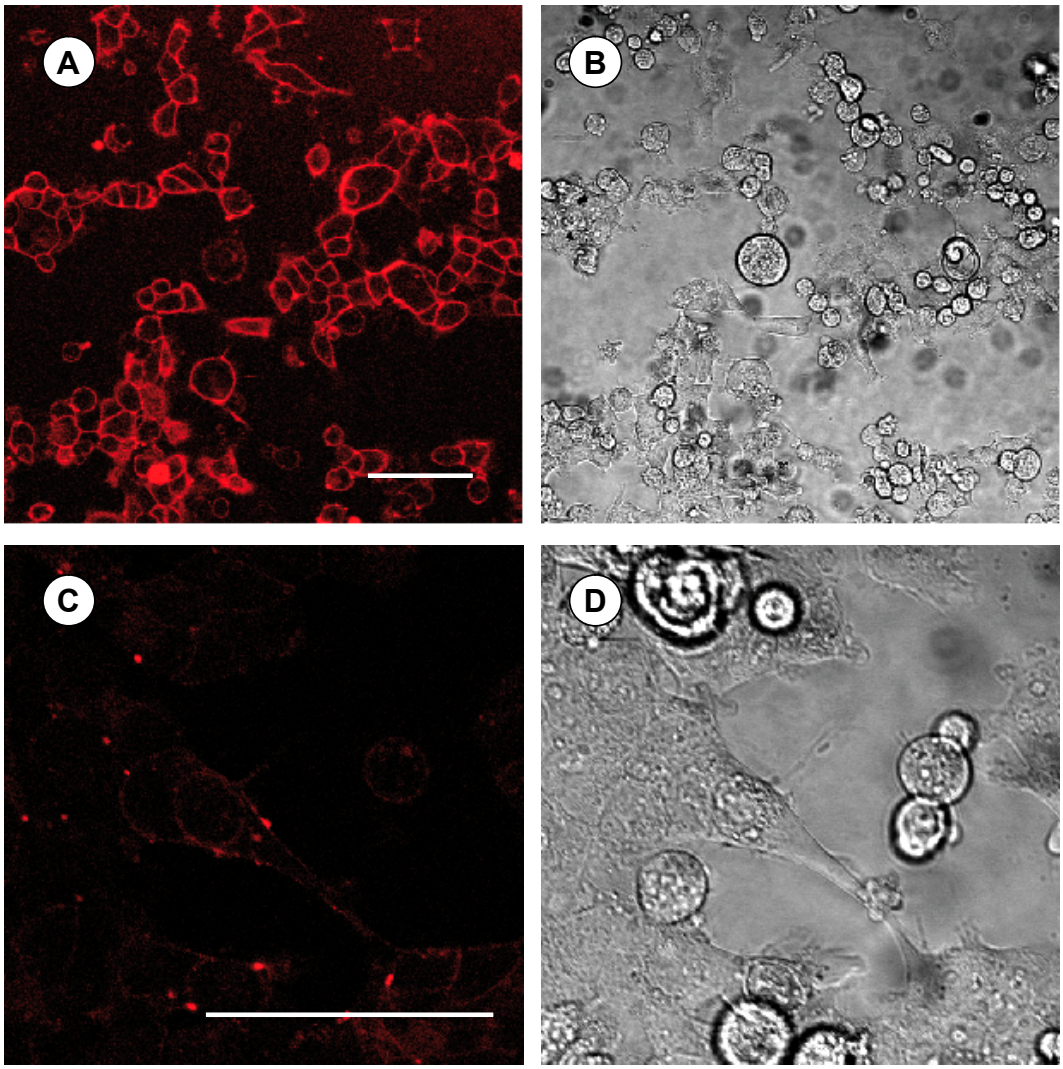

Figure 6: TNFR1-Fas binds sTNF with high affinity. HEK293 Flp-In T-REx cells expressing TNFR1-Fas (**A** and **B**) or $\Delta A1_{CRD1}$-TNFR1-Fas (**C** and **D**) were incubated with Alexa-546-coupled sTNF for 4 min. on ice. The dye-labeled sTNF was diluted six-fold by addition of fresh medium and cells were placed into a humidified, CO_2 and tempereature controlled chamber. Analysis for bound sTNF (red fluorescence, **A** and **C**) was performed by confocal microscopy. Transmission microscopy images of cells are shown in **B** and **D**. The images in Figs. A and B are the avarage of four sections taken at the same vertical position after 10 min. at 37°C. Figures C and D were taken after 16 min. at 37°C and are the average of six sections and in addition in Fig. C the voltage of the photo-multiplier tube was raised 2.5-fold over (A) to visualize TNF binding. Scale bars are 75 μm. Shown data were typical for three independent experiments.

3.1.4. The CRD1 is required for functional receptor interactions

Next, the signaling capability of the three receptor constructs was analyzed by two different assays. First, as the expression of high numbers of receptors containing a death domain is known to induce spontaneous, i.e. ligand independent signaling (Boldin et al., 1995), the HEK cells were analyzed for cell death after induction (Fig. 7). In control experiments, all three cell lines could be easily grown in induction-medium that contained the pan-caspase

inhibitor zVADfmk (20 μM, Figs. 7C, F, and I). In the absence of the caspase inhibitor, however, TNFR1-Fas cells had almost completely detached in induction medium showing a strongly stressed phenotype (Fig. 7B). The ΔA1 mutant displayed an intermediate phenotype (Fig. 7E) whereas the ΔCRD1-TNFR1-Fas cells displayed no observable response at all (Fig. 7H). Assuming that large receptor-receptor aggregates are essential for ligand-independent signaling and knowing that deletion of the CRD1 abolishes the detachment of cells, the CRD1 seems to be required for signaling-competent receptor-receptor interactions in the absence of ligand. As the deletion mutant of $A1_{CRD1}$ displayed an intermediate detachment phenotype, this type of ligand-independent interaction may be weakened. This question was indirectly tested in the following experiment. Among the many signaling pathways, wild type (*wt*) TNFR1 is known to induce the expression and secretion of IL-8, a chemokine that attracts neutrophils to sites of inflammation. As the parental cell line constitutively expresses low numbers of the *wt* TNFR1, uninduced HEK 293 Flp-In T-REx cells were stimulated with TNF and the secretion of IL-8 could easily be detected with an IL-8 specific ELISA (Figs. 8A - C; triangles). After the induction of cells with doxycycline, IL-8 secretion was completely blocked in TNFR1-Fas positive cells (Fig. 8A, filled circles), unchanged or even slightly enhanced in ΔCRD1-TNFR1-Fas (Fig. 8C, filled circles) or showed an intermediate phenotype in $\Delta A1_{CRD1}$-TNFR1-Fas (Fig. 8B). The expression levels of the respective molecules were always monitored in parallel by FACS analysis (Figs. 8D - F) and the average values from four individual IL-8 release experiments are shown in Figs. 8G - I.

As Fas is also known to induce non-apoptotic signals (Wajant et al., 2003) and for instance leads to secretion of IL-8 (Watermann et al., 2007), several control experiments were performed. Parental HEK293 Flp-In T-REx cells were positive for cell-surface Fas expression as determined by FACS analyses (not shown). In addition, IL-8 release was determined by ELISA after stimulation of endogenous Fas with FLAG-FasL that was multimerized with an FLAG-specific antibody (M2) or not; as a positive control, HT1080 cells were used. Cells were kept in zVADfmk to avoid apoptosis induction by Fas stimulation. In accordance with reported data (Watermann et al., 2007), HT1080 cells secreted IL-8, however, no IL-8 was detected for the HEK293 Flp-In T-REx cells (not shown). Thus, the secretion of IL-8 in the induced ΔA1-TNFR1-Fas HEK293 Flp-In T-REx cell line emanated from TNFR1 and not from the chimeric receptor.

In summary, the data indicated that CRD1 is required for functional signaling as determined by ligand-free signaling and for the formation of mixed receptor complexes as determined from the dominant inhibition assay.

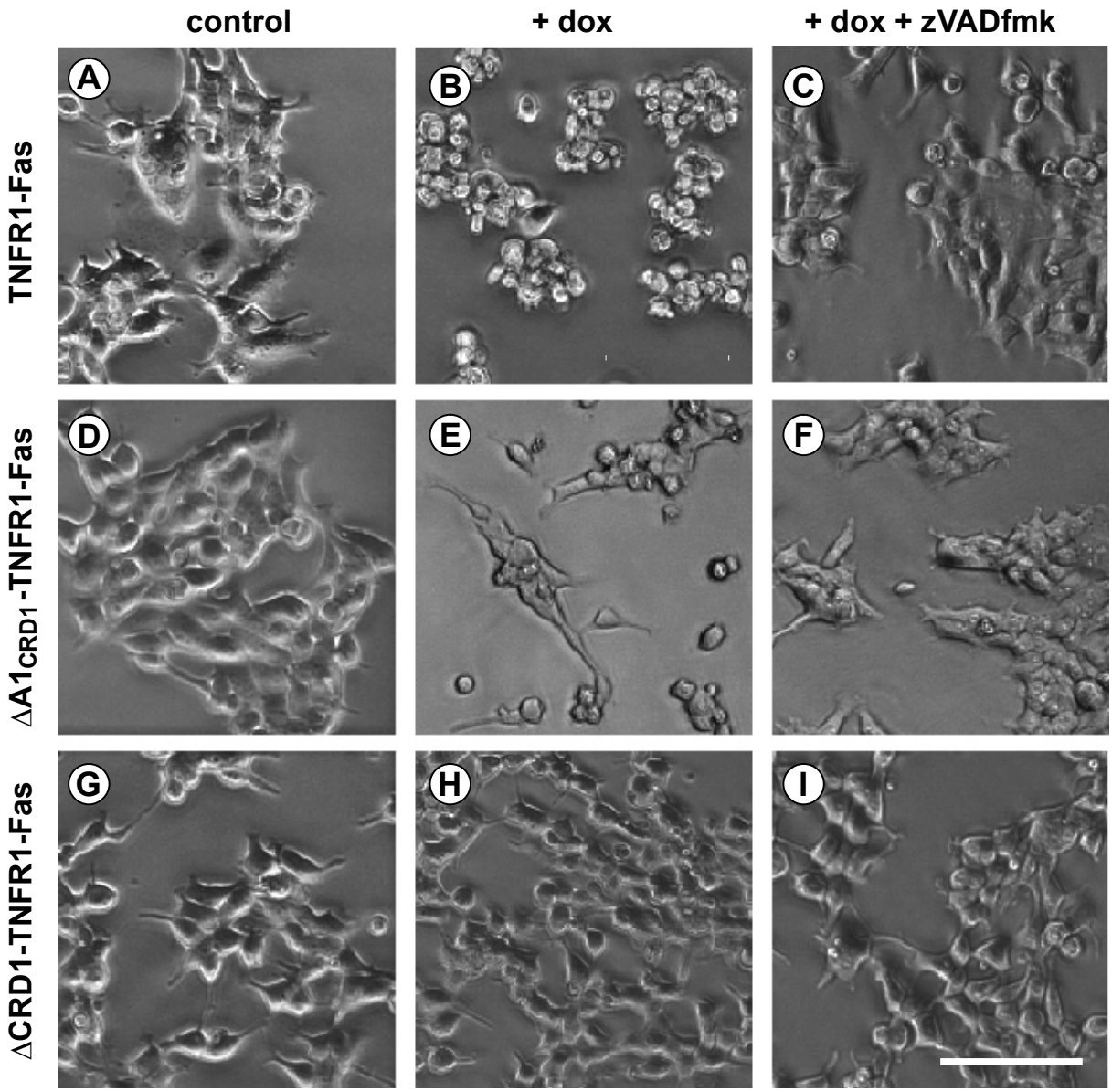

Figure 7: The B2 module of CRD1 is required for spontaneous TNFR1 signaling. HEK293 Flp-In T-REx cells stably transfected with TNFR1-Fas (A-C), $\Delta A1_{CRD1}$-TNFR1-Fas (D-F) or ΔCRD1-TNFR1-Fas (G-I) were seeded in 6-well plates over night. Receptor expression was induced by incubation with doxycycline (dox; 4 ng/ml) with or without the caspase inhibitor zVADfmk (20 μM) and phase contrast images were taken after 24h. The scale bar shown in (I) is representative for all figures and is 100 μm in length. Shown data are representative of five independent experments.

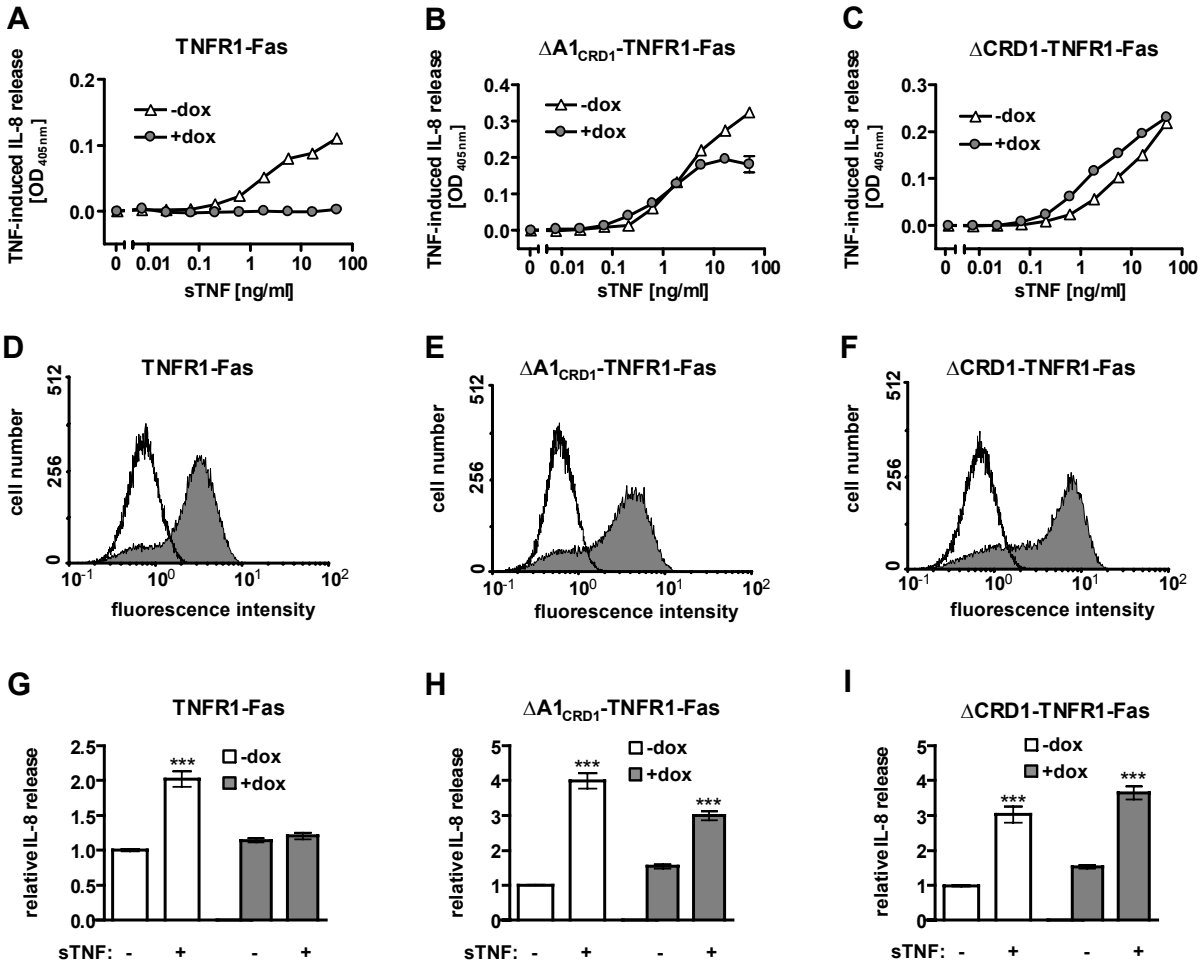

Figure 8: Dominant inhibition of TNFR1-mediated IL-8 release requires the CRD1 of chimeric TNFR1-Fas receptors. HEK293 Flp-In T-REx cells inducibly expressing TNFR1-Fas (A, D and G), $\Delta A1_{CRD1}$-TNFR1-Fas (B, E and H), or ΔCRD1-TNFR1-Fas (C, F and I), were treated with and without doxycycline (- dox and + dox, respectively) for 18h. Cells were kept in presence of zVAD-fmk (20µM) throughout the experiments. **A-C**, TNF-induced IL-8 release. After induction of the chimeric receptors by doxycycline treatment cells were stimulated with and without serial dilutions of sTNF (50 - 0.007 ng/ml) for 24h. Supernatants were analyzed for IL-8 production by ELISA. **D-F**, FACS analyses. The expression of chimeric receptors was analyzed by flow cytometry using a TNFR1-specific monoclonal antibody (mAb225). Cells were treated with doxycycline (shaded gray) or were left uninduced (open histogram). The shown data from figures A-F were taken from a single typical experiment. **G-I,** IL-8 release in HEK293 Flp-In T-REx cells treated with and without TNF (50 ng/ml). Shown are the average values of four independent experiments, each performed in triplicates. Data were normalized within the individual experiments to the control values (without TNF, without induction). Asterisks above the bars indicate p<0.001.

3.1.5. The CRD1 can be functionally exchanged between receptors

To analyze if the effect of the CRD1 deletion was due to a conformational defect, the deleted ΔCRD1-TNFR1-Fas molecule was reconstituted with the CRD1 of TNFR2. The resulting $CRD1_{TNFR2}$-TNFR1-Fas molecule was stably expressed in MEFs as described before and was expected to i) bind to TNF with high affinity and ii) signal with sTNF. The chimeric exchange molecule could be easily detected by a TNFR1-specific monoclonal antibody on

the surface of cells (Fig. 9C). As a control, the ΔCRD1-TNFR1-Fas (Fig. 9A) or TNFR1-Fas cells were used (Fig. 9B).

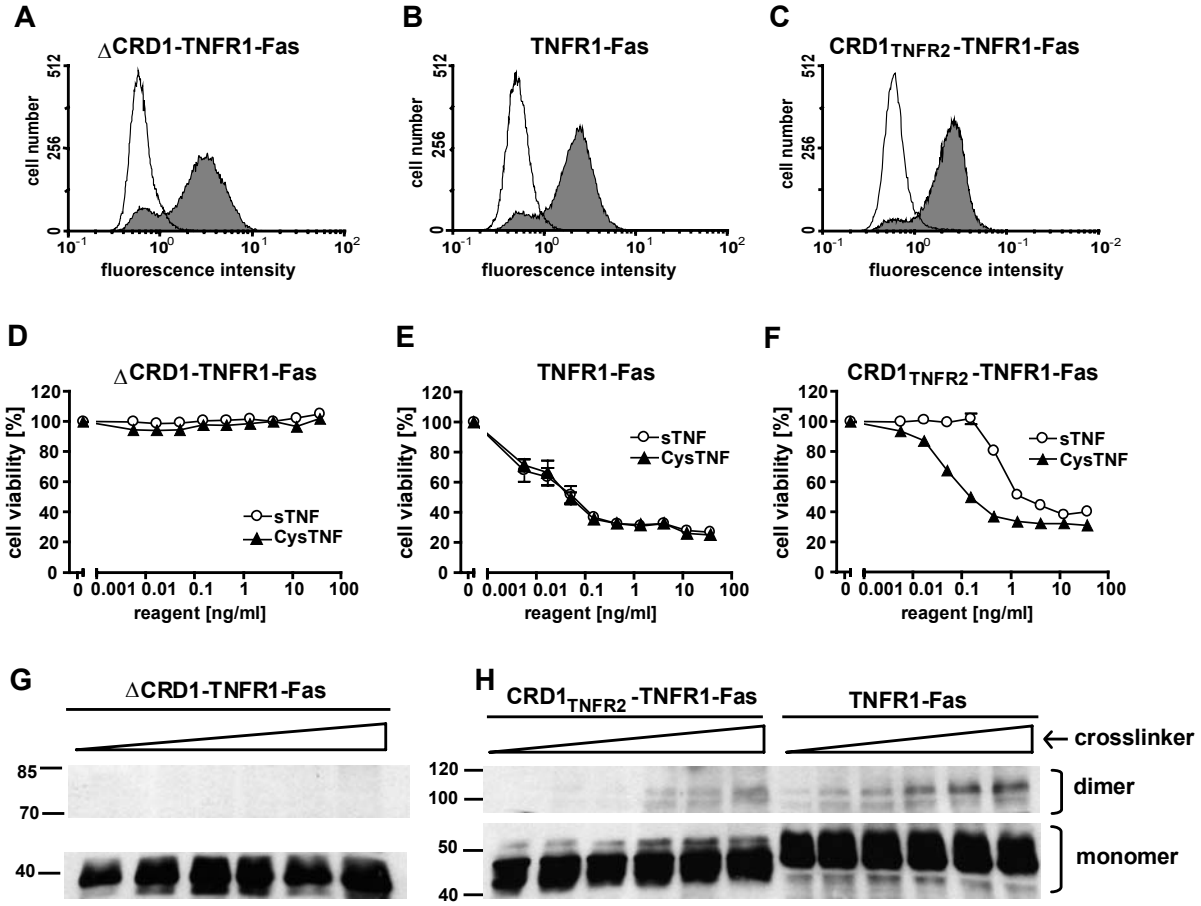

Figure 9: The CRD1 is required for TNF responsiveness and is involved in the discrimination between soluble and membrane-bound ligand. A – **C**, FACS analyses. MEFs stably expressing chimeric TNFR1-Fas (B), ΔCRD1-TNFR1-Fas (A) or the exchange mutant $CRD1_{TNFR2}$-TNFR1-Fas (C) were stained for cell surface expression with a TNFR1-specific monoclonal antibody (mAb225) and analyzed by flow cytometry (gray histograms; open histograms were only stained with the secondary antibody). **D** – **F**, Cytotoxicity assays. Indicated cells were left untreated or were treated for 16 hours with serial dilutions of sTNF or CysTNF (33 – 0.006 ng/ml). Live cells were quantified by crystal violet staining and cell viability is given as percentage of unstimulated cells. Note that TNFR1-Fas (E) is about 10-fold more sensitive towards sTNF as compared to the CRD1 exchange mutant (F). **G and H** Chemical crosslinking. Cells were incubated with increasing concentrations of the chemical crosslinker BS^3 and cell lysates (protein amounts loaded were adjusted to cell surface expression) were subjected in parallel to reducing SDS-PAGE and Western Blotting using a Fas-specific antibody (clone B10). The monomeric, as well as the crosslinked species are indicated at the right (monomer, dimer). Note that TNFR1-Fas (H) can be better crosslinked as compared to the CRD1-exchange mutant. The experiments (A – H) were performed in parallel, repeated three times and presented data were from a single, typical experiment.

Cytotoxicity assays were performed as before (Fig. 2E and H) and confirmed that TNFR1-Fas was responsive towards both ligand forms (sTNF and CysTNF) whereas the ΔCRD1 mutant was not (Fig. 9E and D). The CRD1 exchange mutant showed an intermediate phenotype: Whereas expressing cells remained equally responsive towards CysTNF (Fig. 9F, black triangles), a clear shift of the EC50 value for sTNF to higher concentrations (Fig.

9F, open circles) was observed. Thus, the exchange mutant prefers CysTNF that has a higher valency as compared to sTNF.

3.1.6 The CRD1 contributes to receptor-receptor interactions and sTNF responsiveness

To analyze the reason for the higher EC50 values, two different types of experiments were performed, namely chemical crosslinking and saturation binding studies shown further below. It had been reported previously that TNFR1 and -2 are pre-assembled via their pre-ligand binding assembly (PLAD) domains that requires the membrane-distal CRD1 to be functional (Chan et al., 2000). To address the question if the receptors used here show differences regarding their self-association, experiments using the water soluble, homo-bi-functional and amino-reactive chemical crosslinker BS^3 were performed (Fig. 9G and H). In brief, cells stably expressing TNFR1-Fas, ΔCRD1- or $CRD1_{TNFR2}$-TNFR1-Fas were incubated with increasing BS^3 concentrations and protein lysates were subjected to reducing SDS-PAGE and Western Blotting. In contrast to reported data (Chan et al., 2000), the molecular species that could be readily identified under these conditions were dimers of TNFR-Fas and not trimers. Further experiments showing dimeric TNF-receptors will be presented in the following sections (Figs. 11 and 12). Nevertheless, crosslinked TNFR1-Fas (Fig. 9H, upper right lane) or $CRD1_{TNFR2}$-TNFR1-Fas (Fig. 9H, upper left lane) could be easily detected. In contrast, under the same exposition conditions, no crosslinked species were detected when the receptor lacked its CRD1 (Fig. 9G). Interestingly, it appeared that TNFR1-Fas could be crosslinked more efficiently already at lower BS^3 concentrations as compared to the exchange mutant $CRD1_{TNFR2}$-TNFR1-Fas (Fig. 9H). Densitometric analysis of three independent experiments confirmed this observation (data not shown).

Another possibility for the reduced EC50 value of the CRD1 exchange mutant could be that the molecule, due to its chimeric nature, is somehow skewed or conformationally affected and thus has a reduced affinity to bind to TNF. Therefore saturation binding experiments were performed at 4°C (Fig. 10). The data confirmed high affinity binding of TNFR1-Fas with a K_D value of 117 pM ± 14 pM (Fig. 10B and C) and no specific binding for ΔCRD1-TNFR1-Fas (Fig. 10G and H). The CRD1 exchange mutant also showed high affinity for iodinated TNF (Fig. 10E and F) with a K_D value of 88 ± 26 pM. Interestingly, during these experiments, the chimeric exchange molecule displayed the tendency to have a higher affinity for sTNF as compared to TNFR1-Fas (Fig. 10i). A similar phenotype was observed for the wild type TNFR2 and TNFR1 molecules with K_D values of 60 pM and 100 pM, respectively (Grell et al., 1998).

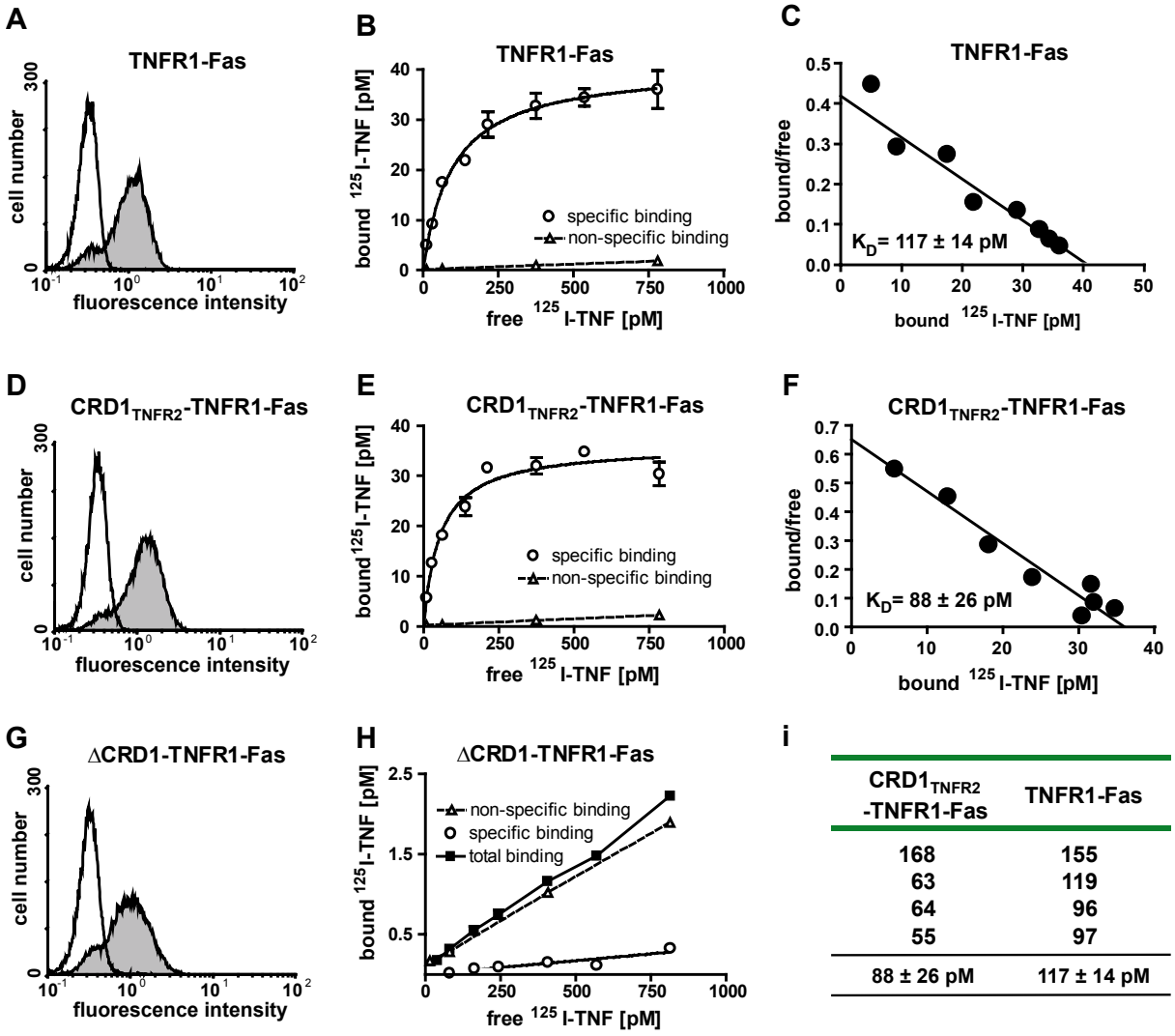

i

$CRD1_{TNFR2}$ -TNFR1-Fas	TNFR1-Fas
168	155
63	119
64	96
55	97
88 ± 26 pM	117 ± 14 pM

Figure 10: The CRD1-exchange mutant folds properly. A, **D**, **G**, Mouse embryonic fibroblasts expressing TNFR1-Fas (A), $CRD1_{TNFR2}$-TNFR1-Fas (D) or ΔCRD1-TNFR1-Fas (G) were stained with a TNFR1-specific monoclonal antibody (mAb225, gray histograms) or secondary antibodies only (FITC-labeled, open histogram) and analyzed for cell surface expression by flow cytometry. **B**, **E**, **H**, Saturation binding experiments. Cells were incubated with increasing amounts of ^{125}I-labeled TNF or in presence of excess un-labeled TNF (non-specific binding, NSB). Note that ΔCRD1-TNFR1-Fas (H) cells show no specific binding, as total binding is parallel to NSB. **C** and **F**, Scatchard plots of the data from Figs. B and E, respectively (K_D values are given with S.E.M errors). Shown data are representative of four indvidual experiments. **i**, individual K_D values from four independent experiments are shown for TNFR1-Fas and $CRD1_{TNFR2}$-TNFR1-Fas.

Thus, the CRD1 is required for the stabilization of CRD2 and to some degree influences the responsiveness towards soluble or membrane-like ligand. The latter is likely due to influencing the receptor-receptor association strength as were determined by crosslinking experiments.

3.1.7 The stem and transmembrane regions as determinants of sTNF responsiveness

Searching for other components that could influence the preferred responsiveness of TNFRs with sTNF or CysTNF the so-called “stem” (S) and “transmembrane” (TM) regions (Fig. 1A) were exchanged between TNFR1 and TNFR2 (Messerschmidt, 2006) and expressed in MEFs as described (Krippner-Heidenreich et al., 2002). The resulting receptors, TNFR1-$(S/TM)_{TNFR2}$-Fas and TNFR2-$(S/TM)_{TNFR1}$-Fas showed the reverse phenotype towards sTNF, as compared to the receptors TNFR1-Fas and TNFR2-Fas that contained the extracellular *wt* sequences (Table 3). This means that molecules containing S/TM_{TNFR2} required CysTNF for efficient signaling. In addition, the dissociation rates of sTNF from S/TM-exchanged receptors were determined [(1)]; Table 3. However, although these values correlated with the sTNF responsivities of TNFR1 and TNFR2 as described (Grell et al., 1998), the (S/TM) exchange mutants were different; for instance, sTNF bound to TNFR2-$(S/TM)_{TNFR1}$-Fas and displayed a half-time of only 1.8 min., yet was responsive towards sTNF (Table 3). As the working hypothesis was that the formation of ligand-receptor clusters is required for efficient signaling, it could by hypothesized that the sum of receptor-ligand and receptor-receptor interactions determine if signaling occurs or not. Therefore, chemical crosslinking with BS^3 was performed (Fig. 11) to analyze if differences between receptor self-association exist. As described before (Fig. 9H), dimeric receptor-species could be detected by Western Blotting using whole-cell lysates from BS^3 treated cells. Remarkably, receptors that were most responsive towards sTNF could be more effectively crosslinked, namely TNFR1-Fas (Fig. 11E, left-upper panel) and TNFR2-$(S/TM)_{TNFR1}$-Fas (Fig. 11F, right-upper panel). These data are in consistence with a strong receptor-receptor interaction. Taken together, these data indicated that two types of interactions are required to form a strong signal. The data from these experiments are summarized in Table 3, below.

chimeric TNFR-Fas receptor:	**TNFR2-$(S/TM)_{TNFR1}$**	**TNFR1**	**TNFR2**	**TNFR1-$(S/TM)_{TNFR2}$**
sTNF:	++	+++	-	+
CysTNF:	+++	+++	++	++(+)
$t_{1/2}$ (min) [(1)]:	1.8 +/- 0.1	30.2 +/- 5.5	1.0 +/- 0.14	7.6 +/- 0.9
R-R crosslinking with BS^3	+++	++	+	(+)

Table 3: Given are the chimeric receptors with their relative sTNF or CysTNF responsivities, as determined from cytotoxicity assays (Messerschmidt, 2006). Cytotoxicity is indicated by the following signs: +++, potent activator; ++, moderate activator; +, weak activator; -, non-responsive. The half-times ($t_{1/2}$) of TNF for binding to corresponding receptors are given [(1)], as well as the determined receptor-receptor (R-R) crosslinking capabilities using BS^3.

[1] A. Krippner-Heidenreich, personal communication.

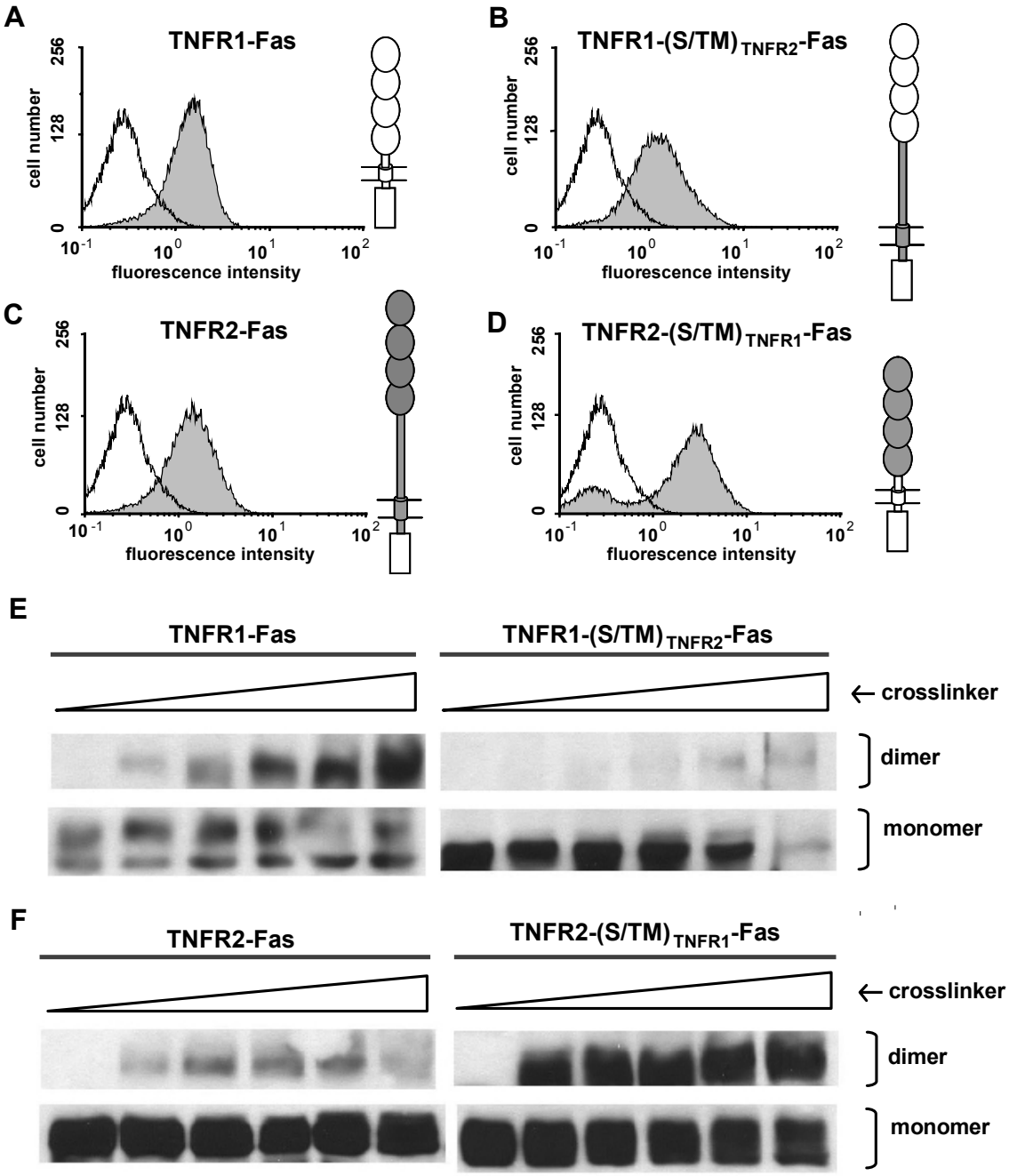

Figure 11: The Stem- and transmembrane regions of TNFRs contribute to receptor crosslinking efficiency. A – D, Flow cytometry. MEFs stably expressing chimeric TNFR1-Fas (A), TNFR1-(S/TM)$_{TNFR2}$-Fas (B), TNFR2-Fas (C) or TNFR2-(S/TM)$_{TNFR1}$-Fas (D) were stained for cell surface expression with specific monoclonal antibodies for TNFR1 (mAb225) or TNFR2 (MR2-1) and analyzed by flow cytometry (gray histograms; open histograms were only stained with the secondary antibody). Schematic drawings of chimeric receptors are shown to the right of corresponding histograms. **E** and **F**, Chemical crosslinking. Cells expressing the indicated chimeric receptors were incubated with increasing concentrations of BS^3 (0, 32, 64, 125, 250 500 mM) and cell lysates were generated. Two discontinuous polyacrylamide gels were prepared from the same solutions (4.5% / 8%) and proteins were subjected in parallel to reducing SDS-PAGE and Western Blotting using a Fas-specific antibody (clone B10). Lysates of TNFR1-Fas and TNFR1-(S/TM)$_{TNFR2}$-Fas were run on one gel (E), and lysates containing TNFR2-Fas and TNFR2-(S/TM)$_{TNFR1}$-Fas were separated in parallel on the second gel (F). Monomeric and dimeric species of TNFR-Fas molecules are indicated at the right (monomer/dimer). Note that there are clear differences in the amount of crosslinkable receptors (dimer). The shown set of data was from typical experiments independently performed four times.

3.2 Chapter II

3.2.1 TNFR1-Fas is a homo-dimer on the cell surface and binds to TNF

The crystal structure of soluble TNFR1, bound to soluble LTα indicated a 3:1 stoichiometry (three receptor chains and one homo-trimeric ligand). These data are in accordance with the observation that saturation binding studies with iodinated TNFR2-specific antibodies at 4°C detected ~2.5 - fold more binding sites on Kym-1 cells, as compared to sTNF (Löhden, 1995). Thus, several membrane-anchored TNFRs may bind to their ligand either in sequential order (one receptor after another) or in few, multivalent steps. To see if TNFR1-Fas molecules are pre-assembled on cells as described for TNFR1 (Chan et al., 2000), stably expressing MEFs were again chemically crosslinked with BS^3 as described above. With increasing concentrations of crosslinker dimeric TNFR1-Fas species were detected (Fig. 12A). The use of higher BS^3 concentrations (above 1 mM) resulted in the disappearance of bands reflecting monomeric, but also dimeric TNFR1-Fas (not shown). Thus, the dimer is the main pre-multimerized receptor species at these receptor “densities” on the MEF cells. To investigate if TNF also binds to dimeric receptors under conditions where saturation binding experiments were performed (at 4°C), MEFs expressing TNFR1-Fas were first incubated with sTNF on ice and then crosslinked with BS^3 (Fig. 12B, middle panel). As sTNF is a non-covalently linked homotrimer, it can dissociate under conditions of reducing and denaturing SDS-PAGE. To circumvent this problem cells were also incubated with a covalently linked TNF molecule that was termed single-chain TNF (scTNF) following the name of single chain antibody fragments. The use of scTNF made it possible to clearly distinguish between bands caused by TNFR1-Fas dimers alone (Fig. 12B, left panel), receptor dimers crosslinked to subunits of the homotrimeric TNF (Fig. 12B, middle panel) or receptor dimers crosslinked to a complete scTNF (Fig. 12B, right panel). Thus, TNF binds to two TNFR1-Fas molecules at 4°C. However, it should be stressed that the binding mechanism cannot be resolved in such a way; thus it is unclear, if TNF forms simultaneous physical contacts with two receptors or just one receptor, whereas in the latter scenario the second receptor remains indirectly “hooked” to TNF via the first receptor.

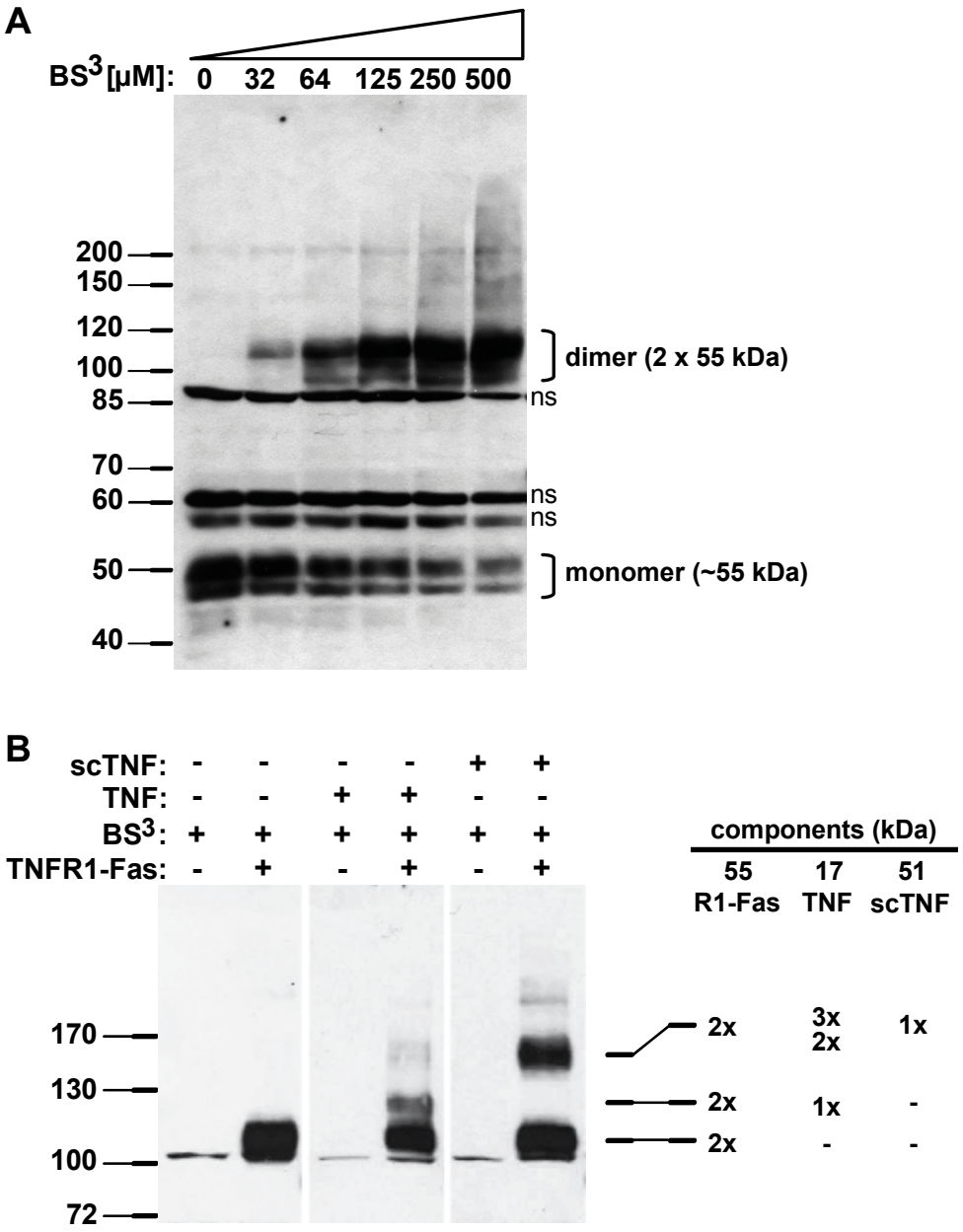

Figure 12: The chimeric molecule TNFR1-Fas exists as a pre-formed dimer on the cell surface. A, MEFs stably expressing TNFR1-Fas were incubated with increasing concentrations of the chemical crosslinker BS^3 and whole cell lysates (soluble protein, 100 µg/lane) were resolved by reducing SDS-PAGE (4.5% stacking-, 8.25% resolution gel) and shown is the Western Blot with a Fas-specific antibody (clone B10). Molecular weight markers are given to the left and TNFR1-Fas species are indicated by two brackets to the right (monomer, dimer); ns = non-specific bands. Note that TNFR1-Fas almost exclusively forms dimers and that a smear is visible at higher BS^3 concentrations that might indicate additional, higher molecular weight TNFR1-species. **B**, MEFs stably expressing TNFR1-Fas (+) or the parental *tnfr1*$^{-/-}$ *tnfr2*$^{-/-}$ cell line (-) were incubated where indicated (+) for 60 minutes on ice with 166 ng/ml of human, soluble TNF or with "single-chain" TNF (scTNF). Chemical crosslinking was performed by adding a saturating concentration of BS^3 (1 mM) for 30 min. on ice. Soluble proteins of the cellular lysates were resolved by reducing SDS-PAGE (3% / 6.25%). Western Blotting was performed as in (A). Protein standards are given to the left and identified molecular species are indicated at the right; R1Fas = TNFR1-Fas. Note that the gel in (B) was choosen to clearly identifiy the crosslinked products, thus the monomeric TNFR1-Fas is not visible. Shown data are representative of three individual experiments.

3.2.2 A first model of a LTα-TNFR1 super-complex

The crosslinking studies with TNFR1-Fas stably expressed on MEFs indicated a pre-formed receptor dimer, whereas others have reported that members of the TNFR family are "likely to be homotrimers" (Siegel et al., 2000; Chan et al., 2000). Both stoichiometries were used to build a receptor-ligand cluster as can be for instance observed under light-microscopes. Therefore, the solved crystal structure of LTα-TNFR1 (Banner et al., 1993) was depicted in a space-filling representation and multiple copies were used to arrange them in a two-dimensional lattice (Fig. 13).

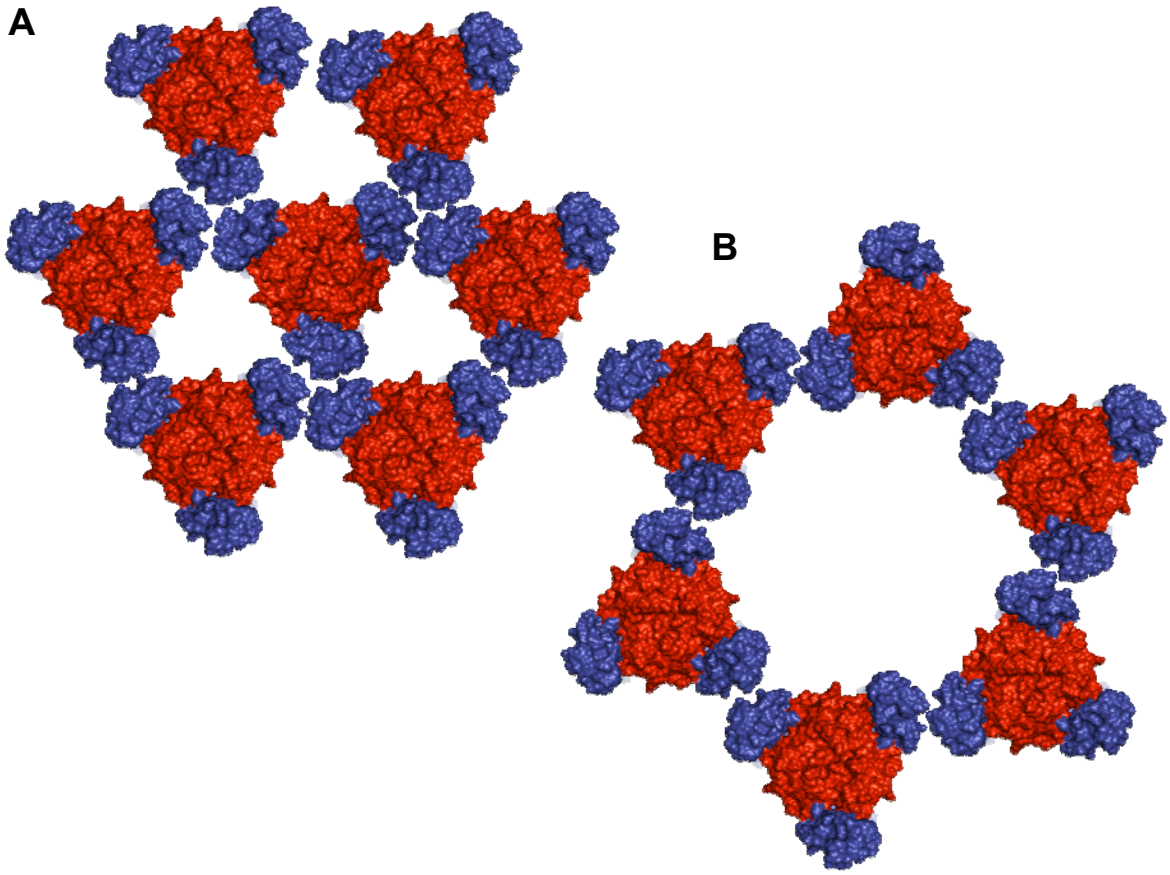

Figure 13: Two possible hexagonal LTα-TNFR1 arrangements lead to large aggregates. Shown are LTα (red) and TNFR1 (blue) molecules in space filling representation and the perspective is such that the plasma-membrane is below molecules. **A**, LTα-TNFR complexes were arranged in a hexagonal lattice with three receptor molecules (blue) forming direct contacts to each other. This composition may represent the "classical" view of pre-formed receptor trimers without ligand. **B**, Within this hexagonal arrangement TNFR1 molecules form dimeric interactions. This view better reflects the chemical crosslinking studies performed during this work showing dimeric pre-formed TNFR-Fas receptors.

Both stoichiometries resulted in the formation of a hexagonal lattice. Whereas the trimeric receptor-interaction cluster is relatively compact, the dimeric receptor-interaction cluster displays relatively large "wholes" in the lattice (Fig. 13B). To see if *wt* TNFR1 also forms homo-multimers, a green fluorescent protein-tagged variant (TNFR1-GFP) was transiently

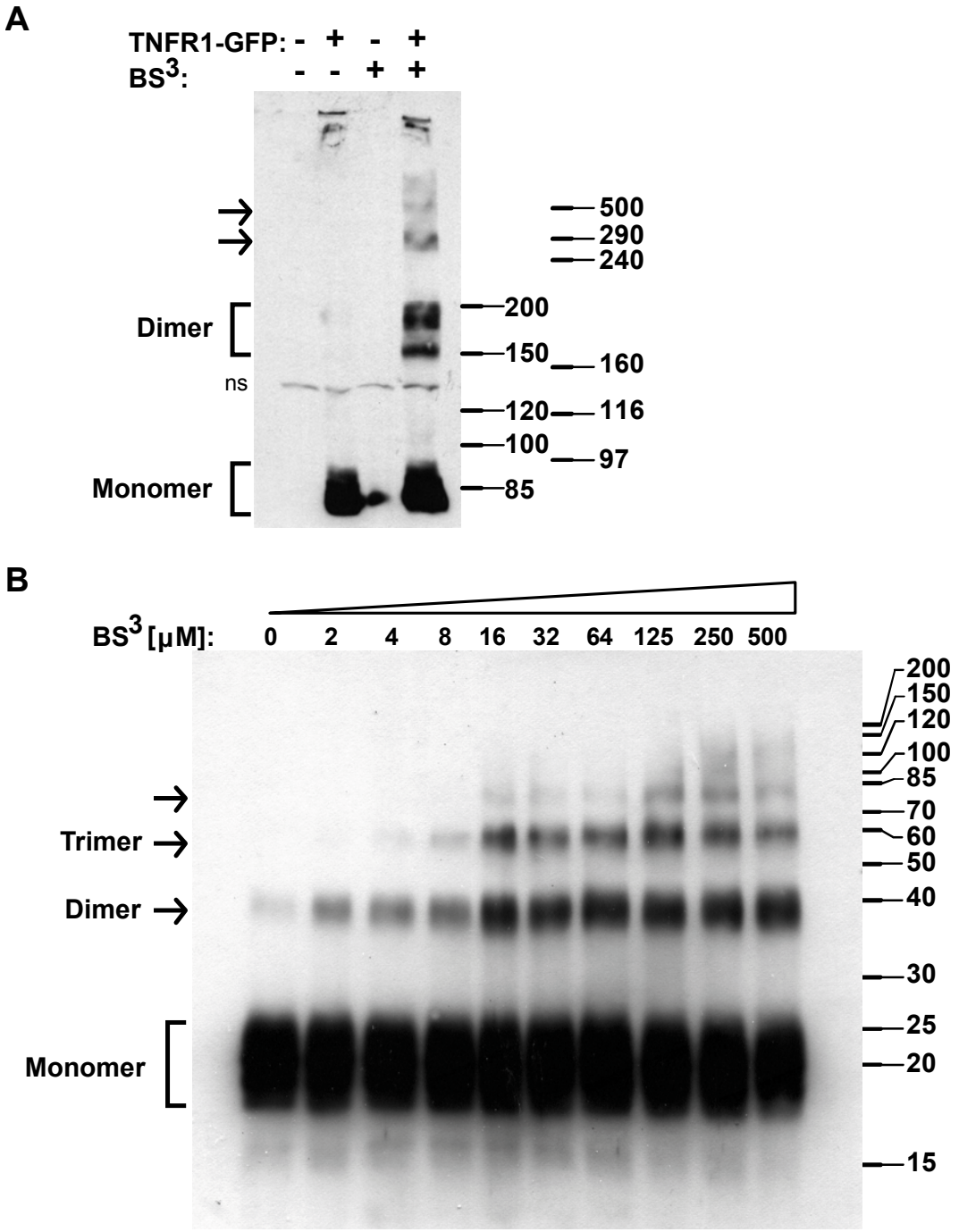

Figure 14: TNFR1 forms aggregates on cells and in solution. A, HEK293 cells were transiently transfected with TNFR1-GFP (+) or not (-) and incubated for 24h in the presence of zVAD-fmk (20 µM). Cells were harvested, aliquoted and incubated for 30 min on ice with the chemical crosslinker BS^3 (+) or not (-). Soluble proteins were separated by reducing SDS-PAGE and analyzed by Wesern Blotting with GFP-specific antibodies. Monomeric, dimeric and higher MW species are indicated by brackets and arrows to the left, whereas the two used protein standards are given to the right; ns = non-specific bands. **B**, The recombinant, purified extracellular domain (600 ng of soluble TNFR1) was incubated with increasing concentrations of BS^3 (2-500 µM). Proteins were analyzed by reducing SDS-PAGE and Western Blot analysis using a TNFR1-specific antibody (clone H5). The positions of unstained molecular mass markers are indicated in kDa at the right. The arrows and brackets identify monomer-, dimer- and trimer formation of TNFR1. Representative experiments out of three are shown.

expressed in the presence of the caspase inhibitor zVADfmk and then crosslinked with BS^3 (Fig. 14A). Using a GFP-specific antibody, the TNFR1-GFP-dimer could be easily detected, as well as higher molecular weight species of above 240 kDa (Fig. 14A) probably indicating a the formation of a TNFR1-GFP trimer under these expression conditions. To analyze if TNFR1 can homo-multimerize without the stem-, transmembrane- and intracellular regions, a baculovirus expressed and purified soluble variant of TNFR1 (Moosmayer et al., 1996) was analyzed by chemical crosslinking (Fig. 14B). Here, two effects were observed. First, even high concentrations of BS^3 were not capable to quantitatively crosslink the soluble, extracellular part of the receptor, as is evident from high amounts of the monomeric species. Second, and in contrast to all membrane-anchored receptors analyzed so far, the soluble TNFR1 variant formed a ladder that consisted of dimers, trimers, tetramers and probably even higher molecular weight species (Fig. 14B). To analyze if the purified, full-length *wt* TNFR2 molecules also homo-multimerize, the affinity-purified protein (Moosmayer et al., 1996) was also analyzed and was found to mainly form a dimer after crosslinking (Fig. 15).

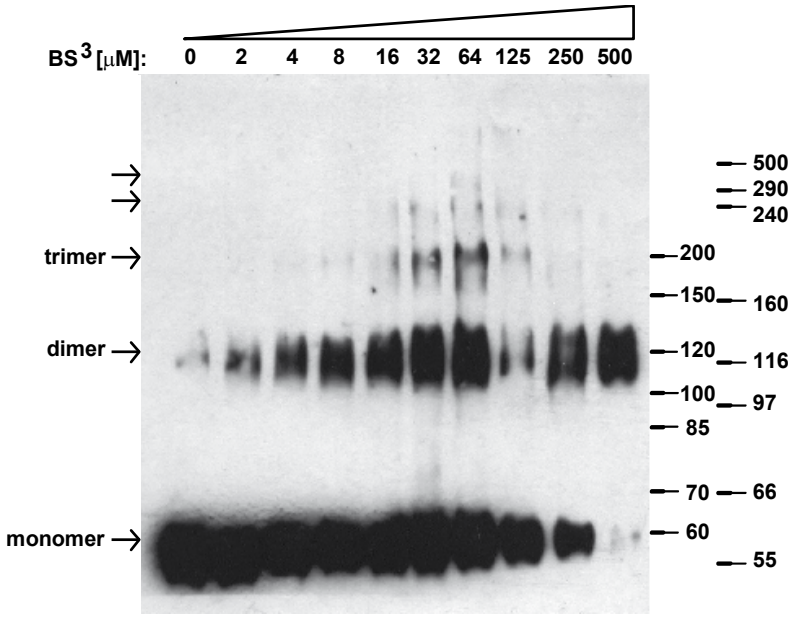

Figure 15. TNFR2 mainly forms dimers in solution. Crosslinking of recombinant, purified, human, full-length TNFR2. Identical amounts of protein (600 ng/lane) were incubated 30 min. on ice with increasing concentrations of crosslinker (BS^3). TNFR2 complexes were resolved by reducing SDS-PAGE (4.5% / 6.25%) and analyzed by Western Blotting with a monoclonal antibody (goat-anti TNFR2, R&D). Shown is a typical experiment performed four times. The two molecular weight markers used are shown at the right.

In addition, the reaction was nearly quantitative, as the monomer decreased almost completely with increasing BS^3 concentrations. Thus, both receptors for TNF have the capability to form ligand-independent interactions that may lead to hexagonal arrangements on the cell surface after ligand binding.

3.2.3 Recombinant CRD1 of TNFR2 shows only a very weak self-association

Currently all anti-rheumatic therapies with drugs biotechnologically produced target TNF. The side-effects, likely due to the blockade of both TNF-receptors, are the increased risk for opportunistic infections, reactivation of latent tuberculosis and so far unexplained cardiovascular effects (Schiff et al., 2006). Therefore, a receptor-selective modulation of TNF signaling could be of advantage. As the CRD1 of TNFR1 and TNFR2 is crucial for functional receptors during i) ligand binding and ii) complex formation, an excess of CRD1 proteins could potentially be used to target TNFR1 or TNFR2. In addition, the CRD1 should form homo-multimers. The proteins could be tested *in vivo* with mice that overexpress human TNFR2 and develop spontaneous auto-inflammatory syndromes (Douni and Kollias, 1998). The methylotrophic yeast *Pichia pastoris* was used to express the coding sequences of CRD1 of TNFR2 ($CRD2_{TNFR2}$). The peptide was composed of the $A1_{CRD1}$ and the $B2_{CRD1}$ modules, fused to a myc and his_6 sequence via a protease-cleavable linker (Fig. 16A).

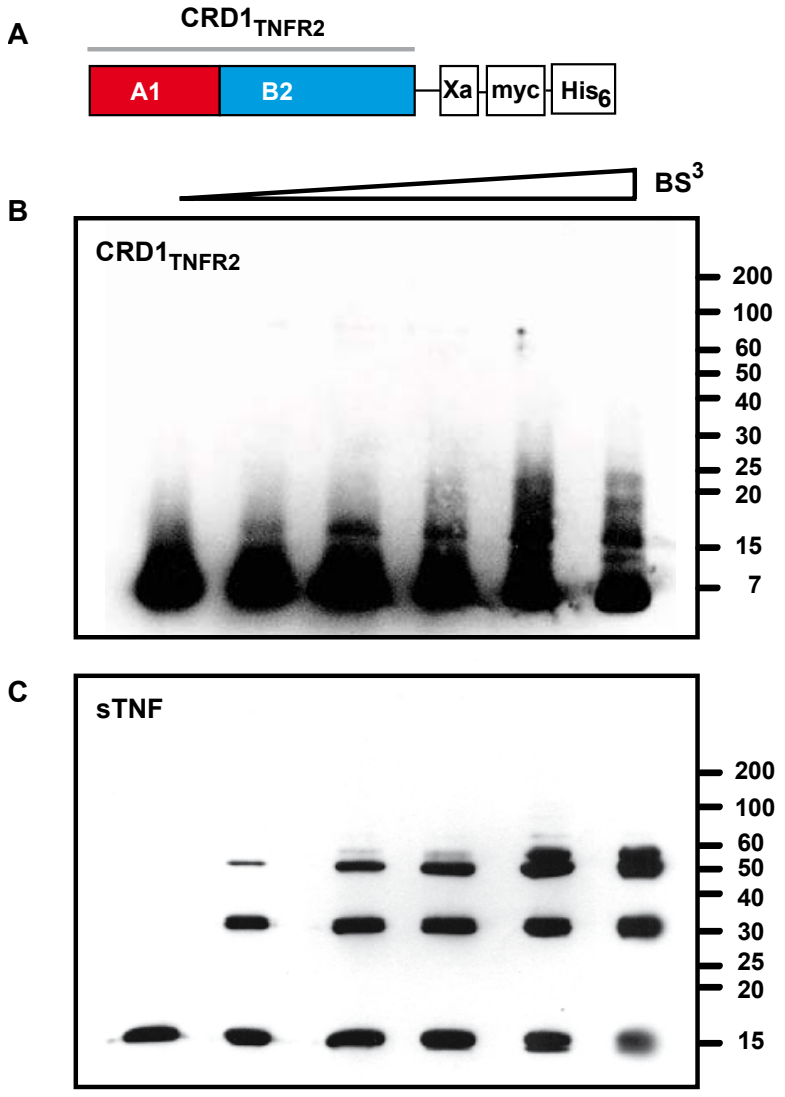

Figure 16: The CRD1 promotes homophilic interactions. (See below)

Figure 16: The CRD1 promotes homophilic interactions. A, Schematic drawing of $CRD1_{TNFR2}$. The molecule consists of an A and a B module, fused to a myc- and a His-tag that can both be cleaved-off via protease treatment (Factor Xa site). **B** and **C,** Chemical crosslinking. The CRD1 from TNFR2 without any tag (B) and soluble, human TNF (C) were treated with increasing amounts of the crosslinker BS^3, separated by reducing SDS-PAGE (4.5% / 12.5%) and detected with specific antibodies for TNFR2 (goat anti-huTNFR2, R&D) or human TNF (mouse-anti TNF, clone T3). Fig. 16B was overexposed. Shown data were from a single typical experiment independently performed three times.

Bacteria appeared to be not well suited, since six cysteines have to form three disulfide bridges and potential N-glycosylation sites exist within the CRDs. In addition, the yeast secretes the protein into the supernatant, uses defined chemical, simple media and contains no endotoxins such as lipopolysaccharide (LPS). Whereas the $CRD1_{TNFR2}$ could be expressed with *Pichia* in 500 ml flask cultures at concentrations of ~2 mg/l the $CRD1_{TNFR1}$ could not be expressed; the reasons remain unclear. To see if the $CRD1_{TNFR2}$ interacts with itself, the protein was analyzed by crosslinking (Fig. 16B) and sTNF was used as a positive control (Fig. 16C). Whereas an overexposed Western Blot of BS^3 treated $CRD1_{TNFR2}$ showed some multimeric species correlating with a dimer or trimer, TNF displayed almost equally strong bands of a monomer, dimer and trimer at moderate BS^3 concentrations. These data indicate that the self-association of $CRD1_{TNFR2}$ is very weak. In addition, $CRD1_{TNFR2}$ was analyzed by mass spectrometry (Fig. 17A, lower panel) and high-performance liquid chromatography (HPLC; Fig. 17B) for molecular size and radius. In accordance with the calculated mass, a peak was detected at 6.8 kDa that represents $CRD1_{TNFR2}$ (Fig. 17A, lower panel). As a positive control, carrier-free sTNF was used (Fig. 17A, upper panel) and detected at 17.3 kDa. Thus, the sizes and amino acid sequences were as expected. Due to the predicted globular shape of CRD1 from the TNFR1 crystal structure, HPLC appeared to be suitable to analyze if $CRD1_{TNFR2}$ shows any signs of aggregation in solution. Using physiologic salt conditions (PBS as the mobile phase), the protein eluted before the cytochrome *c* (12.4 kDa) standard (Fig. 17B, upper panel), indicating a dimer. If this were the case, high salt conditions should disrupt any polar protein-protein interactions and dissociate potential $CRD1_{TNFR2}$ dimers. Thus, increasing salt amounts were added into the mobile phase (Fig. B, lower panel). Whereas the $CRD1_{TNFR2}$ peptide indeed eluted at later time points, the cytochrome *c* marker eluted earlier. Both effects contributed to the apparent shift of the $CRD1_{TNFR2}$ elution peak towards the smallest standard protein used (aprotinin, 6.5 kDa). However, it was not possible to dissociate the CRD1 peptide into two clear, equally high elution peaks with varying salt amounts (not shown). Thus, non-specific adsorption to the column material seems to have caused a peak of apparent dimeric $CRD1_{TNFR2}$ in PBS. Thus, the majority of the $CRD1_{TNFR2}$ peptide was likely to be not functional.

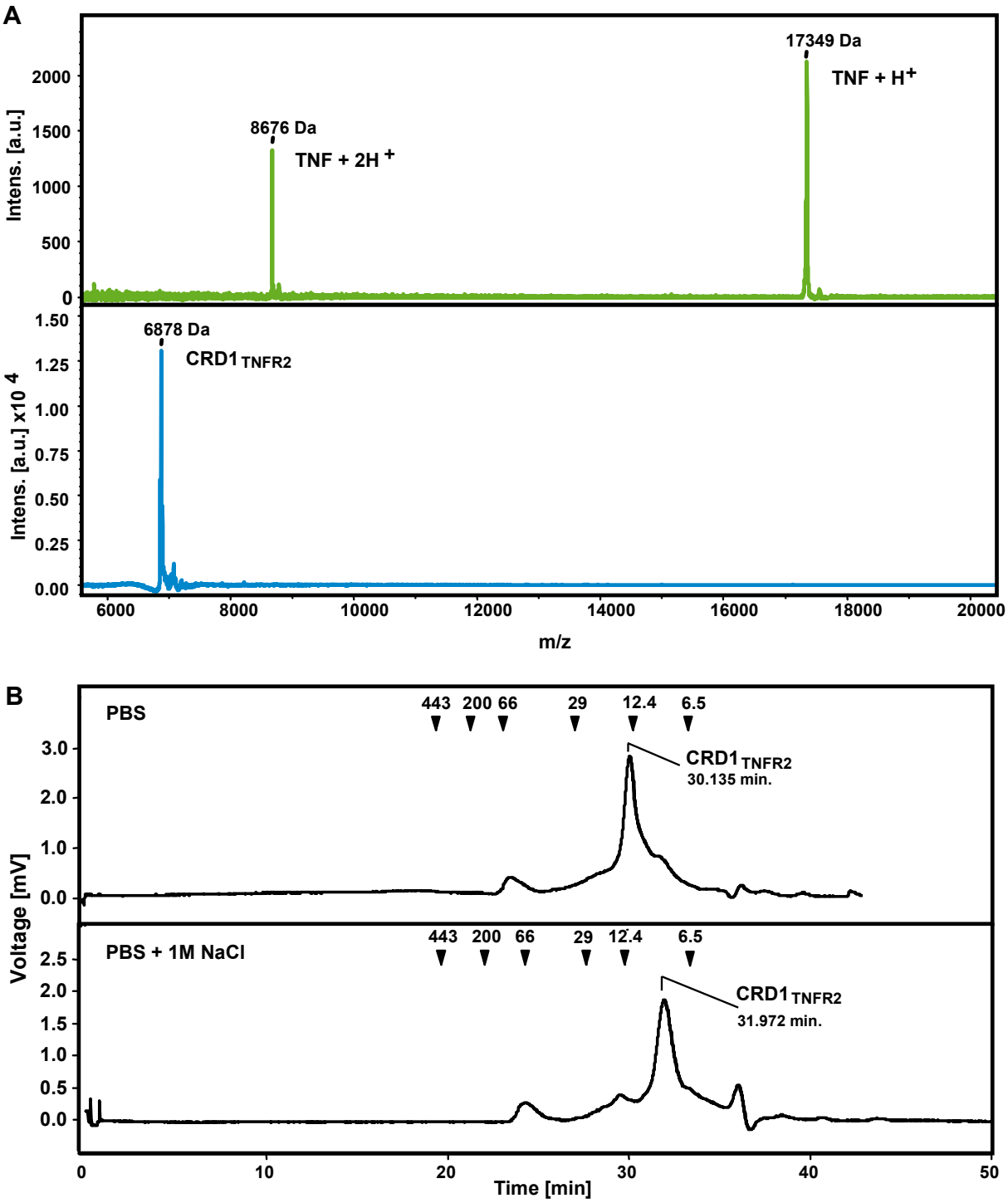

Figure 17: Molecular characterization of purified CRD1$_{TNFR2}$. A, Mass spectroscopy of soluble TNF (upper panel, green) and CRD1$_{TNFR2}$ (lower panel, blue). The determined masses (Da) and protonation statuses (H^+) are given. **B**, Size exclusion chromatography/HPLC of CRD1$_{TNFR2}$ under low-salt (PBS, upper panel) or high salt (PBS + 1M NaCl, lower panel) conditions. The elution times of MW-standards (in kDa) are indicated by arrowheads. Note that CRD1$_{TNFR2}$ elutes before cytochrome *c* (12.4 kDa) at low salt conditions and between cytochrome *c* and aprotinin (6.5 kDa) at high salt conditions. The peak around 38 min. is the running front of the buffer. Shown data were typical for three independently performed experiments.

3.3 Chapter III

3.3.1 Different crystal structures can be used to built *in silico* a large ligand-receptor cluster, but this complex may be non-functional

As mentioned before, several crystal structures have been determined for TNFR1. Whereas the LTα-TNFR1 structure showed no receptor-receptor interaction (Banner et al., 1993), all structures without ligand displayed dimers of soluble TNFR1 molecules (Naismith et al., 1995; Naismith et al., 1996a; Naismith et al., 1996b). Naismith and colleagues have therefore proposed a signaling mechanism that anticipated the formation of clusters composed of trimeric ligands connected by two interacting receptors (Naismith et al., 1995). However, the scientific view since the seminal publication of David Banner and colleagues in 1993 was that the trimerization of receptors, induced by the homotrimeric ligands of the TNF superfamily, induced receptor-signaling. This view has been refined recently into a model in which TNF "slides" into pre-formed receptor trimers (Chan, 2000). As increasing evidence of large receptor-ligand clusters is available (Krippner-Heidenreich et al., 2002; Siegel et al., 2004; Henkler et al., 2005), the idea similar to what Naismith and colleagues had proposed was approached. Therefore, an *in silico* cluster was built by "fusing" the available crystal structures of LTα-TNFR1 (pdb entry 1TNR; Fig. 18A) with that of the parallel, dimeric TNFR1 structure obtained at pH 7.5 (pdb entry 1NCF; Fig. 18B). The resulting intermediate (Fig. 18C) was used to add an additional LTα-TNFR1 complex (Fig. 18D). Whereas the overlay of TNFR1 from the two crystal structures almost perfectly fitted, the two individual LTα-TNFR1 complexes were tilted towards each other by 38.5° (Fig. 18D and E). This is due to the fact that in the dimeric/parallel crystal structure (Fig. 18B) receptor-receptor contacts are formed by the CRD1 and the CRD4: Whereas the CRD1 receptor chain A is in touch with chain B on the front, CRD4 of chain A contacts chain B on the back side. Thus the structure looks like "two embracing bananas", therefore resulting in the observed rotation of the built complex. The result from the experiment therefore showed that a change in receptor orientation has to occur if (i) interactions found within the two crystal structures are existent on a cell and if (ii) aggregates form by dimeric receptor interactions as discussed here.

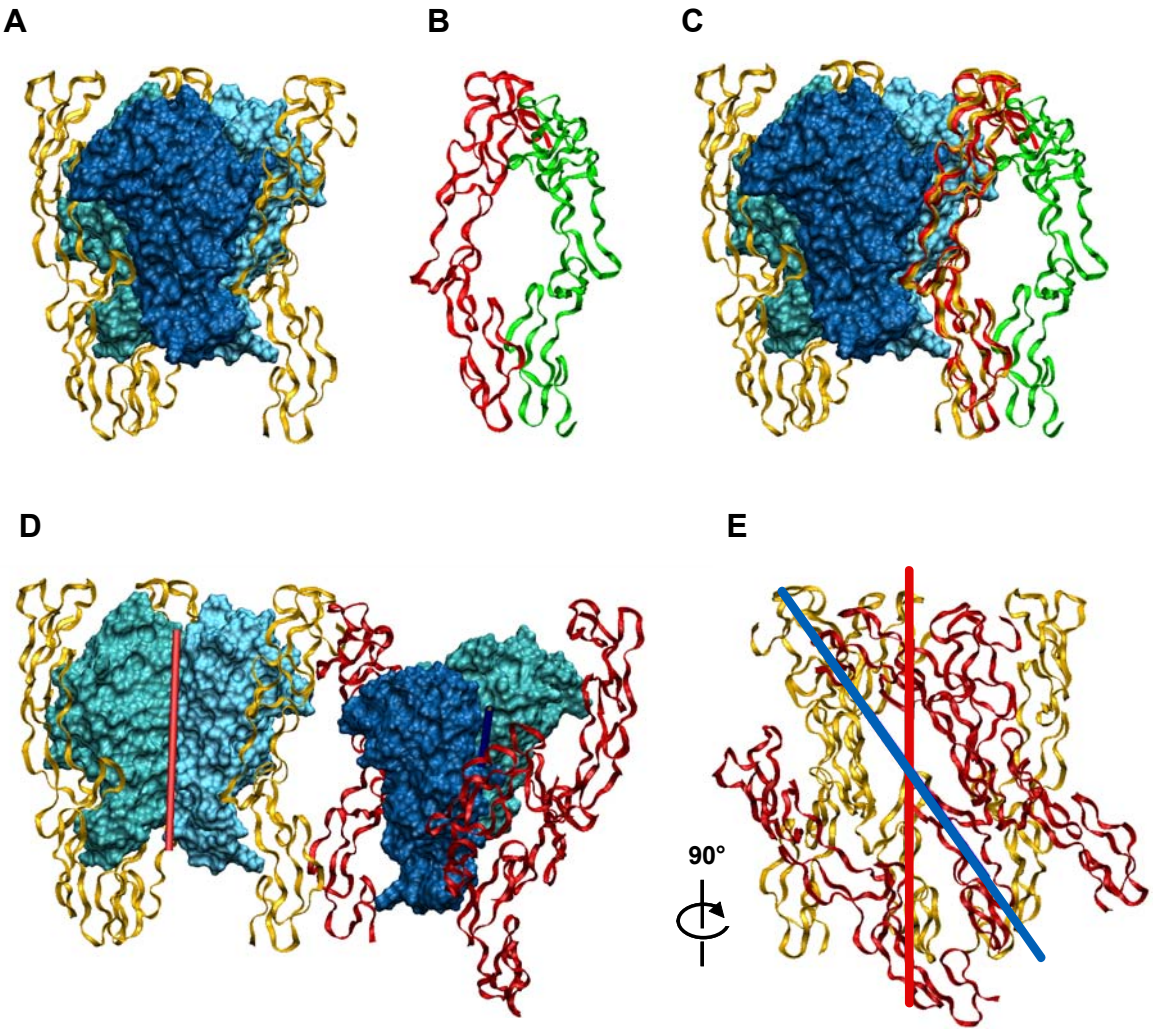

Figure 18: The crystal structures of the bound and the unbound (parallel) TNFR1$_{ex}$ can be superimposed, but leads to a cluster of [LTα-TNFR1$_{ex}$] units that are tilted by 38 degrees. A, The crystal structure of the homotrimeric cytokine LTα with three bound TNFR1$_{ex}$ chains is shown (1TNR.pdb). The cytokine is depicted as a space-filling model with blueish colors for each subunit and the receptor chains are shown in ribbon representation in yellow. **B**, TNFR1$_{ex}$ crystals that were obtained at pH 7.5 (1NCF.pdb) are in parallel orientation. The two chains are in ribbon representation and are shown in red (chain A) and green (chain B). **C**, Receptor chain A of the parallel structure (shown in Fig. B) was superimposed with a receptor chain of the bound structure (shown in Fig. A). Note that free receptor (red) is only slightly more curved than bound receptor (yellow). **D**, The bound structure (shown in Fig. A) was superimposed with the second receptor chain of the moved dimeric structure (green color, Fig. C). Shown are the central LTα molecules as space-filling models (blue colors) and three receptor chains (ribbon representation; orange and red) for each LTα molecule. To demonstrate that the two [LTα:TNFR1$_{ex}$] complexes are tilted towards each other, one of the three subunits of LTα was removed to show the central axis of each complex as a red or blue cylinder. **E**, Same as in (Fig. D), but the LTα molecules were completely removed and the complex was vertically rotated by 90 degrees to show the angular tilt, demonstrated by the red and blue lines that indicate the vertical axes of the two complexes.

3.3.2 An alternative, compact hexagonal arrangement of ligand-receptor complexes

In an additional approach to generate a large receptor-ligand aggregate a molecular docking experiment was performed in cooperation with the group of Prof. Dr. M. Zacharias (University of Bremen). Therefore, the LTα-TNFR1 complex (Fig. 18A) was treated as a single molecule that was allowed to arrange with other identical complexes. The result, as shown in Fig. 19A, was a compact hexagonal cluster of six LTα-TNFR1 complexes. The individual LTα-TNFR1 complexes, when viewed from the top, may be regarded as triangles. In contrast to the lattice shown previously (Fig. 13B), this arrangement utilizes the edges of the triangles to form the contacts between complexes (Fig. 19A). Although these data are preliminary, the arrangement proposed would require stabilizing steric and electrostatic interactions provided by receptor(s) and ligand(s).

Therefore the electrostatic potential of the LTα-TNFR1 complex was calculated. The result is shown in Fig. 19B. Interestingly, the charge distribution was found to be complementary between two adjacent complexes and perfectly matched to each other (Fig. 19B). By continuing the formation of a lattice as in Fig. 19 the formation of a central “ring” of six TNFR1 molecules (in blue color) was observed. This feature is not found in the dimeric, “wide” arrangement (Fig. 13B). In addition, the receptor-receptor contacts in Fig. 19A are different and likely to be rather weak, because only small parts of the CRD1 form contacts to each other. Thus additional stabilizing mechanisms such as the plasma-membrane are likely to be required.

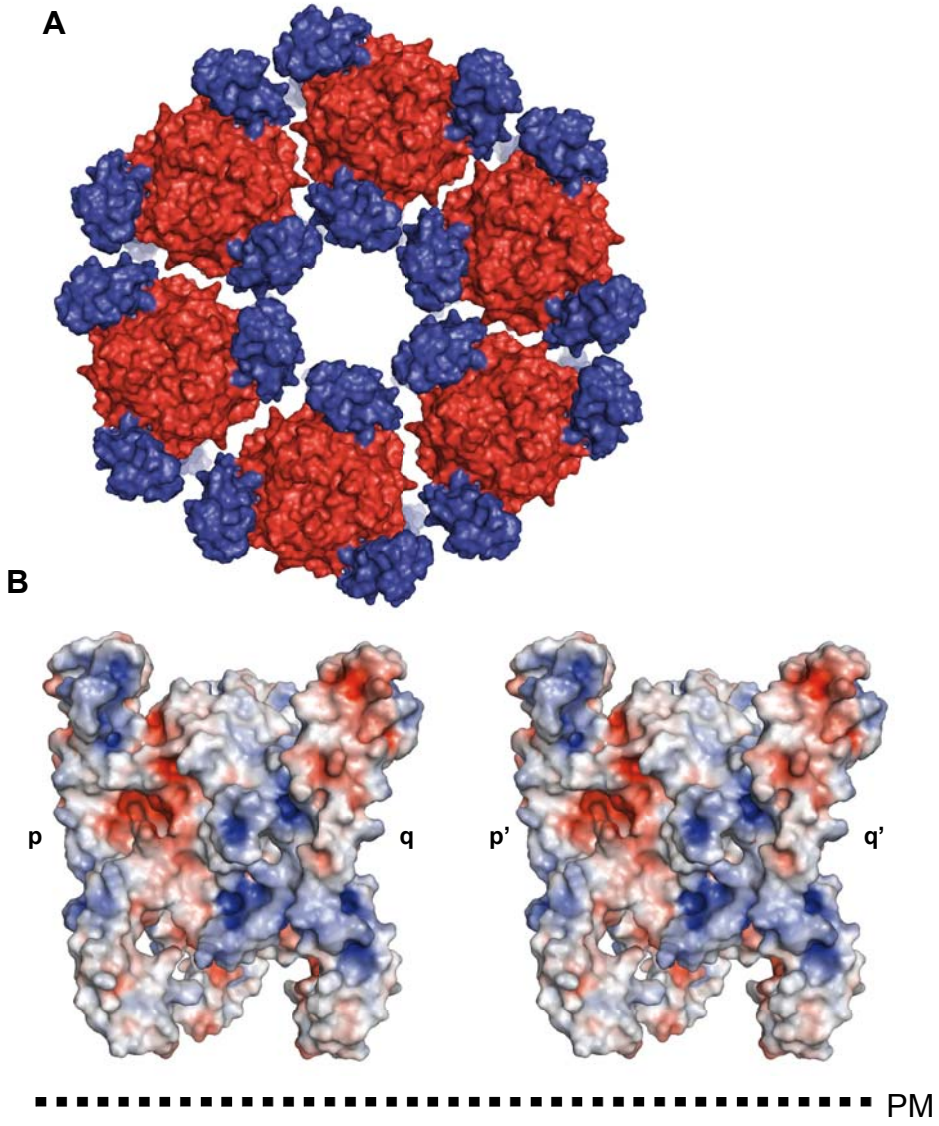

Figure 19: An alternative, compact model of a ligand-receptor lattice. A, Protein docking experiments. In cooperation with Prof. Martin Zacharias (University of Bremen), LTα-TNFR1 complexes were allowed to arrange themselves *in silico* into a two-dimensional lattice by translational and rotational movement. The result of the experiment is showed that LTα-TNFR1 complexes (receptors = blue; homotrimeric LTα = red) are arranged into a hexagonal lattice. Six LTα-TNFR1 complexes are shown. For clarity, complexes were manually separated to better distinguish between them. Note, that the contact interface between individual complexes includes ligands and receptors. **B**, Electrostatic potential of two LTα-TNFR1 complexes. Shown are two complexes that were horizonally rotated by 90°, such that the plasma-membrane (PM, indicated by a dashed line) would be below the receptors. Complexes are depicted as an “open book view” to visualize the contact interface discribed in (A). The negative potential was colored red and is displayed at -4*k*T level, the positive potential was colored blue and is displayed at +4*k*T level (T = 310K). The letters indicate which sides of the complexes interact in an arrangement as described in (A), namely p with q‘ and q with p‘. Note that the charges and sufaces are complementary.

4. Discussion

4.1. The multiple roles of CRD1 from TNFR1

The first part of the presented work focuses on the membrane-distal, first out of four TNFR-characteristic cysteine rich domains (CRD1). Lenardo and colleagues deleted the CRD1 of several members of the TNFR family (e.g. TNFR1, TNFR2, Fas) in all cases leading to molecules unable to bind their respective fluorescently labeled ligand, as determined by FACS analyses. It was argued that a defective pre-association into trimeric receptors is the cause for the loss of ligand binding. In accordance with Lenardo and colleagues, the deletion of CRD1 from TNFR1 or TNFR2 leads to receptors completely unresponsive towards sTNF or CysTNF at physiological concentrations (Fig. 2). As will be discussed later, an avidity-based effect is likely to contribute to high affinity binding of TNF to TNFR1. We used here a highly sensitive method to detect bound ligand applying radiolabeled TNF, which should still allow the detection of TNF bound to a single receptor. However, when the CRD1-deleted TNFR1 mutants were analyzed, no specific binding of sTNF could be detected using two different expressing cell lines (Figs. 5E and 10H). Similar results were obtained for TNFR2 molecules lacking CRD1 (not shown). To analyze if the deletion of CRD1 has a structural effect on the CRD2, molecular dynamics simulations of TNFR1 were performed. Indeed, these data indicated that the first module of CRD2 (namely $A1_{CRD2}$) which is essential for ligand binding undergoes major conformational changes when the CRD1 is lacking (Fig. 3D). Three additional findings support this scaffolding hypothesis.

First, Lenardo and colleagues generated TNFR1 point mutants to analyze dominant interference (associated with receptor-receptor interactions) and ligand binding (Chan et al., 2000). Two aa mutations within CRD1 (KY19/20AA and K32A) were argued as to be unexpected to disturb the overall structure. However, looking in detail at the localization within the TNFR1-LTα structure, K19 and Y20 are located on the $A1_{CRD1}$ and K32 is located on $B2_{CRD1}$. Importantly, K32 and Y20, although at different sequential positions, localize at the same three-dimensional site, namely at the interface between CRD1 and CRD2, directly on top of the A1 of CRD2. Whereas Y20 packs against H66 of $A1_{CRD2}$, K32 comes from the opposite side, reaches through the receptor and also packs against the $A1_{CRD2}$, namely aa E64N65. Accordingly, the Y20 and K32 residues are involved in the herein described scaffolding of CRD2, although localized on CRD1. On the other hand, the single mutation of K19E had no effect, which can be understood since this aa is located at the surface of TNFR1 and points away from the receptor and from the ligand.

Second, when the CRD1 of TNFR2 was first fused with the CRD2 of TNFR1 ($CRD1_{TNFR2}$-TNFR1-Fas), the molecule produced was unresponsive towards sTNF (data not shown). This was in accordance with Lenardo and colleagues who reported a similar observation (Chan et al., 2000). This first fusion protein consisted of the $CRD1_{TNFR2}$, fused by an aspartate to

$CRD2_{TNFR1}$. A closer view at the amino acid sequences of both TNFRs revealed, however, that the CRD1s and CRD2s are separated in both cases by two amino acids, rather by a single one (Supplement 6.2). Thus the restoration of a spacer composed of two amino acids between these two CRDs also restored the functionality of the chimeric receptor analyzed here (Fig. 9F). In light of these data, it seems likely that in the first approach the CRD1 was "too close" to CRD2, thus probably pressing against the A1 of CRD2 and causing a non-functional deformation that abolished ligand binding. Interestingly, the CRD1 deleted Fas molecule (ΔCRD1-Fas) was reported also not to be capable of ligand binding and the molecule could be rescued with the CRD1 of TNFR1 (Orlinick et al., 1997).

Third, the TNFR1-related molecule HVEM also consists of four CRDs. CRD1 and CRD2 of HVEM each show amino acid sequences typical for A1 and B2 modules and are thus similar to TNFR1 and TNFR2 (Naismith and Sprang, 1998). HVEM can be bound by the herpes simplex virus glycoprotein D (gD) and deletion of CRD1 or CRD2 abolished gD binding (Whitbeck et al., 2001). The crystal structure of HVEM in complex with gD confirmed that gD binds to the CRD1 as well as to a small region of three aa of the subsequent CRD2 (Carfi et al., 2001). However, later mutational analyses of the contact sites between gD and HVEM revealed that the CRD2 is only indirectly required for gD binding (Connolly et al., 2002). The authors thus proposed that the CRD2 is required to stabilize the gD binding site located on the B2 of CRD1. These results are in accordance with the scaffolding hypothesis of CRD2 provided for CRD1 in the TNFR1 molecule.

Deletion of only the A1 of CRD1 also leads to a functional TNFR1 molecule displaying high affinity ligand binding (Figs. 4D and 5C). These data are in accordance with reported $A1_{CRD1}$ deletions of CD40 (Malmborg Hager et al., 2003) and Fas (Siegel et al., 2000) which can still bind to CD40L and FasL, respectively. When expressed in high numbers on HEK293 Flp-In T-REx cells, $\Delta A1_{CRD1}$-TNFR1-Fas molecules were capable of inducing spontaneous cytotoxic effects, although less effective as compared to the full-length TNFR1-Fas molecule (Fig. 7B and E). In addition, the IL-8 release assay showed that TNFR1-Fas can fully inhibit *wt* TNFR1 signaling (Fig. 8), most likely via the formation of non-functional TNFR1:TNFR1-Fas receptor complexes. Similarly, down-regulation of signaling by the formation of receptor heteromeres has also been recently discussed for the TRAILR system (Clancy et al., 2005; Merino et al., 2006). Therein decoy-receptors without intracellular domains may be expressed simultaneously with the full-length receptors (Marsters et al., 1997).

The dominant effect of the TNFR1-Fas molecules on TNFR1 signaling was shown to be dependent on the CRD1, as the deletion (ΔCRD1-TNFR1-Fas) showed no inhibitory phenotype (Figs. 8C and I). However, this molecule could also not bind to TNF. The $\Delta A1_{CRD1}$-deleted molecule was capable of ligand binding and showed inhibition of *wt* TNFR1 signaling, however only at higher TNF concentrations. This observation indicates a ligand-

dependent recruitment into non-functional complexes and a weak receptor-receptor interaction. When MEFs expressing the $\Delta A1_{CRD1}$-TNFR1-Fas molecule where analyzed shortly after their FACS-sorting they displayed high affinity for sTNF (not shown), albeit requiring CysTNF for cytotoxicity induction (Fig. 4D). This effect is likely to be caused by a decreased receptor-receptor interaction, also suggested by the functional studies with the inducible HEK293 cells (Fig. 7). Thus, the disulfide-linked CysTNF molecules may have provided the multimerization that the $\Delta A1_{CRD1}$-TNFR1-Fas molecule lacks, but is essential for the formation of a functional ligand receptor aggregate.

An alternative argument would be that low receptor numbers (~4000 binding sites) are present on the cell surface of MEFs and thus CysTNF is required for efficient cluster formation. However, when calculating the amount of occupied receptors at concentrations of 100 ng/ml with an affinity of ~200 pM, approximately 90% of all receptors are saturated. Thus, several thousand receptors are ligated, yet are not functional, whereas *wt* TNFR1 is on some cells expressed in numbers of few hundred and still is capable to induce receptor-ligand clusters and thus signaling.

The use of chemical crosslinking to analyze if $\Delta A1_{CRD1}$-TNFR1-Fas molecules have a reduced self-association gave no clear results (data not shown). In cell lines investigated, (MEFs and inducible HEK cells) the intensities of bands from Western Blotting corresponding to monomeric $\Delta A1_{CRD1}$ were very high and did not correlate with the amount detected by FACS analyses. Thus, it may be that a fraction of ΔA1 does not fold properly and is retained within the cell. Such effects are quite well known and may result in the so-called unfolded protein response, UPR (Wu and Kaufman, 2006). However, the UPR was not investigated, as it is not likely to interfere with the functional analysis of CRD1. In accordance with the Western Blot analysis, the amount of binding sites detected with sTNF on $\Delta A1_{CRD1}$-TNFR1-Fas HEK Flp-In cells was always smaller as compared to full-length TNFR1-Fas HEK Flp-In cells. Whether this non-binding receptor species represents an abnormal, probably disulfide-linked class of molecules is not known. However such a mechanism may explain why only ~50% of $\Delta A1_{CRD1}$-TNFR1-Fas expressing MEFs died upon CysTNF stimulation, whereas non-responsive cells may have higher amounts of miss-folded receptors that somehow inhibit signaling (Fig. 4D). Since the PLAD-function seemed to be intact to some degree, it could well be that these receptors form disulfide linked dimers on the cell surface, or already within the cell. Such a mechanism has been reported to be one cause for a disease termed TNFR1-associated auto-inflammatory disease, TRAPS (Lobito et al., 2006; Todd et al., 2004). TRAPS patients display spontaneous inflammatory responses, sometimes locally restricted and have mutations localized mainly within the CRD1 (McDermott et al., 1999). More precisely, the most penetrating effects are caused by mutations that target the cysteines of CRD1, thus leaving one cysteine without an intra-chain binding partner.

Although speculative, the accumulation of disulfide-connected TNFR1 molecules could start the ligand-independent signaling of TNFR1 when reaching a certain threshold of molecules and thus lead to local inflammation.

Nevertheless, the $\Delta A1_{CRD1}$ deletion mutant bound to TNF with high affinity (Fig. 5C). However, during microscopical analysis, a low amount of bound labeled TNF was detected (Fig. 6C). The incubation time of 20 min. for Alexa-546-coupled sTNF during confocal microscopy may have been too short to reach saturation in ligand binding. However, the red staining did not increase during the microscopical analysis, although labeled TNF was present throughout the experiment (not shown). This may indicate a different mechanism. For instance TNF molecules may only transiently be bound but are lost quickly. Alternatively or in addition, the initially, microscopically observed homogeneous staining for full-length TNFR1-Fas could in fact already represent some kind of aggregation involving an avidity based binding mechanism. Thus if the receptor-receptor interaction is weakened for the ΔA1 molecule less ligand is effectively bound.

4.2 Molecular localization of the PLAD and its role in sTNF responsivity

Herein, the pre-ligand binding assembly domain (PLAD) has not been identified and data presented do not allow the molecular localization. However, using chimeric TNFR1-Fas molecules it is shown that the $B2_{CRD1}$ is required for i) ligand-independent signaling ii) ligand binding and iii) dominant inhibition of TNFR1 after ligand binding. In the simplest interpretation, the same parts of CRD1 are responsible for receptor-receptor association before and after ligand binding. However, since the CRD1 deletion also affects the CRD2, the pre-ligand binding domain may also be partly located on the CRD2. Indeed, in the anti-parallel crystal structure two TNFR1 molecules interact via their CRD2 domains (Fig. 20B). Thus, the CRD1 may also contain a distinct post-ligand binding domain required for functional ligand-receptor complexes after ligand binding. How TNFRs are arranged on the surface of the plasma-membrane and which domains are involved in each conformation is not known. However, there appears to be a hierarchy of domains that influence receptor self-association. The CRD1 contributes the major part to self-association, as deletion of CRD1 dramatically reduces crosslinking efficiency with BS^3 (Fig. 9G). Interestingly, the CRD1 exchange mutant displayed weaker sTNF responsiveness, interpreted as a reduced receptor self-association from chemical crosslinking studies (Fig. 9H). Accordingly, this molecule displayed a higher demand for ligand-mediated multimerization (Fig. 9F). In addition, there was a tendency for a higher TNF binding affinity at 4°C (Fig. 10E and i). Although contradictory at first sight, these data fit together with that of TNFR2. This molecule also displayed a higher saturation binding affinity constant (and faster k_{on}) at 4°C as compared to TNFR1 (Grell et al., 1998), yet requires a membrane-like ligand to signal.

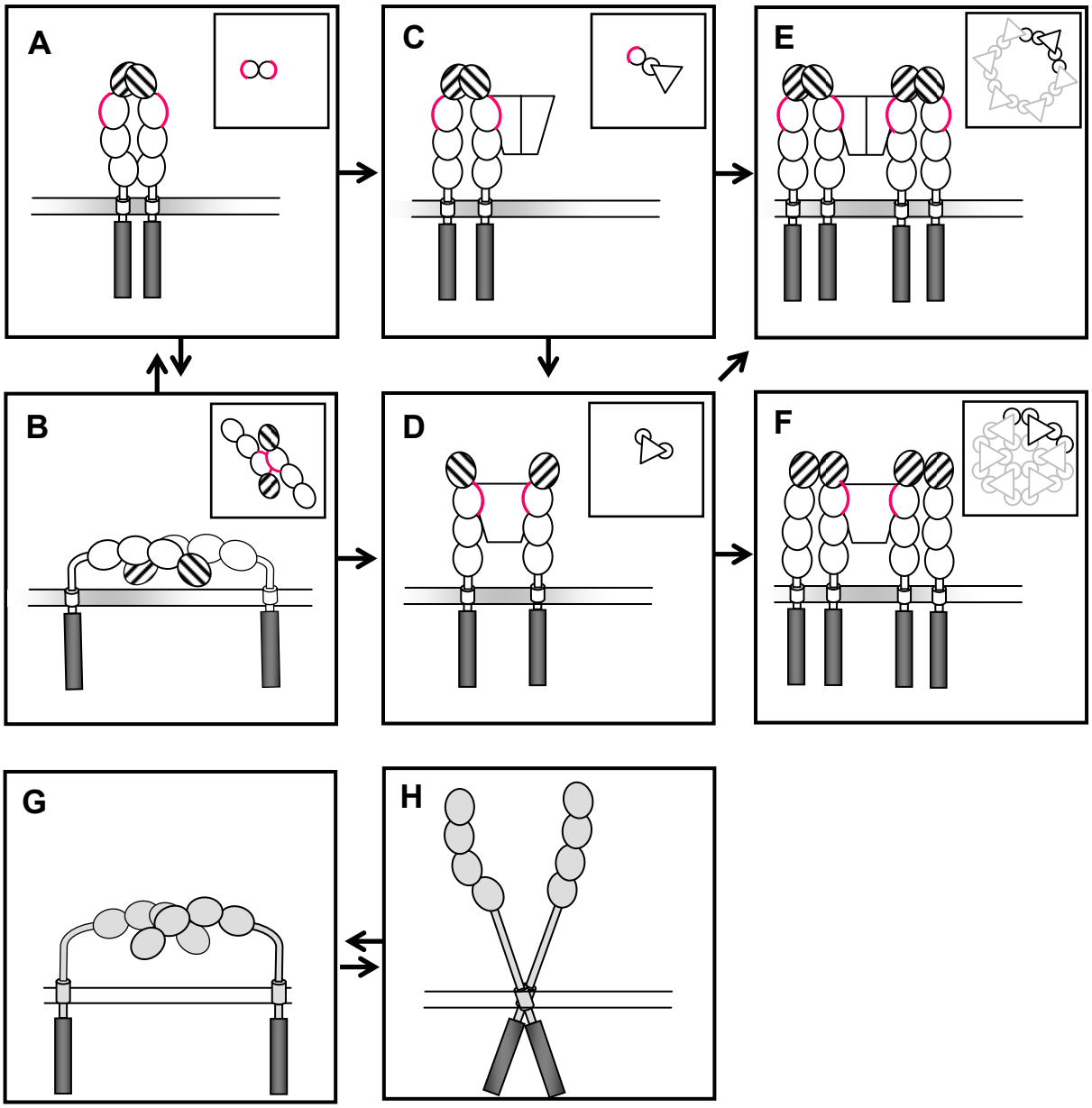

Figure 20: Possible early events in TNFR signaling. Schematically shown are TNFR1-Fas molecules (A-F) and TNFR2-Fas molecules (G and H). The intracellular Fas domain is shown as a rectangle (dark gray). The four CRDs are indicated by four ovals, whereas the CRD1 of TNFR1 is hatched. The insets show the top view of respective molecules. The ligand binding site is highlighted by a red line and the homotrimeric ligand is shown as a trapezoid (C, D, E, F). Note that the views in C and E are different from D and F: The third receptor binding site is indicated by a vertical line within the ligand in C and E. The plasma membrane is shown as two horizontal lines. Potential lipid microdomains are given as gray shades within the plasma membrane (A-F). **A** and **B,** TNFR1 may exist in two conformtional stages that both do not signal without ligand. Upon addition of the ligand, one (**C**) or two (**D**) receptor chains may bind to TNF. Note that a structural change has occured upon ligand binding (A vs. C and B vs. D). Depending on the aggregate formed, either a rather open (**E**) or tight (**F**) hexagonal lattice may form. The molecules that are shown in E and F are depicted within the inset as black lines whereas the addition of further molecules leading to the hexagonal lattice are shown in light gray. For TNFR2, similar (**G**) or additional (**H**) homophilic receptor interaction types as compared to TNFR1 may exist, but are also hypothetical. The shortening of the long TNFR2 stem region may facilitate a receptor arrangement such as depicted for TNFR1 within (A). Further details for A - H are given within the text.

Although speculative, the CRDs may be involved in keeping the receptor in a non-signaling state. Thus the dimeric receptor may be in equilibrium between several conformational states (see Fig. 20). However, if such a potential silencing mechanism would exist it may not require the CRD1, as the ΔCRD1-TNFR1-Fas molecule resulted in no spontaneous cytotoxic signaling when induced to be expressed in HEK293 Flp-In T-REx cells in high amounts (Fig. 7H). If the pre-ligand, maybe PLAD-mediated homo-multimerization is very strong, then ligand cannot bind. Again, the anti-parallel dimeric crystal structure nicely reflects these demands since the extracellular parts of TNFR1 are arranged such that the TNF binding site is buried (Fig. 20B). However, alternative receptor arrangements may exist that are not signaling competent without ligand (Fig. 20A). If the pre-ligand PLAD affinity is rather weak, it allows the easy transition into the second state, thereby enabling ligand binding. Either ligand binding may occur sequentially (Figs. 20A → C → E) or two receptors bind to the homotrimeric ligand in a single step (Figs. 20A and B → C). Such a scenario of a weak pre-ligand binding self-association may hold true for TNFR2, probably facilitated by a long "stalk" region that increases the TNFR2 radius of action and allows efficient ligand binding at 4°C (see Fig. 20H). At 37°C, however, secondary effects involving the plasma-membrane may take place, as discussed further below. If the pre-ligand binding assembly domain is located on CRD1 and CRD2 or additional CRDs remains to be shown. For instance the CRD1 exchange molecule ($CRD1_{TNFR2}$-TNFR1-Fas) could be used to analyze if a dominant inhibition of *wt* TNFR1 signaling occurs as was observed for the TNFR1-Fas molecule in the inducible HEK293 cell system (Fig. 8A and G).

4.3 The stoichiometry of TNFRs in the absence of ligand

The question remains of whether TNFR1 forms a homotrimer or not. Data of crosslinked receptors have been presented that were separated under non-reducing conditions and detected by Western Blotting (Chan et al., 2000; Siegel et al., 2000). As in these experiments the disulfide bridges were left intact, the receptors should remain in their typical elongated structures. Further, the used molecular weight references used in these studies are likely to have been dye-labeled, because the indicated molecular weights are identical with those of a commercial set of pre-stained markers. In addition, for TNFR1 three marker proteins (62, 82 and 175 kDa) were used to infer that a species of TNFR1 (apparent Mw of 62 kDa) is a trimer, since specific bands of crosslinked receptors were detected close above and below the 175 kDa marker. In the presented work, reducing conditions could be applied due to a non-reducible crosslinker (BS^3 was used here instead of the crosslinker DTSSP). Thus, the characteristic elongated shape of TNFRs plays no role in size determination here. Second, unstained protein standards were used and gels were chosen to optimize resolution for the expected molecular weight range. When TNFR1-GFP was transiently overexpressed and

then crosslinked, the majority of crosslinked species was a dimer of TNFR1-GFP with indeed an additional species that could represent a trimer (Fig. 14A). However, for all TNFR1-Fas derivatives stably expressed in MEFs only a dimer could be detected. The increase in crosslinker concentration (above 1 mM) resulted in a near to quantitative crosslinking, as the monomer band disappeared, however, the dimer band disappeared as well. Thus, at receptor “concentrations” on the plasma-membrane of MEFs (~35,000 binding sites for ^{125}I-TNF) the majority of TNFR1-Fas molecules are likely to be assembled as homo-dimers (Figs. 9H, 11E and 12A). In accordance with these data it was reported that HVEM and the p75 nerve growth factor (NGF)-receptor are homo-dimers (Connolly et al., 2002; He and Garcia, 2004). Both molecules are members of the TNFRSF and are composed of four CRDs, as are TNFR1 and TNFR2.

Increasing the amount of cell-surface TNFR1 molecules could probably enhance the fraction of the trimeric species. Thus, receptors could be thought of being in a dynamic equilibrium of monomers, dimers, trimers and probably even higher multimers, as revealed from the crosslinking of soluble TNFR1 (Fig. 14B). However, the plasma-membrane and/or cytoplasmatic part seem to limit the allowed conformations to a dimer and/or trimer and in addition ease the crosslinking reaction if the proper stem and transmembrane region are present (discussed in 4.4).

When purified, full-length TNFR2 (Moosmayer et al., 1996) was crosslinked (Fig. 15), a near quantitative shift of the monomer to the dimer was observed, in contrast to the soluble TNFR1 consisting of CRD1-4, where large amounts remained monomeric (Fig. 14B). Three reasons may account for this effect, besides a low affinity of TNFR1 towards itself. First, the increased number of reactive amino side chains for the chemical crosslinking reaction, second, the TM-domain and third the intracellular part of TNFR2:

i) Soluble TNFR1 contains 11 lysines residues, but full-length TNFR2 contains 15 lysines, so the numeric increase in lysines may facilitate crosslinking.

ii) TM-domains are hydrophobic and thus “stick” to each other in aqueous buffers. Additionally, three potentially reactive lysine residues are located as a secretory stop-signal just after the TM-domain of TNFR2. Furthermore the TNFR2 TM-domain contains a so-called GxxxG motif (see primary structure in Supplement 6.2) that has recently gained considerable interest (Senes et al., 2004). This motif, composed of two glycines, separated by any three amino acids is thought to generate a flat interface that is used for protein-protein interactions within hydrophobic surroundings. Whether such an interaction holds true also true for TNFR2 remains to be investigated.

iii) Moosmayer and colleagues noticed during cytotoxicity assays on Kym-1 cells that purified, full-length TNFR2 has a superior TNF-neutralization capacity as compared to the soluble, extracellular TNFR2 (Moosmayer et al., 1996). An additional molecule in which the

TM of TNFR2 was deleted was found to be ~65-fold more effective as compared to soluble TNFR2. The authors therefore concluded that the intracellular part of TNFR2 must confer a stabilizing effect. However, although death domains that are found within TNFR1 or Fas are known to mediate aggregation, so far no domain present within TNFR2 (e.g. TRAF binding domains) have been reported to mediate homo-multimerization.

4.4 The effects of the stem- and transmembrane regions on sTNF responsiveness

TNF receptors type 1 and type 2 display different requirements for the ligand in order to initiate signaling. This phenotype has been correlated with the dissociation rate (Grell et al., 1998). This is due to the relationship between the off-rate (k_{off}) and how long a receptor-ligand interaction remains stable ($t_{1/2}$ = ln2/k). When the stem- and transmembrane regions had been exchanged between TNFR1-Fas and TNFR2-Fas (Fig. 11) the signaling capabilities were also switched (Table 3). Thus, a TNFR2-Fas molecule that was constructed to contain the stem and TM region of TNFR1 was responsive towards sTNF. However, the determined half-times of the respective ligand/receptor complexes (Table 3) could not explain this phenotype. One can envisage that a strong receptor-receptor interaction, in combination with a strong ligand-receptor binding leads to cellular signaling. The performed crosslinking studies with BS^3 indeed indicated that this may be true for the analyzed chimeric TNFRs. Therefore, the TNFR2-$(S/TM)_{TNFR1}$-Fas molecule can signal with sTNF because it displays strong self association (Fig. 11F, right upper panel) and in addition the ligand remains bound for ~2 min (Table 3). The TNFR1-$(S/TM)_{TNFR2}$-Fas protein, although having a ligand/receptor half-time of ~8 min does not signal with sTNF, because it has a very weak self-association tendency as determined by chemical crosslinking (Fig. 11E, upper right panel). Thus, crosslinking studies of receptors are important complementary data to the “classical” analysis of receptor-ligand interactions. However, the molecular mechanisms behind the crosslinking phenotypes are not shown and can be discussed in three ways, namely in context with the stem domain, the TM domain and chemical reactivity with BS^3.

First, it is unclear which of the two exchanged domains (stem or TM) are responsible for the responsivities towards sTNF. Whereas the stem of TNFR1 is rather short (14 aa; Supplement 6.2) the stem of TNFR2 is quite long (59 aa; Supplement 6.2) and was reported to be O-glycosylated (Pennica et al., 1993). The computationally predicted transmembrane domains are also different in length. TNFR1 has a “classical” TM length of 22 aa that are perfectly suited to span a membrane as an alpha-helix. On the other hand TNFR2 contains a hydrophobic stretch of 33 aa (Supplement 6.2). Whereas the transfer-stop signal for the membrane-insertion of TNFR2 seems to be clear (three lysines, KKK) and mark the end of a putative TM domain, the “start” is rather unclear. In addition, as mentioned above, TNFR2 contains one or maybe two putative glycine-rich self-association motifs (GxxxG; Supplement

6.2). In addition, recent data indicate that especially the TM parts of receptors determine the localization into specialized lipid micro domains (Pike, 2006). These domains are thought to be enriched with certain lipids such as ceramide and are biochemically characterized by their resistance to detergent extraction on ice and are therefore also called detergent resistant membranes (DRMs) or rafts. Although the raft field may be facing physical-technical limitations (Jacobson et al., 2007), the experiments usually performed to analyze them are nevertheless useful since they allow discrimination between molecules and different stimulation protocols. For instance the pro-apoptotic TNFR family member Fas has been shown to be localized to “lipid rafts” where receptors of type I cells are pre-associated (Muppidi and Siegel, 2004). It had been shown earlier, that for Fas the lipid ceramide is required to form aggregates (Hueber et al., 2002; Cremesti et al., 2001). Several reports are available that also discuss a “raft” association for CD40 (Bock and Gulbins, 2003; Grassme et al., 2002a; Grassme et al., 2002b). The localization of TNFR1 within different membrane domains has been discussed as a discriminator between NF-κB or apoptosis signaling (Muppidi et al., 2004; Legler et al., 2003). Therefore molecules containing the TM-domain of TNFR1 may be stabilized in their (PLAD) interaction by a certain lipid microenvironment (Fig. 20A) and in addition may be locally concentrated. If such microenvironments are large enough a lipid-mediated retention mechanism would help to explain how only a few hundred TNFR1 molecules can produce a signal. As mentioned, usually the distribution into microdomains is studied by detergent extraction at 4°C followed by density gradient centrifugation (e.g. on sucrose). The protocol applied here to extract crosslinked proteins was principally identical (1% Triton X-100 at 4°C), however without the density gradient centrifugation. The crosslinking studies could be performed in combination with disruption of lipid rafts by methyl-β-cyclodextrin (MCD)-mediated cholesterol depletion to see if the amount of dimerized receptors decreases. Similar experiments have been performed for the Fas system (Muppidi and Siegel, 2004). These authors showed that some T-cells die after incubation with soluble FasL. These sensitive T-cells had pre-associated Fas molecules within “rafts” that could be better chemically crosslinked as compared to Fas of resistant T-cells. In favour of such a second interaction type is the observation that overexposed Western Blots of chemically crosslinked CRD1-deleted TNFR-Fas molecules expressed on MEFs revealed bands representing receptor dimers (not shown). This may indicate secondary, but weak receptor-receptor interactions likely to be mediated by other CRDs, the TM-domain or the intracellular Fas domain. However, the main contributor to receptor-receptor dimerization is the CRD1, as this deletion dramatically reduces detectable receptor dimers (Fig. 10G, upper lane).

Second, the long stem-region of TNFR2 may hinder receptor self-association. This may be due to an increase in overall flexibility that could initially ease ligand binding, but secondly

disturb signal transduction into the cell. Interestingly, when the stem-region within the chimeric molecule TNFR1-(S/TM)$_{TNFR2}$-Fas was shortened down to 14 aa yielding TNFR1-(ΔS/TM)$_{TNFR2}$-Fas [(2)], this receptor became responsive towards sTNF (data not shown). However, subsequently performed chemical crosslinking studies showed no increase in self-association (data not shown). Thus, the stem- and TM regions may contribute differentially towards sTNF responsiveness or the chemical crosslinker BS^3 is not suited to distinguish these receptors (discussed further below).

Third, the stem-region of TNFR1 contains a lysine (K174), whereas that of TNFR2 does not. Thus the stem-exchange also altered the number of lysines available for crosslinking. However, whereas TNFR2-Fas contains six extracellular lysines (see Supplement 6.2) and showed an intermediate crosslinking capability (Fig. 11F, upper left panel), the exchange mutant TNFR2-(S/TM)$_{TNFR1}$-Fas gained only one additional lysine through the stem region and displayed strongest crosslinking capability (Fig. 11F, upper right panel). Also, the TNF-unresponsive TNFR1-(S/TM)$_{TNFR2}$-Fas contains eleven lysines available for BS^3, but displayed the weakest dimeric receptor band (Fig. 11E, right upper panel). Thus, the number of lysines available for crosslinking seems not to be the limiting factor for the chemical stabilization of pre-formed receptor dimers. However, this only holds true as long as every lysine can be equally used for chemical crosslinking, which seems rather unlikely due to tertiary and quaternary protein structures. Alternatively, TNFR1 may be in equilibrium between two conformations, the ligand-binding permissive conformation being stabilized by the TM-domains held together maybe via the mentioned DRMs (Fig. 20A). Thus, the TM brings the stem-regions into close proximity and allows for efficient crosslinking between receptors at position K174. The corresponding crystal structure for this hypothesis would be the parallel, head-to-head oriented organization in which soluble receptors form contacts between CRD1:CRD1 and CRD4:CRD4 (Fig. 20A). Interestingly, yeast-2-hybrid data indicated that CRD1 as well as CRD4 [(3)] can form homophilic interactions. However, the parallel oriented TNFR1 molecules cannot be used exactly as determined from the crystal structure to build a large ligand-receptor cluster, as this would lead to a twisting of individual ligand-receptor complexes (see Fig. 18E). Maybe the membrane-anchorage or ligand-binding could alter the CRD4 interaction and lead to a different vertical orientation of the two receptor chains (Figs. 20A versus 20 C). Thus, the head-to-head oriented ligand-free crystal structure may indicate homophilic interactions between CRD1 and CRD4 however may be not precisely identical as if the full-length receptors were within the PM and ligated.

Such a conformational change mechanism in combination with a shift of the equilibrium form a non-signaling towards an easy signaling configuration may also be the case for the

[2] A. Krippner-Heidenreich and A. Zappe, personal communication.
[3] Group of M. Lenardo, personal communication.

discussed data of the TNFR1-(ΔS/TM)$_{TNFR2}$-Fas mutant with the shortened stem sequence. However, since preliminary data [4] indicated that TNFR2 is not associated with cholesterol-rich microdomains, the mechanism of how the deletion of parts of the stem-region affects efficient signaling may be different for the two TNFRs. Probably the O-glycosylation of the TNFR2 stem serves to keep the membrane proximal regions apart and thus helps to keep TNFR2 in a resting, non-signaling state (Fig. 20G). Shortening the stem region may shift TNFR2 into an easily signaling conformation (such as shown for TNFR1 in Fig. 20A). Thus, TNFR1-(ΔS/TM)$_{TNFR2}$-Fas can efficiently signal with sTNF. However, since there is no lysine available within the shortened stem region of TNFR2 for crosslinking, there is almost no difference observable between TNFR1-(S/TM)$_{TNFR2}$-Fas and TNFR1-(ΔS/TM)$_{TNFR2}$-Fas during chemical crosslinking studies. Site-directed mutagenesis could be used to introduce a lysine into the *wt* (long) as well as into the shortened stem of TNFR2-Fas to see if these molecules are different in chemical crosslinking experiments. In addition, a TNFR2 molecule with a shortened stem region (TNFR2-(ΔS/TM)$_{TNFR2}$-Fas) would be interesting to be investigated for sTNF responsiveness. Further investigations are required to clarify the discussed mechanisms.

4.5. The CRD1 as a target for the modulation of TNFR-signaling

Besides being a scaffold for CRD2, the CRD1 is also the target for the binding of two monoclonal antibodies, namely the antagonistic TNFR1-specific H398 and the synergistic TNFR2-specific 80M2 (Fig. 2B and D, respectively). Whereas H398 remains its antagonistic effect as a monovalent Fab fragment, the synergism of 80M2 is lost when used as a Fab fragment. Moreover, in very sensitive assay systems of TNF responses, the full-length IgG of H398 showed agonistic effects (Menegazzi et al., 1994). Similar observations were made for 80M2 on some cell lines expressing high amounts of TNFR2-Fas molecules [5]. The binding of these two antibodies was also tested with the receptor in which the CRD1 domains had been exchanged i.e. CRD1$_{TNFR2}$-TNFR1-Fas MEFs (data not shown). Both antibodies failed to bind to the exchange mutant, indicating that the epitope maps to a region governing parts of CRD1 and CRD2. Similarily it was reported that the recognized epitope of agonistic Fas antibodies is the connective region between CRD2 and CRD3 (Fadeel et al., 1998). Thus the hinges between the CRDs may be preferred immunogenic targets.

Whereas 80M2 might act by keeping TNFR2 in a conformation ready to signal if further multimerized by soluble or membrane-like TNF, the antagonistic and TNFR1-specific H398 acts by displacing TNF (data not shown). This may be due to a (allosteric) conformational change of TNFR1 that leads to a structural shift of the A1$_{CRD2}$ similar to what was shown for

[4] Dr. Carsten Tietz (3rd Physical Institute, University of Stuttgart); personal communication.
[5] G. Holeiter (IZI, University of Stuttgart); personal communication.

the ΔCRD1 mutant (Fig. 3D). Alternatively, or in addition, H398 may occupy regions necessary for ligand binding, such as the $A1_{CRD2}$ but still requires CRD1 for efficient binding with some of its CDR loops. An H398-induced dissociation of TNFR1 homo-multimers would be an additional possible mechanism that might be complicated to analyze if different receptor conformations exist as predicted from crystal structures (Naismith et al., 1995; Naismith et al., 1996b; Naismith et al., 1996a). Thus, the effect(s) on signaling (agonistic, synergistic or antagonistic) of antibodies recognizing similar receptor regions are not predictable and have to be individually analyzed. In a study to analyze if there is any correlation between the affinity of an antibody to CD40 and the effect on cellular signaling, Malmborg-Hager and colleagues found that there only was a correlation between the ability to block CD40L binding and to activate CD40 (Malmborg Hager et al., 2003). In addition, the strongest activator, as well as the weakest tested activator, both required the A1 domain of CRD1, whereas CD40L binding was preserved. Similarly, when H398 was tested on $\Delta A1_{CRD1}$-TNFR1-Fas expressing HEK293 Flp-In T-REx cells, no binding could be detected (data not shown). In summary, the CRD1 and CRD2 interface seem to be an interesting target to achieve TNF-receptor signaling modulating effects. However, the qualities of these effects have to be evaluated in each case.

4.6 The "PLAD" as a therapeutic target

The CRD1 of TNFR2 was recombinantly expressed using the yeast *Pichia pastoris*. In some preparations the C-terminally fused myc-his_6 sequence was cleaved during the expression phase or after dialysis of purified protein at pH 7. Mass spectrometric analysis confirmed that the protein was cleaved by yeast proteases at or around the Factor-Xa site (see schematic drawing in Fig. 16A; data not shown). Similar problems were encountered for a TNF variant genetically modified into one polypeptide chain (scTNF) [(6)] that was cleaved by the yeast's proteases within the linker sequences containing parts of the natural TACE cleavage site. Therefore the expression was conducted in 0.5l scale in Erlenmeyer flasks, as a fermentation performed in 20 l scale showed the degradation of $CRD1_{TNFR2}$ from the first day of induction on (data not shown). Concentrations of purified protein were around 2 mg/l and sufficient to conduct several experiments. Chemical crosslinking experiments were performed with the purified myc-his_6 tagged protein (not shown), as well as with the Factor Xa treated, tag free $CRD1_{TNFR2}$ (Fig. 16B). However, for both proteins the Western Blots had to be overexposed in order to detect any crosslinked species (Fig. 16B). On the other hand the positive controls, TNF (Fig. 16C) or FasL (not shown), could be readily crosslinked with bands corresponding to monomeric, dimeric and trimeric species in equal stoichiometries. Size exclusion chromatography of $CRD1_{TNFR2}$ without any tag (Fig. 17B) indicated a molecular size of

[6] V. Boschert (IZI, University of Stuttgart); personal communication.

greater than 12.4 kDa (cytochrome *c* as a standard), whereas mass spectrometry clearly showed the expected mono-isotropic mass of 6.8 kDa (Fig. 17A). Increasing the salt concentration during HPLC from 150 mM (PBS) to 1.15 M (PBS + 1M NaCl) induced a clear shift of $CRD1_{TNFR2}$ towards a later elution time-point corresponding to a size of ~8 kDa (Fig. 17B, lower panel). However, cytochrome *c* also dramatically changed its elution time under these conditions, indicating non-specific adsorption of the molecules to the column material under low salt conditions. For instance, cytochrome *c* is known to be strongly positively charged in order to interact with lipids of the inner mitochondrial membrane.

Nevertheless the data indicated that $CRD1_{TNFR2}$ showed no strong self-association and two explanations are discussed here. First, the protein concentration may have been far below the K_D for CRD1:CRD1 interactions. The protein concentration was around 100 μg/ml and the Mw is 6.8 kDa, thus the molar concentration was approximately 14.7 μM which seems high enough to form interactions if the structure of the protein is correct. However, it could well be that the affinity in fact is in the μM range which may be sufficient to interact if anchored to the plasma-membrane to form a stable complex. Alternatively, recalling the experiences from the CRD1-deleted receptor, the CRD1 may also require scaffolding provided by the CRD2. Preliminary molecular dynamics simulation experiments [7] suggested that indeed the B2 module of CRD1 from TNFR1 is stabilized by the subsequent A1 of CRD2. If this is also the case for the CRD1 of TNFR2 remains to be shown. However if this were the case, a CRD1 fused with the A1 of CRD2 should display a higher affinity towards itself. The purified $CRD1_{TNFR2}$ was also tested for functionality in several assays, but failed to display significant biologic effects. Using $CRD1_{TNFR2}$-TNFR1-Fas MEFs, no protection from sTNF (1 ng/ml) induced cytotoxicity was observed even at concentrations of 2 μM $CRD1_{TNFR2}$, whereas the positive control (Enbrel®) was protective throughout the complete titration range (2 μm to 8 nM; data not shown). Also, Kym-1 cells that were stimulated with a TNFR2-specific ligand (CysTNF-143N145R) to induce endogenous TNF expression went into autocrine/juxtacrine apoptosis no matter whether $CRD1_{TNFR2}$ was present or not (data not shown). In a third set of experiments, $CRD1_{TNFR2}$-TNFR1-Fas expressing MEFs were incubated with radioactively labeled ^{125}I-TNF on ice with or without the $CRD1_{TNFR2}$ protein. However, in contrast to reported data (Deng et al., 2005), no significant reduction of the amount of bound ^{125}I-TNF was observed (data not shown). Of course it could be that the $CRD1_{TNFR2}$ is the “low-affinity PLAD” as indicated by the crosslinking experiments performed (Fig. 9H), which is in accordance with the observation that for the inhibition of TNFR2 higher amounts of a GST-tagged “PLAD2” protein were required as compared to GST - “PLAD1” required for TNFR1 inhibition (Deng et al., 2005). Indeed, Deng and colleagues also tested the hypothesis to modulate TNFR signaling with recombinant CRD1 proteins from TNFR1 or

[7] A. Aird (3rd Physical Institute, University of Stuttgart) personal communication.

TNFR2 expressed in *E. coli* (Deng et al., 2005). Although the authors mentioned no concentrations, they reported that CRD1 proteins had to be used at 1,000-10,000 fold higher amounts as compared to TNF to be effective. It should be stressed, that the proteins used during this published study were N-terminally fused to the glutathione-S transferase (GST) moiety for purification. The GST-induced increase in size could explain that these proteins were effective in altering TNFR signaling by sterically disturbing complex formation. For instance, whereas the CRD1 of TNFR1 is composed of 53 aa, the GST fusion protein consists of 294 aa; supplement in (Deng et al., 2005). In addition, the GST sequence is known to homo-dimerize, therefore the biochemical properties of this fusion protein are rather undefined. The observed immunogenicity of the GST moiety when this fusion protein was injected into mice also limits the potential clinical use. Thus other strategies must be envisaged in order to create a potential therapeutic molecule using PLAD-based proteins. One possibility might by the generation of Fc fusion proteins similar to the TNFR2-Fc fusion protein (Enbrel®) used in clinic. In addition, sterically blocking the aggregation of TNFRs might require an increase in size; this could be achieved for instance by genetically fusing an N-terminal human serum albumin-binding protein. The increase in size would also be beneficial for the putative circulation time in the blood. The effect of PEGylation, also used to increase the circulation time, may be contraindicated if PLAD proteins have low affinity to themselves per se.

4.7 Is there a virus-like and circularly arranged cluster of TNF-TNFR1 complexes?

The last part of the presented work dealt with the construction of a molecular complex that would consider the physiologic observation of large receptor-ligand aggregates. Previous data lead to the view of pre-trimerized receptors in the absence of ligand. Since ligands of the TNF family are also homotrimers, a simple mechanistic model would be the “sliding” of the ligand into a preformed trimeric receptor complex, thus liberating the CRD1 that can search new CRD1s, found in the neighboring TNF-TNFR complex (Figure 1A in (Deng et al., 2005)). The crosslinking studies performed here displayed pre-formed dimeric TNFR1-Fas molecules on the cell surface. Crosslinking of receptors, pre-incubated with TNF also showed preferentially dimeric receptors bound to one ligand (Fig. 12B).

Nevertheless, two arrangements of the known LTα-TNFR1 complex were generated accounting for an either dimeric or trimeric receptor interaction (Fig. 13A and B). It should be kept in mind, however, that the crosslinking experiments were performed at 4°C and cluster formation takes place at 37°C. Thus it may be that receptors are in equilibrium of several aggregation states, but eventually the ligand drives the formation of a signaling-competent state that may result in structures such as depicted in Fig. 13. An additional, third “compact” organization was provided by the group of Prof. Martin Zacharias (Fig. 19A). This complex is

arranged similarly to the relatively “open” hexameric lattice (Fig. 13B), however, the central cavity is much smaller (diameters of 37 Å versus 100 Å). In addition it predicts two types of receptor-receptor interactions. The open-structure mainly involves an A1:A1 interaction and only forms receptor dimers. On the other hand the compact-structure interaction involves the A1 and B2 domains of CRD1 and allows the formation of monomeric, dimeric, up to hexameric TNFR1 molecules finally forming a receptor ring (Fig. 19B). Indeed, when soluble TNFR1 molecules were crosslinked with BS^3, a molecular ladder consisting of monomers, dimers and higher molecular weight products was identified by Western Blotting (Fig. 14B) possibly indicating the existence of higher weight TNFR1 complexes. The formation of either ring-like structure is of particular interest, because, besides their symmetrical beauty, they allow the translation of a trimeric (ligand) into an intracellular, dimeric interaction necessary for caspase and kinase activation. These intracellular interactions could take place between two homotrimeric ligands, rather than exactly beneath them. Similar conclusions have been drawn for the Fas system. For instance, the crystal structure of FADD showed a dimeric molecule that is thought to stabilize the interaction of two receptors; the proposed hexagonal organization was shown on the cover of the respective journal issue (Carrington et al., 2006). Similar conclusions were drawn by the group of Werner who biochemically showed that FADD/FADD interactions are required to stabilize an array of receptors (Sandu et al., 2006). In favor of this argumentation, the crystal structure of a viral flice-inhibitory protein (vFLIP) named MC159 revealed a novel anti-apoptotic mechanism by disrupting the FADD/FADD interaction (Li et al., 2006; Yang et al., 2005), yet leaving intact the caspase-8 recruitment into the death-inducing signaling complex, DISC. The authors have also proposed that the DISC is composed of hexameric, connected rings that are disrupted by MC159, thus preventing induced proximity activation of caspase 8. In addition, a dimeric FasL, engineered by the fusion to the Fc region of an antibody was sufficient to induce apoptosis (Holler et al., 2003). Thus, there is increasing evidence that caspases are activated between two homotrimeric ligands, rather than directly beneath the ligand. This mechanism finally leads to the circular arrangement of TNFRs. Due to the huge molecular size of the DISC that is in principle infinite in size no crystallographic/structural data are available until today. However, other finite death-domain containing complexes have been reported. These include the apoptosome that activates caspase 9 (Acehan et al., 2002; Bao and Shi, 2007) and the PIDDosome that activates caspase 2 (Park et al., 2007). Both have been shown to assemble into wheel-like structures. Thus, in accordance with these names, the true DISC may be called a “DISCosome”. Due to the potentially larger contact interfaces and the complementary charges, the compact, hexagonal arrangement depicted in Fig. 19A seems to be the most likely. Of, course, molecular and biochemical data will be required to prove its existence and some experimental proposals are given further below. Until then, two issues

have to be discussed associated with Fig. 19A. First the glycosylation of receptors and ligands and second the known endocytosis of such large complexes.

i) The effect of TNFR1 N-glycosylation was investigated using the crystal structure of the LTα-TNFR1 complex (Banner et al., 1993). The aa of the three known potential glycosylation sites were increased in size and were found not to disturb a clustering-mode as described in Fig. 19A. Rather, the N-linked sugar chains could fit into the central cavity formed by six receptors. Whereas human TNF is not glycosylated, murine TNF, human FasL and human LTα are (Voigt et al., 1992); it has been demonstrated that the glycosylation is likely to be required for the efficient transport of the ligands to the cell surface (Schneider et al., 1997). In addition, for murine TNF the glycosylation has been reported to lower the bioactivity ten-fold (Koyama et al., 1992). For the Fas system a model structure composed of three Fas molecules and a fully glycosylated, homotrimeric FasL has been proposed (Schneider et al., 1997). If these glycosylation sites (three per FasL subunit) disrupt a complex such as the one proposed here is impossible to say from the given data (Schneider et al., 1997). LTα, however, contains one N-linked sugar chain that is localized at the potential LTα:LTα interaction interface shown in Fig. 19. As the side chain of the affected asparagine can be simply rotated upward the linked sugar chain could lie on top of the adjacent ligand (not shown).

ii) Some ligand-receptor complexes are known to internalize in order to form a secondary signaling complex. Examples include TNF-TNFR1 (Micheau and Tschopp, 2003; Schneider-Brachert et al., 2004; Jacobelli et al., 2006) and FasL-Fas (Lee et al., 2006). The role of internalization for TRAIL-TRAILR is, however, rather unclear (Kohlhaas et al., 2007). Alternatively TNFR1 is released as full-length protein in vesicles called exosomes that range in diameter between 20 to 50 nm (Hawari et al., 2004) or is cleaved within the stem region by the metalloproteinase TACE (Reddy et al., 2000) to release CRDs 1-4. The proposed hexameric clusters of 6 homotrimeric ligands and 18 receptors (Fig. 19A) can be easily extended by adding more receptors and ligands. Thus, many hexagons are connected. However, they do not allow the simultaneous bending in two directions to form a cavity required for internalization. Therefore additional, smaller rings have to be integrated. The resulting structure would be similar to a soccer ball, composed of pentagons and hexagons. However, the interactions between the [ligand-receptor]:[ligand-receptor] complexes would not be exactly equivalent, a problem that is well known from the architecture of viral capsids. This issue has been solved by the idea of quasi-equivalency, a hypothesis stating that subunits that have nearly the same local environment thus form nearly identical interactions with their neighbors. Besides viruses, the cage of clathrin coated vesicles is also formed of pentagons and hexagons, although the basic units are the triscelions (Fotin et al., 2004). On the other hand, it is quite likely that nature had not planned to form clusters of TNF-TNFRs in

the μm size. Thus, physiologic cluster sizes may be small enough to allow some bending necessary for internalization and the expression of large receptor numbers would lead to huge structures that may be almost crystalline and cannot be internalized any more. Such structures were in fact observed to be stable for several hours (Henkler et al., 2005). Thus, internalization should not be a problem.

Interestingly, the structure of another TNF ligand family member, BAFF (also known as TALL-1, THANK, BlyS, and zTNF4) is quite different from all other TNF ligand family members because it does not stop ligand-association at the homo-trimer level. Rather, it forms a "super ligand" composed of 20 homotrimers that are arranged as a true icosahedron (Liu et al., 2002; Cachero et al., 2006). This BAFF virus-like cluster consists of pentagons and hexagons that are likely to dictate the grid of receptor aggregation. In order to form such an aggregate, the ligand has evolved a specialized loop (termed the flap region) that contacts the groove of a neighboring homotrimeric BAFF. As this groove normally is used for receptor binding, the BAFF receptor binds with its tips to the bottom of the clustered ligands. Although speculative, this mechanism may have evolved because the three receptors contain only one cysteine rich domain (BAFFR, BCMA) or two (TACI). Recently it was shown that TACI in fact only uses its membrane proximal CRD for ligand binding (Hymowitz JBC 2005). Thus, one CRD may not be enough to realize ligand binding and receptor self association; therefore the BAFF ligand may have evolved additional multimerization mechanisms.

4.8 Does TNF induce a ligand-mediated conformational change?

The mechanism discussed here for TNFR signaling involves a ligand-induced change in receptor conformation. Accordingly, TNFRs are in a non-signaling state, because equilibrium prefers the respective conformation (maybe an anti-parallel orientation). For TNFR1, anti-parallel oriented TNFR1 molecules have been proposed as a silent receptor conformation, because the ligand binding site (CRD2) is occupied by the receptor-receptor interaction and C-termini are apart by 100 Å (Naismith et al., 1995). The respective receptor organization is schematically shown in Fig. 20B. An increase in receptor concentration should enhance the likeliness to form the signaling-competent state and thus ligand-independent signaling. As the proposed ligand-induced change mechanism bears some similarities to the allosteric activation of proteins the two TNFR1 conformations may also be called the T (tense = inactive) or R (relaxed = active) state in accordance with the terms introduced by Monod, Wyman and Changeux (MONOD et al., 1965). Both states may be reflected by the pH 7.5 crystal structure without ligand that was found to include parallel receptors with solvent accessible ligand binding sites (R-state) as well as anti-parallel receptors with blocked binding sites (T-state) (Naismith et al., 1995). Naismith and colleagues also proposed that

both ligand-free structures are likely to be almost equally stable due to similar contact areas. Thus the stem would function as a hinge that allows the flipping of receptors between two orientations. Such a change in direction can be structurally accomplished by a γ-turn involving three aa or a β-turn consisting of four aa. Residues with small side chains such as glycine, aspartate, serine, asparagine, cysteine and proline are found preferentially within turns. Indeed, TNFR2 contains several prolines within its stem and TNFR1 contains a sequence of small aa before the TM domain (Asp_{178}-Ser-Gly-Thr_{181}). This putative TNFR1 "hinge-site" is conserved 100% in mouse, rat and human (bovine sequence is Asp-Pro-Gly-Thr). Mutational analysis of the TNFR1 hinge-site may lead to receptors with increased TNF sensitivities (lower EC50 values) as compared to the *wt* TNFR1 or even constitutively active molecules. Next, binding of TNF or LTα may shift equilibrium from the T- into the R-state. Further clustering of parallel oriented receptors bound to ligand(s) leads to a close arrangement of the intracellular parts of TNFRs. Thus intracellular proteins (ubiquitinating proteins, caspases and kinases) are effectively recruited and activated by close proximity. The existence of a receptor conformation "blind" for TNF may also serve as an explanation for the above mentioned observation that iodinated TNFR2-specific antibodies detected more binding sites as compared to iodinated TNF (Löhden, 1995). Pathophysiologic situations can be envisaged in which many receptors are in the R-state. Such a scenario may be the case in TRAPS patients who have mutations affecting cysteines within the CRD1. These mutations lead to the covalent stabilization of TNFR1 molecules (Lobito et al., 2006), probably in the R-state. As this arrangement leads to ligand-independent signaling it is clear that a sometimes used "classical" anti-TNF (Jacobelli et al., 2006) cannot be efficacious in treating TRAPS patients.

Yet another possibility of early signaling events would be that TNFR1 molecules are arranged in parallel as seen in the crystal structure at pH 7.5 (Fig. 18B and Fig. 20A). The binding of TNF to one receptor chain may then lead to the transient liberation of the second receptor that can now bind to one of the two free TNF sites (Fig. 20C → 20D). Similarily, ligand binding to one receptor chain of the anti-parallel organization (Fig. 20B) would likely lead to a ligand complexed with two receptor chains (Fig. 20D). Both scenarios may lead to a strong ligand binding through an avidity driven stabilization. As the post-ligand binding PLAD is now free, it can be utilized to contact an adjacent receptor-ligand complex. Thus, TNF would serve as a catalyst that lowers the activation energy between two conformational receptor states.

Several examples are known in which cytokine receptors are multimerized and signal after a ligand-induced conformational change. For instance, the erythropoietin (EPO) receptor is a non-covalently linked dimer (Livnah et al., 1999) that is activated by an EPO-induced conformational change (Remy et al., 1999; Lu et al., 2006). Human growth hormone (GH)

receptor dimerizes with the help of the transmembrane domain and is activated by rotation of the receptor chains after binding of the ligand (Brown et al., 2005). The human epidermal growth factor (EGF) receptor, also known as HER1, is composed of four extracellular domains (I-IV) that are “auto-inhibited” (Ferguson et al., 2003) and undergo large conformational changes after binding of the ligand that reveals the receptor-dimerization interfaces composed of the cysteine rich domain II and domain IV (Dawson et al., 2005). This process then leads to an allosteric activation of the intracellular HER1 kinase domains (Zhang et al., 2006). Although the transmembrane domains of the HER family have been reported to contribute to receptor dimerization through the aforementioned GxxxG motif (Mendrola et al., 2002), the function remains rather unclear. As a point-mutation within the transmembrane part of HER2 leads to constitutively active molecules, the GxxxG motif in the HER system may be used to silence receptors. Within the TNFR family a ligand-induced conformational shift has not been proposed so far, however, some reports indicate that after ligand binding receptors change their relative orientations. For instance, disulfide-linking of receptors after ligand binding has been reported for CD40 (Reyes-Moreno et al., 2004) and TNFR2 (Grazioli et al., 1994). The pro-apoptotic Fas molecule is known to shift into SDS-stable aggregates termed “hiDISC” after stimulation with FasL consisting of four to six Fas molecules (Algeciras-Schimnich et al., 2002; Feig et al., 2007). In addition, if TNFR1 is kept in a non-signaling competent T-state, then the CRDs should be essential for this silencing mechanism. Accordingly, fusing the stem-, transmembrane and intracellular regions of TNFR1 with the extracellular parts of the EPO receptor was reported to lead to a constitutively active molecule (Bazzoni et al., 1995). Thus, a ligand-induced re-arrangement of members of the TNFR family is likely to occur during signaling. If these include rather small (Figs. 20A $\rightarrow$ C) or large (Figs. 20B $\rightarrow$ D; 20C $\rightarrow$ D) conformational re-arrangements as hypothetically discussed here remains to be shown.

4.9 Outlook

The proposed receptor-ligand clusters will not be easily verified. However, some potential experiments briefly described hereafter may help to clarify some of the discussed issues.

Although the structure of many membrane proteins have been determined since the seminal report of the photosynthetic reaction centre in 1982 by Hartmut Michel and co-workers, there still is a lack of sufficient structures from eukaryotic, full length membrane receptors. In the TNF family, ligands and receptors have been crystallized as soluble proteins. However, the membrane-bound native state receptor(s) bound to their ligands in a 2-dimensional crystal should reveal the super-structural organization of these proteins. Crystallized in two-dimensional membranes receptor-ligand complexes could be analyzed by cryo-electron microscopy or atomic force microscopy (AFM). For instance, light harvesting complexes of photosynthetic bacteria have been demonstrated to be rings by the use of AFM (Engel and Muller, 2000; Scheuring et al., 2001). As AFM can be performed in aqueous buffers, fixation artifacts could be excluded in such experiments. Probably more easy to accomplish, sterical modifications of TNF at hypothetical interfaces between two homotrimeric ligands should ease the assessment of the proposed hexagonal lattices. For instance, by using phage-display technology a Japanese group has reported the generation of a lysine deficient TNF variant that displayed normal receptor-binding capability (Yamamoto et al., 2003). From this mutant, one of the six lysines of the TNF molecule (K65, aa sequence PSKQN) is part of the putative ligand : ligand interaction face shown in Fig. 19. The K65 position could be retained and used for site-specific PEGylation. An alternative approach to increase the space at this site would be to generate point mutants (e.g. K65W) or to introduce a small loop at this position. These strategies should lead to TNF molecules almost unchanged in their affinities for TNFRs during saturation binding studies at 4°C. However, do to the introduced sterically hindrances, the EC50 values of these mutants are expected to change.

Another structural approach would be to couple a scTNF variant with one C-terminal cysteine (Cys-scTNF) to small colloidal gold particles. Electron microscopy could be used to analyze if these gold-TNF-molecules arrange in any regular structure on cells expressing high numbers of TNFRs.

Biochemical methods like chemical crosslinking could also be used to determine if TNF molecules are in close proximity when incubated at 37°C with cells expressing TNFRs. As BS^3 is reactive towards any available lysine a site directed photo-crosslinking could be applied. Such a system which introduces an UV-inducible crosslinker at defined aa-positions by using *in vitro* translation has been developed by Josef Brunner from the ETH in Zurich. For instance the interaction sites of a secretory signal sequence to different subunits of the endoplasmatic reticulum translocation complex have been determined in such a way (High et

al., 1993). The *in vitro* translation of TNF could thus be used to introduce an UV-inducible photo-crosslinker.

Concerning the putative interaction of the TM domains of TNFRs, genetic systems based on yeast-two-hybrid have been developed to analyze the interactions of membrane proteins (Stagljar et al., 1998; Iyer et al., 2005). The so-called split-ubiquitin system is based on the release of a transcription factor through the cleavage by an ubiquitin-binding protease after the membrane-protein-induced unification of two ubiquitin halves. An alternative method could be the bimolecular fluorescence complementation (BiFC) technique (Kerppola, 2006). Here, the two TM sequences could be fused to one of the two halves of a slit-GFP molecule. Expressing cells could then be analyzed by confocal microscopy for fluoerscening membranes. In addition, cells expressing TNFR1-Fas or TNFR2-Fas together with the respective TM-domains could be analyzed for the capability to signal cytotoxicity with TNF.

4.10 Conclusion

In summary, the understanding of how complexes composed of ligands and receptors of the TNF superfamily are built may allow the generation of receptor selective and signaling modifying tools. These could include antibodies specific for receptors or small molecules that disrupt receptor self-association. Small peptides resembling the subdomain 4 of ErbB2 have for instance been shown to be efficient in abolishing receptor- dimerization and signaling (Berezov et al., 2002). Clearly the field of TNFR research will remain fascinating in the future.

5. Reference List

Acehan,D., Jiang,X., Morgan,D.G., Heuser,J.E., Wang,X., and Akey,C.W. (2002). Three-dimensional structure of the apoptosome: implications for assembly, procaspase-9 binding, and activation. Mol. Cell *9*, 423-432.

Aggarwal,B.B. (2003). Signalling pathways of the TNF superfamily: a double-edged sword. Nat. Rev. Immunol. *3*, 745-756.

Algeciras-Schimnich,A., Shen,L., Barnhart,B.C., Murmann,A.E., Burkhardt,J.K., and Peter,M.E. (2002). Molecular ordering of the initial signaling events of CD95. Mol. Cell Biol. *22*, 207-220.

Baker,N.A., Sept,D., Joseph,S., Holst,M.J., and McCammon,J.A. (2001). Electrostatics of nanosystems: application to microtubules and the ribosome. Proc. Natl. Acad. Sci. U. S. A *98*, 10037-10041.

Banner,D.W., D'Arcy,A., Janes,W., Gentz,R., Schoenfeld,H.J., Broger,C., Loetscher,H., and Lesslauer,W. (1993). Crystal structure of the soluble human 55 kd TNF receptor-human TNF beta complex: implications for TNF receptor activation. Cell *73*, 431-445.

Bao,Q. and Shi,Y. (2007). Apoptosome: a platform for the activation of initiator caspases. Cell Death. Differ. *14*, 56-65.

Bazzoni,F., Alejos,E., and Beutler,B. (1995). Chimeric tumor necrosis factor receptors with constitutive signaling activity. Proc. Natl. Acad. Sci. U. S. A *92*, 5376-5380.

Berezov,A., Chen,J., Liu,Q., Zhang,H.T., Greene,M.I., and Murali,R. (2002). Disabling receptor ensembles with rationally designed interface peptidomimetics. J. Biol. Chem. *277*, 28330-28339.

Bidere,N., Snow,A.L., Sakai,K., Zheng,L., and Lenardo,M.J. (2006). Caspase-8 regulation by direct interaction with TRAF6 in T cell receptor-induced NF-kappaB activation. Curr. Biol. *16*, 1666-1671.

Blotta,M.H., Marshall,J.D., DeKruyff,R.H., and Umetsu,D.T. (1996). Cross-linking of the CD40 ligand on human CD4+ T lymphocytes generates a costimulatory signal that up-regulates IL-4 synthesis. J. Immunol. *156*, 3133-3140.

Boatright,K.M., Renatus,M., Scott,F.L., Sperandio,S., Shin,H., Pedersen,I.M., Ricci,J.E., Edris,W.A., Sutherlin,D.P., Green,D.R., and Salvesen,G.S. (2003). A unified model for apical caspase activation. Mol. Cell *11*, 529-541.

Boatright,K.M. and Salvesen,G.S. (2003). Mechanisms of caspase activation. Curr. Opin. Cell Biol. *15*, 725-731.

Bock,J. and Gulbins,E. (2003). The transmembranous domain of CD40 determines CD40 partitioning into lipid rafts. FEBS Lett. *534*, 169-174.

Boldin,M.P., Mett,I.L., Varfolomeev,E.E., Chumakov,I., Shemer-Avni,Y., Camonis,J.H., and Wallach,D. (1995). Self-association of the "death domains" of the p55 tumor necrosis factor (TNF) receptor and Fas/APO1 prompts signaling for TNF and Fas/APO1 effects. J. Biol. Chem. *270*, 387-391.

Branschädel,M., Boschert,V., and Krippner-Heidenreich,A. (2007). Tumour Necrosis Factors. In ENCYCLOPEDIA OF LIFE SCIENCES, John Wiley & Sons, Ltd: Chichester).

Brown,R.J., Adams,J.J., Pelekanos,R.A., Wan,Y., McKinstry,W.J., Palethorpe,K., Seeber,R.M., Monks,T.A., Eidne,K.A., Parker,M.W., and Waters,M.J. (2005). Model for growth hormone receptor activation based on subunit rotation within a receptor dimer. Nat. Struct. Mol. Biol. *12*, 814-821.

Bryde,S., Grunwald,I., Hammer,A., Krippner-Heidenreich,A., Schiestel,T., Brunner,H., Tovar,G.E., Pfizenmaier,K., and Scheurich,P. (2005). Tumor necrosis factor (TNF)-functionalized nanostructured particles for the stimulation of membrane TNF-specific cell responses. Bioconjug. Chem. *16*, 1459-1467.

Budd,R.C., Yeh,W.C., and Tschopp,J. (2006). cFLIP regulation of lymphocyte activation and development. Nat. Rev. Immunol. *6*, 196-204.

Cachero,T.G., Schwartz,I.M., Qian,F., Day,E.S., Bossen,C., Ingold,K., Tardivel,A., Krushinskie,D., Eldredge,J., Silvian,L., Lugovskoy,A., Farrington,G.K., Strauch,K., Schneider,P., and Whitty,A. (2006). Formation of virus-like clusters is an intrinsic property of the tumor necrosis factor family member BAFF (B cell activating factor). Biochemistry *45*, 2006-2013.

Carfi,A., Willis,S.H., Whitbeck,J.C., Krummenacher,C., Cohen,G.H., Eisenberg,R.J., and Wiley,D.C. (2001). Herpes simplex virus glycoprotein D bound to the human receptor HveA. Mol. Cell *8*, 169-179.

Carrington,P.E., Sandu,C., Wei,Y., Hill,J.M., Morisawa,G., Huang,T., Gavathiotis,E., Wei,Y., and Werner,M.H. (2006). The structure of FADD and its mode of interaction with procaspase-8. Mol. Cell *22*, 599-610.

Carter,P.H., Scherle,P.A., Muckelbauer,J.K., Voss,M.E., Liu,R.Q., Thompson,L.A., Tebben,A.J., Solomon,K.A., Lo,Y.C., Li,Z., Strzemienski,P., Yang,G., Falahatpisheh,N., Xu,M., Wu,Z., Farrow,N.A., Ramnarayan,K., Wang,J., Rideout,D., Yalamoori,V., Domaille,P., Underwood,D.J., Trzaskos,J.M., Friedman,S.M., Newton,R.C., and Decicco,C.P. (2001). Photochemically enhanced binding of small molecules to the tumor necrosis factor receptor-1 inhibits the binding of TNF-alpha. Proc. Natl. Acad. Sci. U. S. A *98*, 11879-11884.

Cha,S.S., Sung,B.J., Kim,Y.A., Song,Y.L., Kim,H.J., Kim,S., Lee,M.S., and Oh,B.H. (2000). Crystal structure of TRAIL-DR5 complex identifies a critical role of the unique frame insertion in conferring recognition specificity. J. Biol. Chem. *275*, 31171-31177.

Chan,F.K. (2000). The pre-ligand binding assembly domain: a potential target of inhibition of tumour necrosis factor receptor function. Ann. Rheum. Dis. *59 Suppl 1*, i50-i53.

Chan,F.K., Chun,H.J., Zheng,L., Siegel,R.M., Bui,K.L., and Lenardo,M.J. (2000). A domain in TNF receptors that mediates ligand-independent receptor assembly and signaling. Science *288*, 2351-2354.

Chen,Y., Molloy,S.S., Thomas,L., Gambee,J., Bachinger,H.P., Ferguson,B., Zonana,J., Thomas,G., and Morris,N.P. (2001). Mutations within a furin consensus sequence block proteolytic release of ectodysplasin-A and cause X-linked hypohidrotic ectodermal dysplasia. Proc. Natl. Acad. Sci. U. S. A *98*, 7218-7223.

Clancy,L., Mruk,K., Archer,K., Woelfel,M., Mongkolsapaya,J., Screaton,G., Lenardo,M.J., and Chan,F.K. (2005). Preligand assembly domain-mediated ligand-independent association between TRAIL receptor 4 (TR4) and TR2 regulates TRAIL-induced apoptosis. Proc. Natl. Acad. Sci. U. S. A *102*, 18099-18104.

Coley,W.B. (1896). The therapeutic value of the mixed toxins of the streptococcus of erysipelas in the treatment of inoperable malignant tumors, with a report of 100 cases. American Journal of Medical Sciences *112*, 251-281.

Compaan,D.M. and Hymowitz,S.G. (2006). The crystal structure of the costimulatory OX40-OX40L complex. Structure. *14*, 1321-1330.

Connolly,S.A., Landsburg,D.J., Carfi,A., Wiley,D.C., Eisenberg,R.J., and Cohen,G.H. (2002). Structure-based analysis of the herpes simplex virus glycoprotein D binding site present on herpesvirus entry mediator HveA (HVEM). J. Virol. *76*, 10894-10904.

Corti,A., Fassina,G., Marcucci,F., Barbanti,E., and Cassani,G. (1992). Oligomeric tumour necrosis factor alpha slowly converts into inactive forms at bioactive levels. Biochem. J. *284 (Pt 3)*, 905-910.

Cremesti,A., Paris,F., Grassme,H., Holler,N., Tschopp,J., Fuks,Z., Gulbins,E., and Kolesnick,R. (2001). Ceramide enables fas to cap and kill. J. Biol. Chem. *276*, 23954-23961.

Dawson,J.P., Berger,M.B., Lin,C.C., Schlessinger,J., Lemmon,M.A., and Ferguson,K.M. (2005). Epidermal growth factor receptor dimerization and activation require ligand-induced conformational changes in the dimer interface. Mol. Cell Biol. *25*, 7734-7742.

Deng,G.M., Zheng,L., Chan,F.K., and Lenardo,M. (2005). Amelioration of inflammatory arthritis by targeting the pre-ligand assembly domain of tumor necrosis factor receptors. Nat. Med. *11*, 1066-1072.

Dolinsky,T.J., Nielsen,J.E., McCammon,J.A., and Baker,N.A. (2004). PDB2PQR: an automated pipeline for the setup of Poisson-Boltzmann electrostatics calculations. Nucleic Acids Res. *32*, W665-W667.

Douni,E. and Kollias,G. (1998). A critical role of the p75 tumor necrosis factor receptor (p75TNF-R) in organ inflammation independent of TNF, lymphotoxin alpha, or the p55TNF-R. J. Exp. Med. *188*, 1343-1352.

Engel,A. and Muller,D.J. (2000). Observing single biomolecules at work with the atomic force microscope. Nat. Struct. Biol. *7*, 715-718.

Fadeel,B., Lindberg,J., Achour,A., and Chiodi,F. (1998). A three-dimensional model of the Fas/APO-1 molecule: cross-reactivity of anti-Fas antibodies explained by structural mimicry of antigenic sites. Int. Immunol. *10*, 131-140.

Feig,C., Tchikov,V., Schutze,S., and Peter,M.E. (2007). Palmitoylation of CD95 facilitates formation of SDS-stable receptor aggregates that initiate apoptosis signaling. EMBO J. *26*, 221-231.

Feldmann,M. and Maini,R.N. (2003). Lasker Clinical Medical Research Award. TNF defined as a therapeutic target for rheumatoid arthritis and other autoimmune diseases. Nat. Med. *9*, 1245-1250.

Ferguson,K.M., Berger,M.B., Mendrola,J.M., Cho,H.S., Leahy,D.J., and Lemmon,M.A. (2003). EGF activates its receptor by removing interactions that autoinhibit ectodomain dimerization. Mol. Cell *11*, 507-517.

Fotin,A., Cheng,Y., Sliz,P., Grigorieff,N., Harrison,S.C., Kirchhausen,T., and Walz,T. (2004). Molecular model for a complete clathrin lattice from electron cryomicroscopy. Nature *432*, 573-579.

Friedmann,E., Hauben,E., Maylandt,K., Schleeger,S., Vreugde,S., Lichtenthaler,S.F., Kuhn,P.H., Stauffer,D., Rovelli,G., and Martoglio,B. (2006). SPPL2a and SPPL2b promote intramembrane proteolysis of TNFalpha in activated dendritic cells to trigger IL-12 production. Nat. Cell Biol. *8*, 843-848.

Fu,Z.Q., Harrison,R.W., Reed,C., Wu,J., Xue,Y.N., Chen,M.J., and Weber,I.T. (1995). Model complexes of tumor necrosis factor-alpha with receptors R1 and R2. Protein Eng *8*, 1233-1241.

Galonek,H.L. and Hardwick,J.M. (2006). Upgrading the BCL-2 network. Nat. Cell Biol. *8*, 1317-1319.

Gordon,N.C., Pan,B., Hymowitz,S.G., Yin,J., Kelley,R.F., Cochran,A.G., Yan,M., Dixit,V.M., Fairbrother,W.J., and Starovasnik,M.A. (2003). BAFF/BLyS receptor 3 comprises a minimal TNF receptor-like module that encodes a highly focused ligand-binding site. Biochemistry *42*, 5977-5983.

Grassme,H., Bock,J., Kun,J., and Gulbins,E. (2002a). Clustering of CD40 ligand is required to form a functional contact with CD40. J. Biol. Chem. *277*, 30289-30299.

Grassme,H., Jendrossek,V., Bock,J., Riehle,A., and Gulbins,E. (2002b). Ceramide-rich membrane rafts mediate CD40 clustering. J. Immunol. *168*, 298-307.

Grazioli,L., Casero,D., Restivo,A., Cozzi,E., and Marcucci,F. (1994). Tumor necrosis factor-driven formation of disulfide-linked receptor aggregates. J. Biol. Chem. *269*, 22304-22309.

Grell,M., Wajant,H., Zimmermann,G., and Scheurich,P. (1998). The type 1 receptor (CD120a) is the high-affinity receptor for soluble tumor necrosis factor. Proc. Natl. Acad. Sci. U. S. A *95*, 570-575.

Hawari,F.I., Rouhani,F.N., Cui,X., Yu,Z.X., Buckley,C., Kaler,M., and Levine,S.J. (2004). Release of full-length 55-kDa TNF receptor 1 in exosome-like vesicles: a mechanism for generation of soluble cytokine receptors. Proc. Natl. Acad. Sci. U. S. A *101*, 1297-1302.

He,M.M., Smith,A.S., Oslob,J.D., Flanagan,W.M., Braisted,A.C., Whitty,A., Cancilla,M.T., Wang,J., Lugovskoy,A.A., Yoburn,J.C., Fung,A.D., Farrington,G., Eldredge,J.K., Day,E.S., Cruz,L.A., Cachero,T.G., Miller,S.K., Friedman,J.E., Choong,I.C., and Cunningham,B.C. (2005). Small-molecule inhibition of TNF-alpha. Science *310*, 1022-1025.

He,X.L. and Garcia,K.C. (2004). Structure of nerve growth factor complexed with the shared neurotrophin receptor p75. Science *304*, 870-875.

Henkler,F., Behrle,E., Dennehy,K.M., Wicovsky,A., Peters,N., Warnke,C., Pfizenmaier,K., and Wajant,H. (2005). The extracellular domains of FasL and Fas are sufficient for the formation of supramolecular FasL-Fas clusters of high stability. J. Cell Biol. *168*, 1087-1098.

High,S., Martoglio,B., Gorlich,D., Andersen,S.S., Ashford,A.J., Giner,A., Hartmann,E., Prehn,S., Rapoport,T.A., Dobberstein,B., and . (1993). Site-specific photocross-linking reveals that Sec61p and TRAM contact different regions of a membrane-inserted signal sequence. J. Biol. Chem. *268*, 26745-26751.

Hohmann,H.P., Remy,R., Brockhaus,M., and van Loon,A.P. (1989). Two different cell types have different major receptors for human tumor necrosis factor (TNF alpha). J. Biol. Chem. *264*, 14927-14934.

Holler,N., Tardivel,A., Kovacsovics-Bankowski,M., Hertig,S., Gaide,O., Martinon,F., Tinel,A., Deperthes,D., Calderara,S., Schulthess,T., Engel,J., Schneider,P., and Tschopp,J. (2003). Two adjacent trimeric Fas ligands are required for Fas signaling and formation of a death-inducing signaling complex. Mol. Cell Biol. *23*, 1428-1440.

Hueber,A.O., Bernard,A.M., Herincs,Z., Couzinet,A., and He,H.T. (2002). An essential role for membrane rafts in the initiation of Fas/CD95-triggered cell death in mouse thymocytes. EMBO Rep. *3*, 190-196.

Humphrey,W., Dalke,A., and Schulten,K. (1996). VMD: visual molecular dynamics. J. Mol. Graph. *14*, 33-38.

Hymowitz,S.G., Christinger,H.W., Fuh,G., Ultsch,M., O'Connell,M., Kelley,R.F., Ashkenazi,A., and de Vos,A.M. (1999). Triggering cell death: the crystal structure of Apo2L/TRAIL in a complex with death receptor 5. Mol. Cell *4*, 563-571.

Hymowitz,S.G., Compaan,D.M., Yan,M., Wallweber,H.J., Dixit,V.M., Starovasnik,M.A., and de Vos,A.M. (2003). The crystal structures of EDA-A1 and EDA-A2: splice variants with distinct receptor specificity. Structure. *11*, 1513-1520.

Hymowitz,S.G., Patel,D.R., Wallweber,H.J., Runyon,S., Yan,M., Yin,J., Shriver,S.K., Gordon,N.C., Pan,B., Skelton,N.J., Kelley,R.F., and Starovasnik,M.A. (2005). Structures of APRIL-receptor complexes: like BCMA, TACI employs only a single cysteine-rich domain for high affinity ligand binding. J. Biol. Chem. *280*, 7218-7227.

Iyer,K., Burkle,L., Auerbach,D., Thaminy,S., Dinkel,M., Engels,K., and Stagljar,I. (2005). Utilizing the split-ubiquitin membrane yeast two-hybrid system to identify protein-protein interactions of integral membrane proteins. Sci. STKE. *2005*, l3.

Jacobelli,S., Andre,M., Alexandra,J.F., Dode,C., and Papo,T. (2006). Failure of anti-TNF therapy in TNF-receptor-1-associated periodic syndrome (TRAPS). Rheumatology. (Oxford).

Jacobson,K., Mouritsen,O.G., and Anderson,R.G. (2007). Lipid rafts: at a crossroad between cell biology and physics. Nat. Cell Biol. *9*, 7-14.

Jones,E.Y., Stuart,D.I., and Walker,N.P. (1990). The structure of tumour necrosis factor--implications for biological function. J. Cell Sci. Suppl *13*, 11-18.

Jones,T.A. and Liljas,L. (1984). Structure of satellite tobacco necrosis virus after crystallographic refinement at 2.5 A resolution. J. Mol. Biol. *177*, 735-767.

Karin,M. and Lin,A. (2002). NF-kappaB at the crossroads of life and death. Nat. Immunol. *3*, 221-227.

Kerppola,T.K. (2006). Design and implementation of bimolecular fluorescence complementation (BiFC) assays for the visualization of protein interactions in living cells. Nat. Protoc. *1*, 1278-1286.

Kohlhaas,S.L., Craxton,A., Sun,X.M., Pinkoski,M.J., and Cohen,G.M. (2007). Receptor-mediated endocytosis is not required for TRAIL-induced apoptosis. J. Biol. Chem.

Kovalenko,A. and Wallach,D. (2006). If the prophet does not come to the mountain: dynamics of signaling complexes in NF-kappaB activation. Mol. Cell *22*, 433-436.

Koyama,Y., Hayashi,T., Fujii,N., and Yoshida,T. (1992). Recombinant mouse tumor necrosis factor expressed in mammalian cells: effect of glycosylation on cytotoxic activity. Biochim. Biophys. Acta *1132*, 188-194.

Krippner-Heidenreich,A., Tubing,F., Bryde,S., Willi,S., Zimmermann,G., and Scheurich,P. (2002). Control of receptor-induced signaling complex formation by the kinetics of ligand/receptor interaction. J. Biol. Chem. *277*, 44155-44163.

Lamkanfi,M., Declercq,W., Vanden Berghe,T., and Vandenabeele,P. (2006). Caspases leave the beaten track: caspase-mediated activation of NF-kappaB. J. Cell Biol. *173*, 165-171.

Lamkanfi,M., Festjens,N., Declercq,W., Vanden Berghe,T., and Vandenabeele,P. (2007). Caspases in cell survival, proliferation and differentiation. Cell Death. Differ. *14*, 44-55.

Lee,K.H., Feig,C., Tchikov,V., Schickel,R., Hallas,C., Schutze,S., Peter,M.E., and Chan,A.C. (2006). The role of receptor internalization in CD95 signaling. EMBO J. *25*, 1009-1023.

Legler,D.F., Micheau,O., Doucey,M.A., Tschopp,J., and Bron,C. (2003). Recruitment of TNF receptor 1 to lipid rafts is essential for TNFalpha-mediated NF-kappaB activation. Immunity. *18*, 655-664.

Leist,M. and Jaattela,M. (2001). Four deaths and a funeral: from caspases to alternative mechanisms. Nat. Rev. Mol. Cell Biol. *2*, 589-598.

Li,F.Y., Jeffrey,P.D., Yu,J.W., and Shi,Y. (2006). Crystal structure of a viral FLIP: insights into FLIP-mediated inhibition of death receptor signaling. J. Biol. Chem. *281*, 2960-2968.

Liu,Y., Xu,L., Opalka,N., Kappler,J., Shu,H.B., and Zhang,G. (2002). Crystal structure of sTALL-1 reveals a virus-like assembly of TNF family ligands. Cell *108*, 383-394.

Livnah,O., Stura,E.A., Middleton,S.A., Johnson,D.L., Jolliffe,L.K., and Wilson,I.A. (1999). Crystallographic evidence for preformed dimers of erythropoietin receptor before ligand activation. Science *283*, 987-990.

Lobito,A.A., Kimberley,F.C., Muppidi,J.R., Komarow,H., Jackson,A.J., Hull,K.M., Kastner,D.L., Screaton,G.R., and Siegel,R.M. (2006). Abnormal disulfide-linked oligomerization results in ER retention and altered signaling by TNFR1 mutants in TNFR1-associated periodic fever syndrome (TRAPS). Blood *108*, 1320-1327.

Locksley,R.M., Killeen,N., and Lenardo,M.J. (2001). The TNF and TNF receptor superfamilies: integrating mammalian biology. Cell *104*, 487-501.

Löhden, M. Charakterisierung der Funktion des Tumornekrosefakor-Rezeptors TR80 mit Hilfe von rezeptorspezifischen, die TNF-Antwort modulierenden Antikörpern. 1-1-1995.
Ref Type: Thesis/Dissertation

Lu,X., Gross,A.W., and Lodish,H.F. (2006). Active conformation of the erythropoietin receptor: random and cysteine-scanning mutagenesis of the extracellular juxtamembrane and transmembrane domains. J. Biol. Chem. *281*, 7002-7011.

Malmborg Hager,A.C., Ellmark,P., Borrebaeck,C.A.K., and Furebring,C. (2003). Affinity and epitope profiling of mouse anti-CD40 monoclonal antibodies. Scandinavian Journal of Immunology 517-524.

Marsters,S.A., Frutkin,A.D., Simpson,N.J., Fendly,B.M., and Ashkenazi,A. (1992). Identification of cysteine-rich domains of the type 1 tumor necrosis factor receptor involved in ligand binding. J. Biol. Chem. *267*, 5747-5750.

Marsters,S.A., Sheridan,J.P., Pitti,R.M., Huang,A., Skubatch,M., Baldwin,D., Yuan,J., Gurney,A., Goddard,A.D., Godowski,P., and Ashkenazi,A. (1997). A novel receptor for Apo2L/TRAIL contains a truncated death domain. Curr. Biol. *7*, 1003-1006.

Martinon,F., Burns,K., and Tschopp,J. (2002). The inflammasome: a molecular platform triggering activation of inflammatory caspases and processing of proIL-beta. Mol. Cell *10*, 417-426.

McDermott,M.F., Aksentijevich,I., Galon,J., McDermott,E.M., Ogunkolade,B.W., Centola,M., Mansfield,E., Gadina,M., Karenko,L., Pettersson,T., McCarthy,J., Frucht,D.M., Aringer,M., Torosyan,Y., Teppo,A.M., Wilson,M., Karaarslan,H.M., Wan,Y., Todd,I., Wood,G., Schlimgen,R., Kumarajeewa,T.R., Cooper,S.M., Vella,J.P., Amos,C.I., Mulley,J., Quane,K.A., Molloy,M.G., Ranki,A., Powell,R.J., Hitman,G.A., O'Shea,J.J., and Kastner,D.L. (1999). Germline mutations in the extracellular domains of the 55 kDa TNF receptor, TNFR1, define a family of dominantly inherited autoinflammatory syndromes. Cell *97*, 133-144.

Mendrola,J.M., Berger,M.B., King,M.C., and Lemmon,M.A. (2002). The single transmembrane domains of ErbB receptors self-associate in cell membranes. J. Biol. Chem. *277*, 4704-4712.

Menegazzi,R., Cramer,R., Patriarca,P., Scheurich,P., and Dri,P. (1994). Evidence that tumor necrosis factor alpha (TNF)-induced activation of neutrophil respiratory burst on biologic surfaces is mediated by the p55 TNF receptor. Blood *84*, 287-293.

Merino,D., Lalaoui,N., Morizot,A., Schneider,P., Solary,E., and Micheau,O. (2006). Differential inhibition of TRAIL-mediated DR5-DISC formation by decoy receptors 1 and 2. Mol. Cell Biol. *26*, 7046-7055.

Messerschmidt, S. Molecular determinants of the receptor response capability towards soluble TNF: influence of the cysteine-rich domain 1, the stalk- and transmembrane region of the TNF receptors. 2006.
Ref Type: Thesis/Dissertation

Micheau,O. and Tschopp,J. (2003). Induction of TNF receptor I-mediated apoptosis via two sequential signaling complexes. Cell *114*, 181-190.

MONOD,J., WYMAN,J., and CHANGEUX,J.P. (1965). ON THE NATURE OF ALLOSTERIC TRANSITIONS: A PLAUSIBLE MODEL. J. Mol. Biol. *12*, 88-118.

Moosmayer,D., Wajant,H., Gerlach,E., Schmidt,M., Brocks,B., and Pfizenmaier,K. (1996). Characterization of different soluble TNF receptor (TNFR80) derivatives: positive influence of the intracellular domain on receptor/ligand interaction and TNF neutralization capacity. J. Interferon Cytokine Res. *16*, 471-477.

Muppidi,J.R. and Siegel,R.M. (2004). Ligand-independent redistribution of Fas (CD95) into lipid rafts mediates clonotypic T cell death. Nat. Immunol. *5*, 182-189.

Muppidi,J.R., Tschopp,J., and Siegel,R.M. (2004). Life and death decisions: secondary complexes and lipid rafts in TNF receptor family signal transduction. Immunity. *21*, 461-465.

Muzio,M., Stockwell,B.R., Stennicke,H.R., Salvesen,G.S., and Dixit,V.M. (1998). An induced proximity model for caspase-8 activation. J. Biol. Chem. *273*, 2926-2930.

Naismith,J.H., Brandhuber,B.J., Devine,T.Q., and Sprang,S.R. (1996a). Seeing double: crystal structures of the type I TNF receptor. J. Mol. Recognit. *9*, 113-117.

Naismith,J.H., Devine,T.Q., Brandhuber,B.J., and Sprang,S.R. (1995). Crystallographic evidence for dimerization of unliganded tumor necrosis factor receptor. J. Biol. Chem. *270*, 13303-13307.

Naismith,J.H., Devine,T.Q., Kohno,T., and Sprang,S.R. (1996b). Structures of the extracellular domain of the type I tumor necrosis factor receptor. Structure. *4*, 1251-1262.

Naismith,J.H. and Sprang,S.R. (1998). Modularity in the TNF-receptor family. Trends Biochem. Sci. *23*, 74-79.

Neurath,M.F. (2007). IL-23: a master regulator in Crohn disease. Nat. Med. *13*, 26-28.

Orlinick,J.R., Vaishnaw,A., Elkon,K.B., and Chao,M.V. (1997). Requirement of cysteine-rich repeats of the Fas receptor for binding by the Fas ligand. J. Biol. Chem. *272*, 28889-28894.

Papoff,G., Cascino,I., Eramo,A., Starace,G., Lynch,D.H., and Ruberti,G. (1996). An N-terminal domain shared by Fas/Apo-1 (CD95) soluble variants prevents cell death in vitro. J. Immunol. *156*, 4622-4630.

Papoff,G., Hausler,P., Eramo,A., Pagano,M.G., Di Leve,G., Signore,A., and Ruberti,G. (1999). Identification and characterization of a ligand-independent oligomerization domain in the extracellular region of the CD95 death receptor. J. Biol. Chem. *274*, 38241-38250.

Park,H.H., Logette,E., Raunser,S., Cuenin,S., Walz,T., Tschopp,J., and Wu,H. (2007). Death domain assembly mechanism revealed by crystal structure of the oligomeric PIDDosome core complex. Cell *128*, 533-546.

Park,Y.C., Burkitt,V., Villa,A.R., Tong,L., and Wu,H. (1999). Structural basis for self-association and receptor recognition of human TRAF2. Nature *398*, 533-538.

Pennica,D., Lam,V.T., Weber,R.F., Kohr,W.J., Basa,L.J., Spellman,M.W., Ashkenazi,A., Shire,S.J., and Goeddel,D.V. (1993). Biochemical characterization of the extracellular domain of the 75-kilodalton tumor necrosis factor receptor. Biochemistry *32*, 3131-3138.

Pike,L.J. (2006). Rafts defined: a report on the Keystone Symposium on Lipid Rafts and Cell Function. J. Lipid Res. *47*, 1597-1598.

Pomerantz,J.L. and Baltimore,D. (2002). Two pathways to NF-kappaB. Mol. Cell *10*, 693-695.

Reddy,P., Slack,J.L., Davis,R., Cerretti,D.P., Kozlosky,C.J., Blanton,R.A., Shows,D., Peschon,J.J., and Black,R.A. (2000). Functional analysis of the domain structure of tumor necrosis factor-alpha converting enzyme. J. Biol. Chem. *275*, 14608-14614.

Reed,C., Fu,Z.Q., Wu,J., Xue,Y.N., Harrison,R.W., Chen,M.J., and Weber,I.T. (1997). Crystal structure of TNF-alpha mutant R31D with greater affinity for receptor R1 compared with R2. Protein Eng *10*, 1101-1107.

Remy,I., Wilson,I.A., and Michnick,S.W. (1999). Erythropoietin receptor activation by a ligand-induced conformation change. Science *283*, 990-993.

Reyes-Moreno,C., Girouard,J., Lapointe,R., Darveau,A., and Mourad,W. (2004). CD40/CD40 homodimers are required for CD40-induced phosphatidylinositol 3-kinase-dependent expression of B7.2 by human B lymphocytes. J. Biol. Chem. *279*, 7799-7806.

Salvesen,G.S. and Dixit,V.M. (1999). Caspase activation: the induced-proximity model. Proc. Natl. Acad. Sci. U. S. A *96*, 10964-10967.

Sandu,C., Morisawa,G., Wegorzewska,I., Huang,T., Arechiga,A.F., Hill,J.M., Kim,T., Walsh,C.M., and Werner,M.H. (2006). FADD self-association is required for stable interaction with an activated death receptor. Cell Death. Differ. *13*, 2052-2061.

Scaffidi,C., Krammer,P.H., and Peter,M.E. (1999). Isolation and analysis of components of CD95 (APO-1/Fas) death-inducing signaling complex. Methods *17*, 287-291.

Scheuring,S., Reiss-Husson,F., Engel,A., Rigaud,J.L., and Ranck,J.L. (2001). High-resolution AFM topographs of Rubrivivax gelatinosus light-harvesting complex LH2. EMBO J. *20*, 3029-3035.

Schiff,M.H., Burmester,G.R., and Kent,J.D. (2006). Safety analyses of adalimumab (Humira) in global clinical trial with US postmarketing surveillance of patients with rheumatoid arthritis. Ann. Rheum. Dis. *65*, 889-894.

Schneider,P., Bodmer,J.L., Holler,N., Mattmann,C., Scuderi,P., Terskikh,A., Peitsch,M.C., and Tschopp,J. (1997). Characterization of Fas (Apo-1, CD95)-Fas ligand interaction. J. Biol. Chem. *272*, 18827-18833.

Schneider-Brachert,W., Tchikov,V., Neumeyer,J., Jakob,M., Winoto-Morbach,S., Held-Feindt,J., Heinrich,M., Merkel,O., Ehrenschwender,M., Adam,D., Mentlein,R., Kabelitz,D., and Schutze,S. (2004). Compartmentalization of TNF receptor 1 signaling: internalized TNF receptosomes as death signaling vesicles. Immunity. *21*, 415-428.

Sebban,H., Yamaoka,S., and Courtois,G. (2006). Posttranslational modifications of NEMO and its partners in NF-kappaB signaling. Trends Cell Biol. *16*, 569-577.

Sedger,L.M., Osvath,S.R., Xu,X.M., Li,G., Chan,F.K., Barrett,J.W., and McFadden,G. (2006). Poxvirus tumor necrosis factor receptor (TNFR)-like T2 proteins contain a conserved preligand assembly domain that inhibits cellular TNFR1-induced cell death. J. Virol. *80*, 9300-9309.

Sen,R. (2006). Control of B lymphocyte apoptosis by the transcription factor NF-kappaB. Immunity. *25*, 871-883.

Senes,A., Engel,D.E., and DeGrado,W.F. (2004). Folding of helical membrane proteins: the role of polar, GxxxG-like and proline motifs. Curr. Opin. Struct. Biol. *14*, 465-479.

Siegel,R.M., Frederiksen,J.K., Zacharias,D.A., Chan,F.K., Johnson,M., Lynch,D., Tsien,R.Y., and Lenardo,M.J. (2000). Fas preassociation required for apoptosis signaling and dominant inhibition by pathogenic mutations. Science *288*, 2354-2357.

Siegel,R.M., Muppidi,J.R., Sarker,M., Lobito,A., Jen,M., Martin,D., Straus,S.E., and Lenardo,M.J. (2004). SPOTS: signaling protein oligomeric transduction structures are early mediators of death receptor-induced apoptosis at the plasma membrane. J. Cell Biol. *167*, 735-744.

Stagljar,I., Korostensky,C., Johnsson,N., and te,H.S. (1998). A genetic system based on split-ubiquitin for the analysis of interactions between membrane proteins in vivo. Proc. Natl. Acad. Sci. U. S. A *95*, 5187-5192.

Su,H., Bidere,N., Zheng,L., Cubre,A., Sakai,K., Dale,J., Salmena,L., Hakem,R., Straus,S., and Lenardo,M. (2005). Requirement for caspase-8 in NF-kappaB activation by antigen receptor. Science *307*, 1465-1468.

Todd,I., Radford,P.M., Draper-Morgan,K.A., McIntosh,R., Bainbridge,S., Dickinson,P., Jamhawi,L., Sansaridis,M., Huggins,M.L., Tighe,P.J., and Powell,R.J. (2004). Mutant forms of tumour necrosis factor receptor I that occur in TNF-receptor-associated periodic syndrome retain signalling functions but show abnormal behaviour. Immunology *113*, 65-79.

Voigt,C.G., Maurer-Fogy,I., and Adolf,G.R. (1992). Natural human tumor necrosis factor beta (lymphotoxin). Variable O-glycosylation at Thr7, proteolytic processing, and allelic variation. FEBS Lett. *314*, 85-88.

Wajant,H., Henkler,F., and Scheurich,P. (2001). The TNF-receptor-associated factor family: scaffold molecules for cytokine receptors, kinases and their regulators. Cell Signal. *13*, 389-400.

Wajant,H., Pfizenmaier,K., and Scheurich,P. (2003). Non-apoptotic Fas signaling. Cytokine Growth Factor Rev. *14*, 53-66.

Watermann,I., Gerspach,J., Lehne,M., Seufert,J., Schneider,B., Pfizenmaier,K., and Wajant,H. (2007). Activation of CD95L fusion protein prodrugs by tumor-associated proteases. Cell Death. Differ. *14*, 765-774.

Whitbeck,J.C., Connolly,S.A., Willis,S.H., Hou,W., Krummenacher,C., Ponce,d.L., Lou,H., Baribaud,I., Eisenberg,R.J., and Cohen,G.H. (2001). Localization of the gD-binding region of the human herpes simplex virus receptor, HveA. J. Virol. *75*, 171-180.

Wu,J. and Kaufman,R.J. (2006). From acute ER stress to physiological roles of the Unfolded Protein Response. Cell Death. Differ. *13*, 374-384.

Yamamoto,Y., Tsutsumi,Y., Yoshioka,Y., Nishibata,T., Kobayashi,K., Okamoto,T., Mukai,Y., Shimizu,T., Nakagawa,S., Nagata,S., and Mayumi,T. (2003). Site-specific PEGylation of a lysine-deficient TNF-alpha with full bioactivity. Nat. Biotechnol. *21*, 546-552.

Yang,J.K., Wang,L., Zheng,L., Wan,F., Ahmed,M., Lenardo,M.J., and Wu,H. (2005). Crystal structure of MC159 reveals molecular mechanism of DISC assembly and FLIP inhibition. Mol. Cell *20*, 939-949.

Ye,H., Park,Y.C., Kreishman,M., Kieff,E., and Wu,H. (1999). The structural basis for the recognition of diverse receptor sequences by TRAF2. Mol. Cell *4*, 321-330.

Ye,H. and Wu,H. (2000). Thermodynamic characterization of the interaction between TRAF2 and tumor necrosis factor receptor peptides by isothermal titration calorimetry. Proc. Natl. Acad. Sci. U. S. A *97*, 8961-8966.

Zamzami,N. and Kroemer,G. (2001). The mitochondrion in apoptosis: how Pandora's box opens. Nat. Rev. Mol. Cell Biol. *2*, 67-71.

Zhang,X., Gureasko,J., Shen,K., Cole,P.A., and Kuriyan,J. (2006). An allosteric mechanism for activation of the kinase domain of epidermal growth factor receptor. Cell *125*, 1137-1149.

Zheng,Y., Saftig,P., Hartmann,D., and Blobel,C. (2004). Evaluation of the contribution of different ADAMs to tumor necrosis factor alpha (TNFalpha) shedding and of the function of the TNFalpha ectodomain in ensuring selective stimulated shedding by the TNFalpha convertase (TACE/ADAM17). J. Biol. Chem. *279*, 42898-42906.

6. SUPPLEMENT

6.1 Plasmid maps

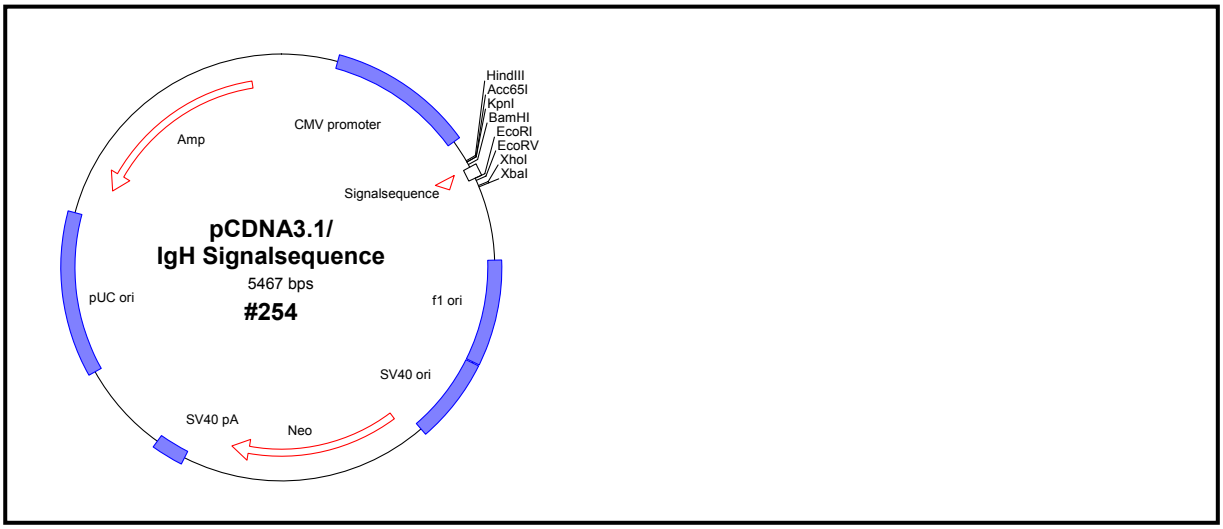

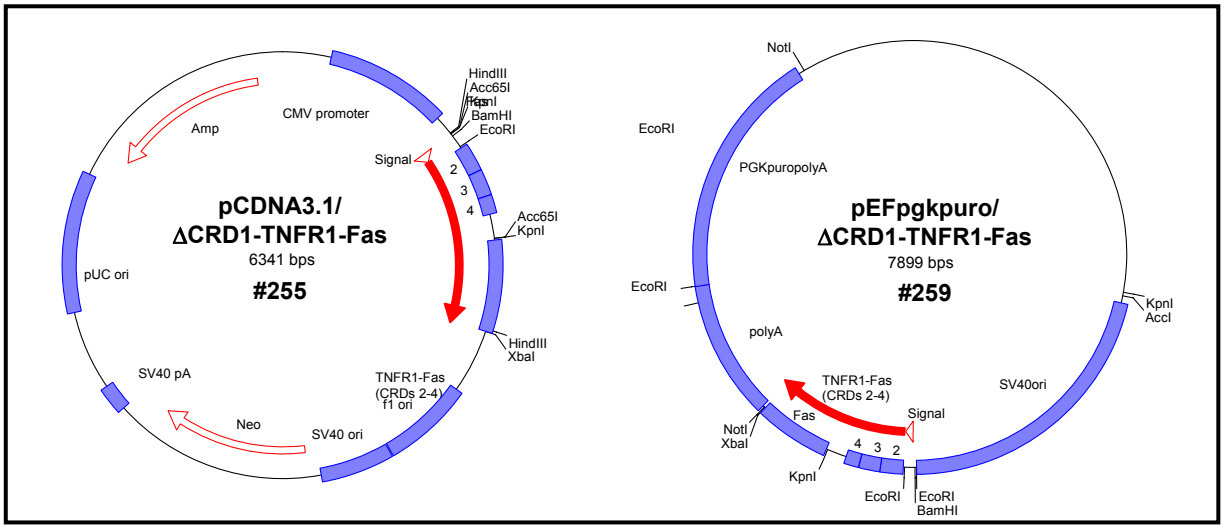

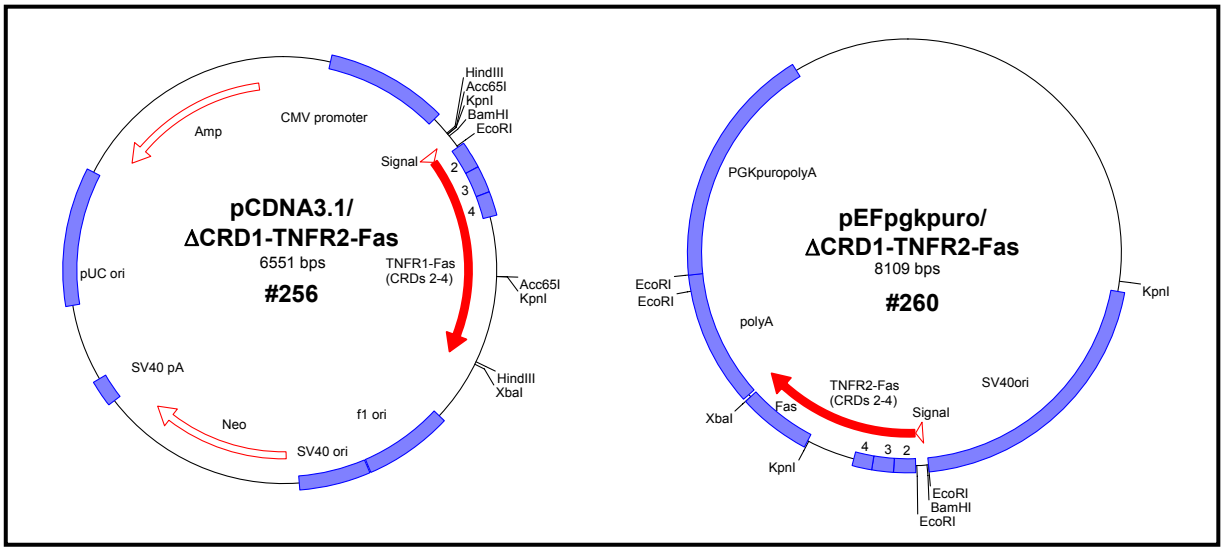

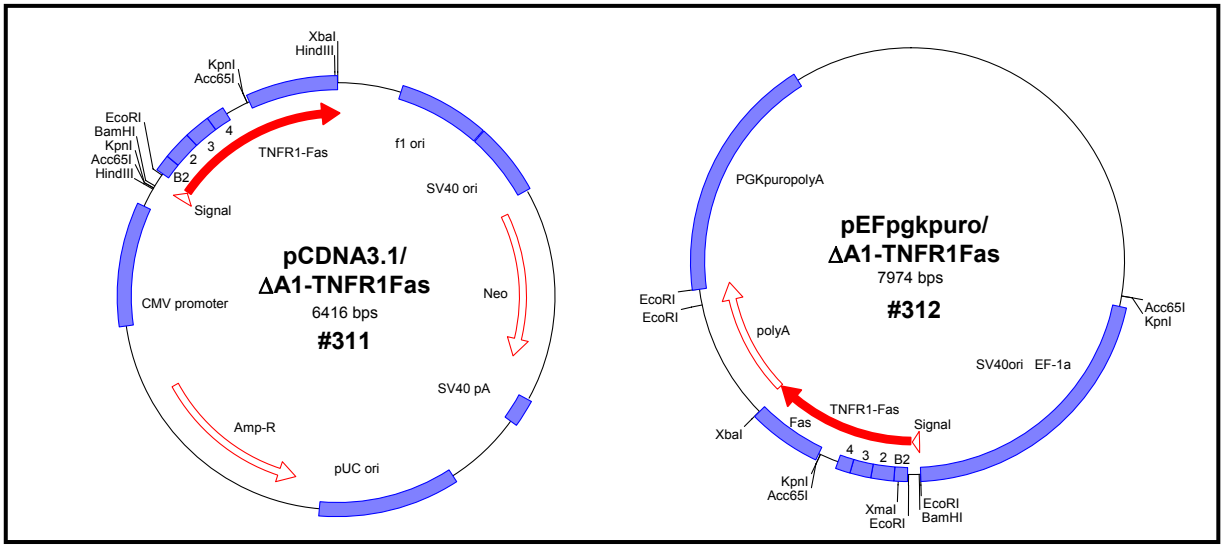
XbaI
HindIII
KpnI
Acc65I
EcoRI
BamHI
KpnI
Acc65I
HindIII
4
3
2
B2
TNFR1-Fas
Signal
f1 ori
SV40 ori
Neo
SV40 pA
Amp-R
pUC ori
CMV promoter
pCDNA3.1/
ΔA1-TNFR1Fas
6416 bps
#311
PGKpuropolyA
pEFpgkpuro/
ΔA1-TNFR1Fas
7974 bps
#312
EcoRI
EcoRI
polyA
Acc65I
KpnI
SV40ori
EF-1a
TNFR1-Fas
Fas
Signal
XbaI
4
3
2
B2
KpnI
Acc65I
XmaI
EcoRI
EcoRI
BamHI

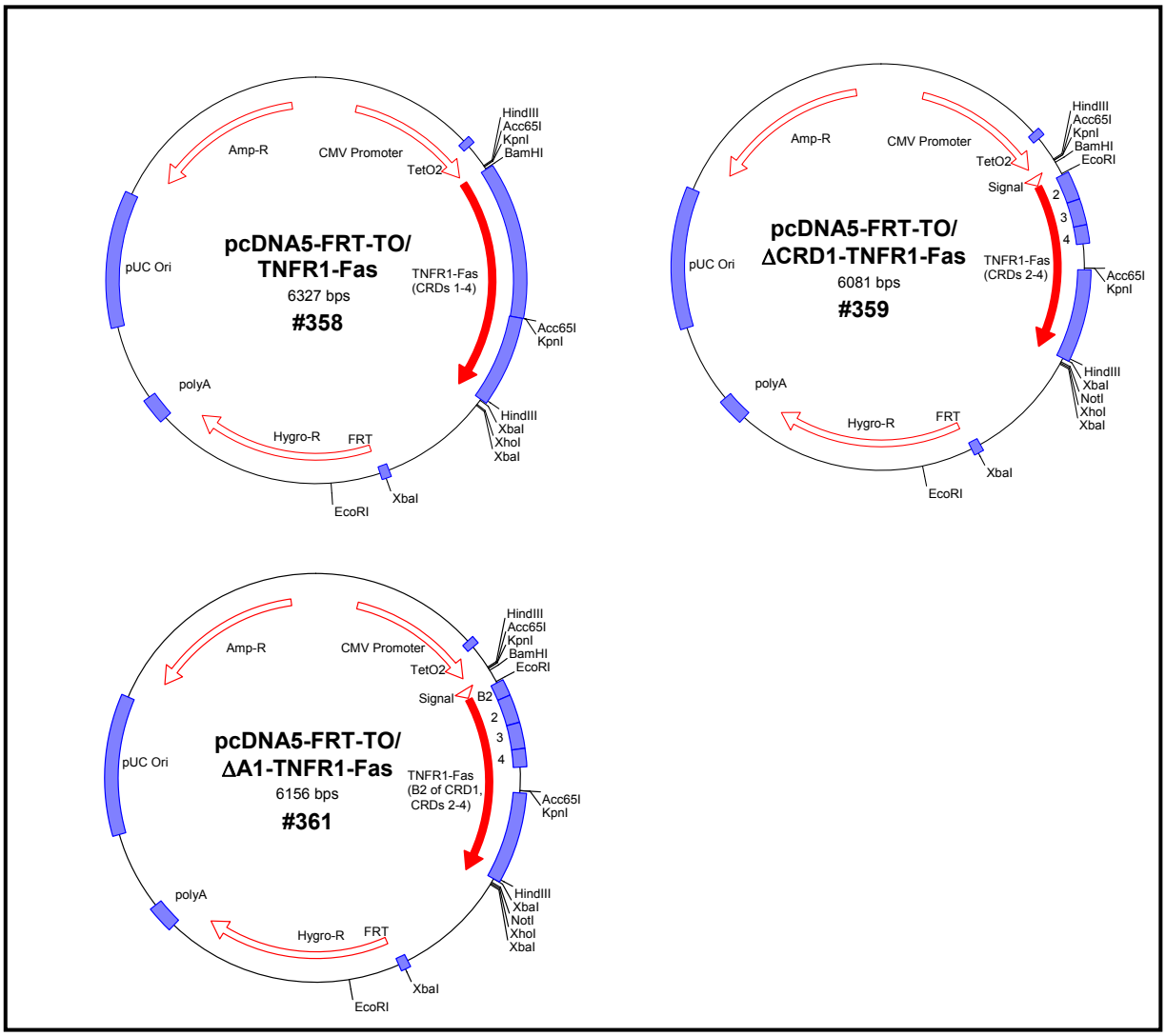
Amp-R
CMV Promoter
TetO2
HindIII
Acc65I
KpnI
BamHI
pUC Ori
pcDNA5-FRT-TO/
TNFR1-Fas
6327 bps
#358
TNFR1-Fas
(CRDs 1-4)
Acc65I
KpnI
polyA
Hygro-R
FRT
HindIII
XbaI
XhoI
XbaI
EcoRI
XbaI
Amp-R
CMV Promoter
TetO2
HindIII
Acc65I
KpnI
BamHI
EcoRI
Signal
2
3
4
pUC Ori
pcDNA5-FRT-TO/
ΔCRD1-TNFR1-Fas
6081 bps
#359
TNFR1-Fas
(CRDs 2-4)
Acc65I
KpnI
polyA
Hygro-R
FRT
HindIII
XbaI
NotI
XhoI
XbaI
XbaI
EcoRI
Amp-R
CMV Promoter
TetO2
HindIII
Acc65I
KpnI
BamHI
EcoRI
Signal
B2
2
3
4
pUC Ori
pcDNA5-FRT-TO/
ΔA1-TNFR1-Fas
6156 bps
#361
TNFR1-Fas
(B2 of CRD1,
CRDs 2-4)
Acc65I
KpnI
polyA
Hygro-R
FRT
HindIII
XbaI
NotI
XhoI
XbaI
XbaI
EcoRI

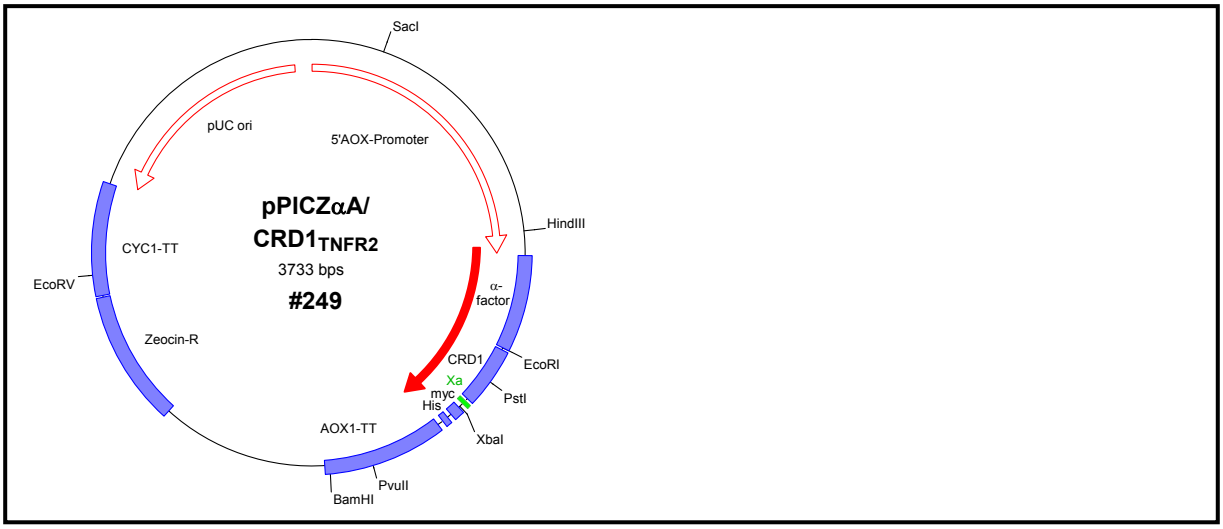

6.2 Amino acid sequences of some relevant proteins

(color coding is given further below)

A) TNFR1-Fas (12 x Lys)

MGLSTVPDLLLPLVLLELLVGIYPSGVIG LVPHLGDREKR

DSVCPQGKYIHPQNNSICCTKCHKGTYLYNDCPGPGQDTDCR

ECESGSFTASENHLRHCLSCSKCRKEMGQVEISSCTVDRDTVCG

CRKNQYRHYWSENLFQCFNCSLCLNGTVHLSCQEKQNTVCT

CHAGFFLRENECVSCSNCKKSLECTKLCLP QIEN VKGTEDSGTT

VLLPLVIFFGLCLLSLLFIGLM YRYL Fas_{cyt}

Δ
TACE
cleavage site

B) TNFR2-Fas (6 x Lys)

MAPVAVWAALAVGLELWAAAHA LPAQVAFTPYAPEP

GSTCRLREYYDQTAQMCCSKCSPGQHAKVFCTKTSDTVCD

SCEDSTYTQLWNWVPECLSCGSRCSSDQVETQACTREQNRICT

CRPGWYCALSKQEGCRLCAPLRKCRPGFGVARPGTETSDVVCK

PCAPGTFSNTTSSTDICRPHQICNVVAIPGNASMDAVCTS

TSPTRSMAPGAVHLPQPVSTRSQHTQPTPEPSTAPSTSFLLPMGPSPPAEGSTGD

FALPVGLIVGVTALGLLIIGVVNCVIMTQV KKKPLCLQREAKVP Fas_{cyt}

GxxxG GxxxxG

C) ΔCRD1-TNFR1-Fas (8 X Lys)

MKCSWVMFFLMAVVTGVNS

RECESGSFTASENHLRHCLSCSKCRKEMGQVEISSCTVDRDTVCG

CRKNQYRHYWSENLFQCFNCSLCLNGTVHLSCQEKQNTVCT

CHAGFFLRENECVSCSNCKKSLECTKLCLP QIEN VKGTEDSGTT

VLLPLVIFFGLCLLSLLFIGLM YRYL Fas$_{cyt}$

D) ΔCRD1-TNFR2-Fas (4 x Lys)

MKCSWVMFFLMAVVTGVNS

DSCEDSTYTQLWNWVPECLSCGSRCSSDQVETQACTREQNRICT

CRPGWYCALSKQEGCRLCAPLRKCRPGFGVARPGTETSDVVCK

PCAPGTFSNTTSSTDICRPHQICNVVAIPGNASMDAVCTS

TSPTRSMAPGAVHLPQPVSTRSQHTQPTPEPSTAPSTSFLLPMGPSPPAEGSTGD

FALPVGLIVGVTALGLLIIGVVNCVIMTQV KKKPLCLQREAKVP Fas$_{cyt}$

E) ΔA1-TNFR1-Fas (11 x Lys)

MKCSWVMFFLMAVVTGVNS DVCTKCHKGTYLYNDCPGPGQDTDCR

ECESGSFTASENHLRHCLSCSKCRKEMGQVEISSCTVDRDTVCG

CRKNQYRHYWSENLFQCFNCSLCLNGTVHLSCQEKQNTVCT

CHAGFFLRENECVSCSNCKKSLECTKLCLP QIEN VKGTEDSGTT

VLLPLVIFFGLCLLSLLFIGLM YRYL Fas$_{cyt}$

F) CRD1$_{TNFR2}$-TNFR1-Fas (12 x Lys)

MAPVAVWAALAVGLELWAAAHA LPAQVAFTPYAPEP

GSTCRLREYYDQTAQMCCSKCSPGQHAKVFCTKTSDTVCD

ECESGSFTASENHLRHCLSCSKCRKEMGQVEISSCTVDRDTVCG

CRKNQYRHYWSENLFQCFNCSLCLNGTVHLSCQEKQNTVCT

CHAGFFLRENECVSCSNCKKSLECTKLCLP QIENVKGTEDSGTT

VLLPLVIFFGLCLLSLLFIGLM YRYL Fas$_{cyt}$

G) TNFR1-(S/TM)$_{TNFR2}$-Fas (11 x Lys)

MGLSTVPDLLLPLVLLELLVGIYPSGVIG LVPHLGDREKR

DSVCPQGKYIHPQNNSICCTKCHKGTYLYNDCPGPGQDTDCR

ECESGSFTASENHLRHCLSCSKCRKEMGQVEISSCTVDRDTVCG

CRKNQYRHYWSENLFQCFNCSLCLNGTVHLSCQEKQNTVCT

CHAGFFLRENECVSCSNCKKSLECTKLCLP GS

TSPTRSMAPGAVHLPQPVSTRSQHTQPTPEPSTAPSTSFLLPMGPSPPAEGSTGD

FALPVGLIVGVTALGLLIIGVVNCVIMTQV KKKPLCLQREAKVP Fas$_{cyt}$

H) TNFR2-(S/TM)$_{TNFR1}$-Fas (7 x Lys)

MAPVAVWAALAVGLELWAAAHA LPAQVAFTPYAPEP

GSTCRLREYYDQTAQMCCSKCSPGQHAKVFCTKTSDTVCD

SCEDSTYTQLWNWVPECLSCGSRCSSDQVETQACTREQNRICT

CRPGWYCALSKQEGCRLCAPLRKCRPGFGVARPGTETSDVVCK

PCAPGTFSNTTSSTDICRPHQICNVVAIPGNASMDAVCTGS QIENVKGTEDSGTT

VLLPLVIFFGLCLLSLLFIGLM YRYL Fas$_{cyt}$

J) Soluble CRD1$_{TNFR2}$ (4 x Lys)

MRFPSIFTAVLFAASSALAAPVNTTTEDETAQIP

Kex2 Ste13

AEAVIGYSDLEGDFDVAVLPFSNSTNNGLLFINTTIASIAAKEEGVSLEKR EA EA EF

LPAQVAFTPYAPEPGSTCRLREYYDQTAQMCCSKCSPGQHAKVFCTKTSDTVCD

TVCDSGAIEGR AAASFL EQKLISEEDL NSAVD HHHHHH

Factor Xa

K) Human *wt* CD95/Fas (13 x Lys)

MLGIWTLLPLVLTSVARLSSKSVNA QVTDINSKGLELRKTVTTVETQ

NLEGLHHDGQFCHKPCPPGERKARDCTVNGDEPDCVPCQEGKEYTDKAHFSSKC

R RCRLCDEGHGLEVEINCTRTQNTKCRCKPNFFCNS

TVCEHCDPCTKCEHGIIKECTLTSNTKCKE EGSRSN LGWLCLLLLPIPLIVWV

KRKEVQKTCRKHRKENQGSHESPTLNPETVAINLSDVDLSKYITTIAGVMTLSQVKG

FVRKNGVNEAKIDEIKN DNVQDTAEQKVQLLRNWHQLHGKKE

AYDTLIKDLKKANLCTLAEKIQTIILKDITSDSENSNFRNEIQSLV

L) Human *wt* TNFR2 (15 x Lys)

MAPVAVWAALAVGLELWAAAHA LPAQVAFTPYAPEP
GSTCRLREYYDQTAQMCCSKCSPGQHAKVFCTKTSDTVCD
SCEDSTYTQLWNWVPECLSCGSRCSSDQVETQACTREQNRICT
CRPGWYCALSKQEGCRLCAPLRKCRPGFGVARPGTETSDVVCK
PCAPGTFSNTTSSTDICRPHQICNVVAIPGNASMDAVCTS
TSPTRSMAPGAVHLPQPVSTRSQHTQPTPEPSTAPSTSFLLPMGPSPPAEGSTGD
FALPVGLIVGVTALGLLIIGVVNCVIMTQV KKPLCLQREAKVPHLPADKARGTQGPE
QQHLLITAPSSSSSLESSASALDRRAPTRNQPQAPGVEASGAGEARASTGSSDSS
PGGHGTQVNVTCIVNVCSSSDHSSQCSSQASSTMGDTDSSPSESPKDEQVPFSKE
ECAFRSQLETPETLLGSTEEKPLPLGVPDAGMKPS

M) Soluble TNFR1 (Baculovirus) (11 x Lys)

MGLSTVPDLLLPLVLLELLVGIYPSGVIG LVPHLGDREKR
DSVCPQGKYIHPQNNSICCTKCHKGTYLYNDCPGPGQDTDCR
ECESGSFTASENHLRHCLSCSKCRKEMGQVEISSCTVDRDTVCG
CRKNQYRHYWSENLFQCFNCSLCLNGTVHLSCQEKQNTVCT
CHAGFFLRENECVSCSNCKKSLEC RL

Color coding for Supplement 6.2:

CRD1 of TNFR1	CRD2, -3, -4 of TNFR1	Stem of TNFR1
CRD1 of TNFR2	CRD2, -3, -4 of TNFR2	Stem of TNFR2
CRD1 of Fas	CRD2, -3 of Fas	Intracellular part of CD95/Fas
His_6-tag	Cysteines belonging to CRDs are in yellow	red underlinded = Factor Xa cleavage site

Further notes:

- All molecules are shown with the secretion signal sequence (letters in gray color) at the beginning.
- The transmembrane domains are double underlined.
- The number of extracellular lysines available for chemical cross-linking are given in brackets next to the heading.
  For recombinant, purified TNFR2 all lysines are given (L).
- The sequences of the chimeric Fas-constructs are only shown until the positions where the intracellular parts of the CD95/Fas molecule starts: $\boxed{Fas_{cyt}}$
  (full CD95/Fas sequence given in Fig. **K**).
- The palmitoylated cysteine of intracellular CD95/Fas (Cys199) is colored in red (Fig. **K**).
- N-terminal of $CRD1_{TNFR2}$ (Fig. **J**) is the yeast alpha-factor signal sequence (gray letters) that is removed by the Kex2 and Ste13 proteases
  (cleavage sites are underlined in blue).
- Cleavage positions of proteases are marked by arrowheads: Δ

ACKNOWLEDGEMENTS

First, I wish to thank Peter for letting me perform this work. I really appreciate that you always had an open door if problems occured that were not necessarily related to laboratory life. I also enjoyed the fruitful and playful discussions that have lead to the development of new hypotheses. The same is essentially true for Anja whom I especially thank for her supportive and very helpful attitude.

In more general, I believe that the good working atmosphere of the past years was also due to the people working in Anja's lab and due to the friendly and helpful colleagues of the whole institute. Present and past members of the Krippner-Heidenrich lab that I want to thank are Verena, Jessica, Monica, Regina, Susanne, Susi, Sylvia, Katja, Katarina, Matthias, Johan, Andrea, Gerlinde, Kornelia, Gosia, Sylvia and Gudrun. Especially Gudrun, who has therefore contributed a lot the success of my work, has taught many essential laboratory techniques to me.

The work would not have been possible without the generous help of many members from the groups of Monilola, Dagmar, Angelika, Jeannette and Jens who unconditionally shared knowledge and provided cell lines, antibodies, ELISAs and several other reagents. Sabine I thank for her kind help with HPLC and Stefan Lange from the Institute of Technical Biology for providing yeast cells. Jürgen from the Fraunhofer Institute has helped with mass spectroscopy measurements. Andrew Aird performed the molecular dynamics simulation experiments and was very patient in explaining.

Many others have contributed to the progression of this work in one way or the other. I am sure that without additional personal efforts of our lovely secretary the final phase of my thesis would have been different.

Finally I wish to thank Susanne and our families for their support, for always being there and for their love.

Stuttgart, in May 2007

LEBENSLAUF

Persönliche Daten

Name:	Marcus Branschädel
Geburtsdatum:	17.04.1975
Geburtsort:	Heilbronn/Neckar
Staatsangehörigkeit:	deutsch

Schulausbildung

03/79 – 06/81	Englischer Kindergarten in Birmingham (GB) und Kaduna (Nigeria)
09/81 – 06/84	Deutsche Schule Kaduna
09/84 – 06/86	Grundschule in Eppingen, Baden-Württemberg
09/86 – 06/95	Gymnasium in Eppingen, Abschluss mit der allgemeinen Hochschulreife
07/95 – 04/96	Wehrdienst: Sanitätsbataillon Horb a.N., Luftl.-sanitätskompanie 250 Ulm
05/96 – 08/96	Firma W. Söhner Präzisionskunsstoffteile GmbH & Co, Schwaigern: Ferienarbeiter

Studium

09/96 – 10/96	Universität Stuttgart, Kurs in Mathematik als Studienvorbereitung
10/96 – 01/03	Universität Stuttgart, Studium der *Technisch orientierten (t.o.) Biologie* - Studieninhalte (u.a.): Bioverfahrenstechnik, Biotechnologie - Vertiefung (u.a.): Zellbiologie, Immunologie - Auszeichnungen: Preise der Technischen Biologie 2001 + 2003
01/03	Studienabschluss zum Diplom-Biologen*, technisch orientiert* (*t.o.*)

Promotion

02/03 – 04/03	Physikalisches Institut, Stuttgart: Vorbereitendes Praktikum (Proteinstruktur-Analysen *in silico*)
05/03 – 03/07	Institut für Zellbiologie und Immunologie, Stuttgart: Interdisziplinäre Promotion Thema: „Analysis of the molecular components essential for the formation of Tumor Necrosis Factor ligand-receptor complexes “

Stuttgart, im Mai 2007